Aus dem Max von Pettenkofer-Institut / Lehrstuhl Virologie
Institut der Ludwig-Maximilians-Universität München

Vorstand: Prof. Dr. med. Oliver T. Keppler

GENERATION OF MACROPHAGE MODELS TO INVESTIGATE THE EFFECT OF HOST FACTORS RESTRICTING HIV AND HSV INFECTION

Dissertation
zum Erwerb des Doktorgrades der Humanbiologie
an der Medizinischen Fakultät der
Ludwig-Maximilians-Universität zu München

vorgelegt von
Qianhao Xiao

aus
Shiyan

Nov 2021

Berichterstatter:	Prof. Dr. med. Oliver T. Keppler
Mitberichterstatter:	Prof. Dr. Rika Draenert
	PD Dr. Hanna-Mari Baldauf
Mitbetreuung durch den promovierten Mitarbeiter:	Prof. Dr. med. Veit Hornung (Lehrstuhlinhaber)
Dekan:	Prof. Dr. med. Thomas Gudermann
Tag der mündlichen Prüfung:	29.11.2021

Table of contents

Contents

Zusammenfassung

Einführung Makrophagen spielen eine zentrale Rolle bei der Immunantwort auf Virusinfektionen. Während zelluläre Antworten stark zelltyp- und pathogenspezifisch sind, ist wenig über angeborene Mechanismen zur Erkennung und Restriktion von Viren in Makrophagen und Makrophagen-ähnlichen Zellen bekannt. MX2 und SAMHD1 wurden kürzlich als antivirale zelluläre Effektoren identifiziert, die auf das humane Immundefizienzvirus Typ 1 (HIV-1) und das Herpes-Simplex-Virus Typ 1 (HSV-1) in Zelllinien abzielen. Makrophagen können produktiv mit HIV-1 und HSV-1 infiziert werden und stellen in vivo wichtige zelluläre Reservoire dar, die Rolle von MX2 und SAMHD1 ist jedoch nur teilweise bekannt.

Ziele Um die zelltypspezifischen Wirtsreaktionen auf diese Viren vollständig zu verstehen, sind experimentelle Modellsysteme erforderlich, die Screening-Ansätze und genetische Manipulationen ermöglichen und physiologisch relevant sind. Hier verfolgten wir die folgenden Ziele: (i) Etablierung und Validierung von *trans*-differenzierten BLaER1-Zellen als genetisch veränderbares Makrophagen-ähnliches Zellmodell für die HIV-1- und HSV-1-Infektion, (ii) Entwicklung eines schnellen und effizienten Protokolls zum Ausschalten von Genen in Primärzellen der Monozyten/ Makrophagen-Linie und (iii) Charakterisierung der antivirale Aktivität von MX2 und SAMHD1 in beiden experimentellen Modellen.

Materialien & Methoden *Trans*-differenzierungs- und Differenzierungsprotokolle sowie phänotypische und funktionelle Analysen von Makrophagen wurden erstellt. Verschiedene Ansätze zur Untersuchung der HIV-1- und HSV-1-Infektion durch Hüllprotein-Pseudotypisierung, Verwendung von Reporterviren, virusähnlichen Partikeln und spezifischen Arzneimitteln wurden optimiert. Angeborene Immunantworten wurden durch PCR und Immunoblot überwacht. Nucleofection-vermittelte, CRISPR/Cas9-basierte Geneditierung in Monozyten wurde entwickelt und die Knockout-Effizienz genetisch und durch Immundetektion validiert.

Ergebnisse (i) *Trans*-differenzierte BLaER1-Zellen nehmen ein myeloisches Genexpressionsprofil an und zeigen Eigenschaften als Reaktion auf eine HIV-1- oder HSV-1-Infektion ähnlich wie primäre Makrophagen. (ii) Im Vergleich zu siRNA-basierten Ansätzen sind CRISPR/Cas9-editierte Makrophagen vital, weisen eine stabile myeloide Marker-Expression auf und genetisch-ausgeschaltete Faktoren werden effizient abgebaut. (iii) Knockouts von MX2 oder SAMHD1 führen zu einer verstärkten HIV-1- und HSV-1-Infektion in *trans*-differenzierten BLaER1-Zellen und primären Makrophagen, was ihre Rolle als Restriktionsfaktoren gegen diesen beiden menschlichen Pathogene bestätigt und erweitert. (iv) In BLaER1-Zellen wird eine Kontamination mit dem Eichhörnchenaffen-Retrovirus (SMRV) entdeckt. (v) BLaER1-

Zellen ermöglichen eine leicht zugängliche Screening-Plattform für zelluläre Faktoren, die für Virusinfektionen funktionell relevant sind.

Fazit Insgesamt legen diese Ergebnisse eine wichtige Methodik für verschiedene Arten von experimentellen Studien zu Virus-Makrophagen-Wechselwirkungen fest. MX2 und SAMHD1 sind breit wirksame Restriktionsfaktoren, die die Infektion von Lentiviren und Herpesviren in menschlichen Makrophagen begrenzen.

Abstract

Introduction Macrophages play a central role in the immune response to viral infection. While cellular responses are highly cell-type and pathogen-specific, little is known about innate mechanisms for sensing and restriction of viruses in macrophages and macrophage-like cells. MX2 and SAMHD1 were recently identified as antiviral cellular effectors targeting Human Immunodeficiency Virus Type 1 (HIV-1) and Herpes Simplex Virus Type 1 (HSV-1) in cell lines. Macrophages can be productively infected by HIV-1 and HSV-1 and constitute important cellular reservoirs *in vivo*, yet the roles of MX2 and SAMHD1 are only partially understood.

Aims To fully understand cell type-specific host responses to these viruses, experimental model systems that allow screening approaches, genetic manipulation and physiologically relevant are needed. Here, we pursued the following aims: (i) Establish and validate *trans*-differentiated BLaER1 cells as a genetically amendable macrophage-like cell model for HIV-1 and HSV-1 infection, (ii) develop a rapid and efficient protocol to knockout genes in monocyte/macrophage primary cells, and (iii) characterize the antiviral potency of MX2 and SAMHD1 in both experimental models.

Materials & methods *Trans*-differentiation and differentiation protocols as well as phenotypic and functional analyses of macrophages were established. Various approaches to study HIV-1 and HSV-1 infection by envelope pseudotyping, use of reporter viruses, virus-like-particles and specific drugs were optimized. Innate responses were monitored by PCR and immunoblotting. Nucleofection-mediated, CRISPR/Cas9-based gene editing in monocytes was developed and knockout efficiencies were validated genetically by immunodetection.

Results (i) *Trans*-differentiated BLaER1 cells adopt a myeloid gene expression profile and display characteristics in response to HIV-1 or HSV-1 infection similar to primary macrophages. (ii) In comparison to siRNA-based approaches, CRISPR/Cas9-edited macrophages are viable, have a stable myeloid marker expression and targeted factors are efficiently depleted. (iii) Knockouts of MX2 or SAMHD1 result in enhanced HIV-1 and HSV-1 infection in *trans*-differentiated BLaER1 cells and primary macrophages, corroborating and expanding their role as restriction factors against these two human pathogens. (iv) A contamination with squirrel monkey retrovirus (SMRV) is discovered in BLaER1 cells. (v) BLaER1 cells can provide an easily accessible screening platform for cellular factors that are functionally relevant for virus infections.

Conclusion Overall, these findings establish critical methodology for different types of experimental studies into virus-macrophage interactions. MX2 and SAMHD1 are

broadly acting restriction factors that limit the infection of lentiviruses and herpesviruses in human macrophages.

List of tables

List of figures

List of abbreviations

Abbreviation	Explanation	Abbreviation	Explanation
AIM2	Absent in melanoma 2	M2	Anti-inflammatory macrophages
AIDS	Acquired immunodeficiency syndrome	MARCH2/8	Membrane-Associated RING-CH 8 or 2 proteins
APOBEC3	Apolipoprotein B mRNA editing enzyme catalytic polypeptide-like 3	MAVS	Mitochondrial antiviral signaling protein
ALRs	Absent in melanoma 2 (AIM2)-like receptors	MDA5	Melanoma differentiation-associated protein 5
ART	Anti-retroviral therapy	MDDC	Monocyte-derived dendritic cells
AGS	Aicardi-Goutières syndrome	MDMs	Monocyte-derived macrophages
CA	Capsid	MFI	Median fluorescence intensities
CARD	Caspase recruitment domain-containing protein 8	MOI	Multiplicity of infection
cGAS	Cyclic GMP-AMP synthase	MX1	Myxovirus resistance 1
cDNA	Complementary DNA	MX2	Myxovirus resistance 2
CNS	Central nervous system	NF-κB	Nuclear factor-κB
Ch25h	Cholesterol-25-hydroxylase	NHEJ	Non-homologous end joining
crRNA	Transcript CRISPR RNA	RNAi	RNA interference
CRISPR/Cas9	Clustered regularly interspaced short palindromic repeats/CRISPR-associated protein 9	Nef	Negative regulatory factor
CRISPRi	CRISPR-mediated interference	NLS	Nuclear localization signal
CRISPRa	CRISPR-mediated activation	NLRs	Nucleotide-binding oligomerization domain (NOD)-like receptors
ctRNP	CrisprRNA composed of RNP	NLRP3	NACHT, LRR and PYD domains-containing protein 3
CypA	Cyclophilin A	NPCs	Nuclear pore complexes
DAI	DNA-dependent activator of interferon	Nups	Nucleoporins
DAMP	Danger-associated molecular pattern	OLRs	Oligoadenylate synthetase (OAS)-like receptors
DCs	Dendritic cells	PAMP	Pathogen-associated molecular pattern
DDX	DexD/H box helicases	PBMCs	Peripheral blood mononuclear cells
DHX	(DEAH-box) proteins	pDCs	Plasmacytoid dendritic cells
DNA-PK	DNA-dependent protein kinase	PIC	Pre-integration complex
dNTP	Deoxynucleoside-triphosphate	PLHIV	People living with HIV
dN	Deoxynucleoside	Pol	polymerase
DSB	double strand break	PRR	Pattern recognition receptor
dsDNA	double stranded DNA	PKR	Protein kinase
dsRNA	double-stranded RNA	qRT-PCR	Quantitative real-time polymerase chain reaction
DTG	Dolutegravir	RIG-I	Retinoic acid inducible gene I
E	Early proteins	RT	reverse transcriptase
EFV	Efavirenz	RLRs	RIG-I-like receptors
Env	Envelope	RNAi	RNA interference (RNAi)
ERT	Endogenous reverse transcription	RNA pol II	RNA polymerase II
FBS	Fetal bovine serum	RNaseL	Latent endoribonuclease
FSC	Forward scatter	RNR	ribonucleotide reductase
Gag	Group-specific antigen	RNPs	ribonucleoproteins
GAS	Gamma-activated sequence	SAMHD1	SAM and HD domain containing protein 1

Abbreviation	Explanation	Abbreviation	Explanation
G3BP1	GTPase-activating protein-(SH3 domain)-binding protein 1	sgRNA	Short guide RNA
GFP	Green fluorescent protein	sgRNP	sgRNA composed of RNP
GBP5	Guanylate-binding protein 5	SG-PERT	SYBR Green I-based real-time PERT assay
GTPases	Guanosine triphosphatases	shRNA	Short hairpin RNA
p.i.	Post infection	SIV	Simian immunodeficiency virus
h	Hour	siRNA	small interfering RNA
HIV	Human immunodeficiency virus	SSC	Side scatter
HHV	Human herpesviruses	ssDNA	Single-stranded DNA
HDR	Homology directed repair	ssRNA	Single-stranded RNA
HSV	Herpes simplex virus	SpCas9	Streptococcus pyogenes
HSCT	Hematopoietic stem cells	tracrRNA	Trans-activating CRISPR RNA
IE	Immediate early proteins	STING	Stimulator of IFN genes
IFI16	Gamma-interferon-inducible protein 16	TALENs	Transcription activator-like effectors nucleases
IRF	Interferon regulatory factor	TBK1	TANK-binding kinase 1
indels	Deletions and insertions	TLRs	Toll-like receptors
IFITM	IFN-inducible membrane-associated cellular factors	TK	Thymidine kinase
IFN-I	type I interferon	TREX1	Three prime repair exonuclease 1
ISGs	Interferon stimulated genes	TRIM5α	Tripartite motif-containing protein 5α
ISG15	Interferon stimulated gene 15	Vif	Viral infectivity factor
JAKs	Janus kinases	Vpr	Viral protein R
kb	kilo-base pair	Vpu	Viral protein U
kDa	kilo dalton	Vpx	Viral protein X
KO	Knockout	Vpx-VLPs	Vpx-containing virus-like particles
L	Late proteins	VSV-G	Glycoprotein of the vesicular stomatitis virus
LGP2	Laboratory of genetics and physiology 2	WHO	World health organization
LRRFIP1	Leucine Rich Repeat of Flightless-1	WT	Wildtype
LTR	Long terminal repeat	ZAP	Zinc-finger antiviral protein
M0	Deactivated macrophages	ZBP-1	Z-DNA binding protein-1
M1	Pro-inflammatory macrophages	ZFNs	Zinc-finger nucleases

1. Introduction

In this introduction, an overview regarding viral infections and innate immune responses in macrophages is outlined. The basic HIV-1 and HSV-1 virology, the principles of the innate immune response and the development of macrophage models in cellular immunology studies are described.

1.1 The viral pandemic, transmission and therapy

1.1.1 Human immunodeficiency virus

The human immunodeficiency virus (HIV) was first recognized as causative virus acquired immunodeficiency syndrome (AIDS) in US in the mid-1980s [1]. According to sequence comparison, HIV infection in humans most likely spread from simian immunodeficiency virus (SIV) to occasionally by cross-species transmission [2]. HIV is divided into two groups: HIV-1 and HIV-2, which both have a wide range of genetic diversity [3]. HIV-1 is most often associated with AIDS worldwide, while HIV-2 is less pathogenic and transmissible reported mainly in West Africa with a few cases in other continents [4]. Four major HIV-1 groups (M, N, O and P) have been identified based on their genetic similarity. Each with a slightly different genetic make-up, the major group M causes the vast majority of infections globally. Within HIV-1 group M, there are at least nine subtypes that vary by about 15% in sequence, with clade C accounting for nearly half of all infections worldwide [5]. HIV-2 infection, on the other hand, has a very low prevalence, with two predominant clades A and B (Figure 1. A). As of 2020, the World Health Organization (WHO) predicts that over 38 million people are infected with HIV/AIDS (Figure 1. C) [6]. In this study, we concentrated on HIV-1 as it is the more common and pathogenic strain. HIV-1 infection is spread through sexual intercourse, contact with contaminated blood, or perinatal transmission [7]. The main transmission worldwide is sexual intercourse and HIV-1 prevalence is high in certain groups who have risk behaviors (Figure 1. B) [8]. Over 75% of all cases of HIV-1 are sexually transmitted via the anogenital mucosa [9]. Another common means of transmission includes intravenous drug abuse with shared needles. Although the next less common, mother to infant transmission can occur via the placenta, during birth, or via breast milk. The last and far less popular transmission includes accidental needle sticks, blood transfusions or organ/tissue transplants that are contaminated with HIV-1 [10].
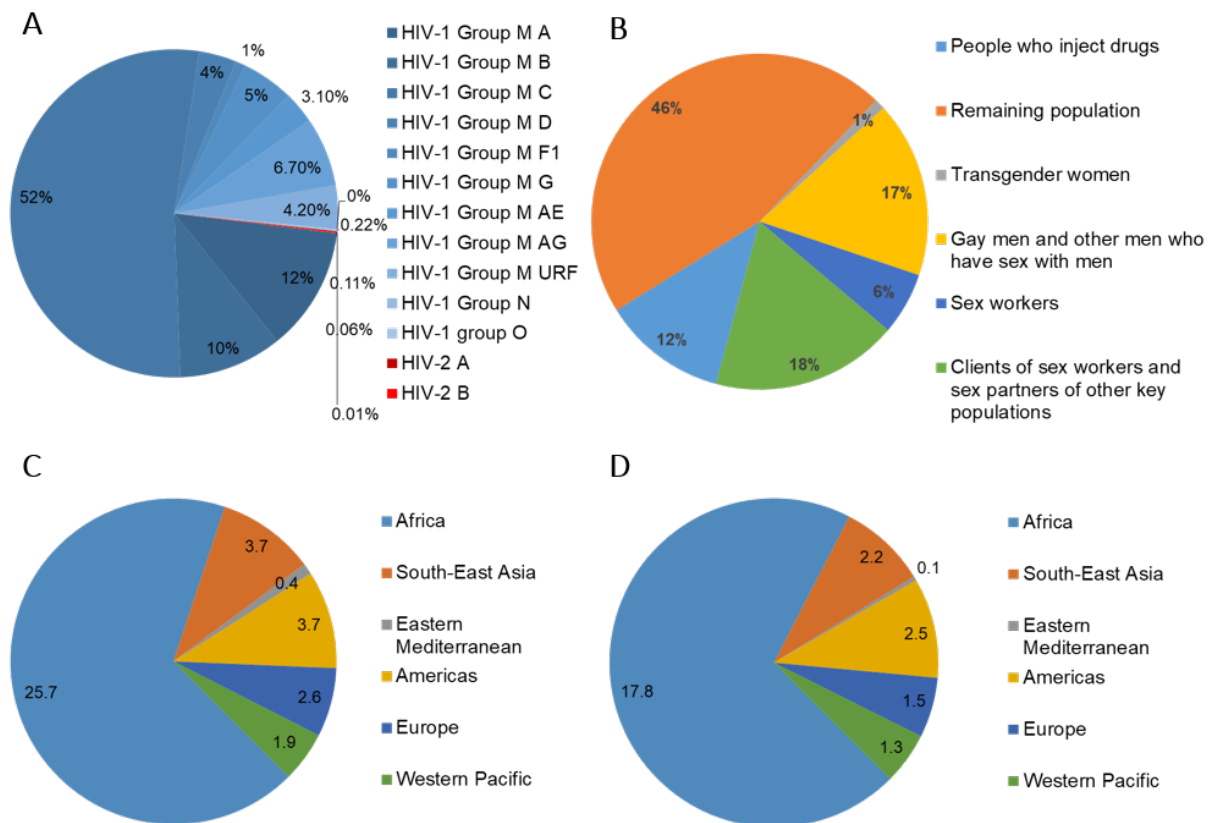
Figure 1*: Global prevalence of HIV by WHO region*
(A) HIV sequence diversity. (B) The percentage of total HIV-1 infections that each clade is responsible for (%). (C) Number of people living with HIV-1 (in millions). (D) People with HIV-1 receiving ART (in millions). Source: [6]

HIV-1 is a member of the *retroviridae* belonging to the order of *lentiviruses*. The HIV-1 virion has a membrane-enveloped capsid (CA) that includes two copies of non-segmented RNA genome (9 kb) and a number of viral proteins [11]. The retroviral RNA genome contains three genes: gag, where it codes for group-specific structural antigens; pol, that either codes for reverse transcriptase, integrase, and protease; and env, that codes for envelope structural proteins. Unlike other retroviruses, HIV gene expression is regulated by tat, rev, nef, vpr, vpu and vif, that aid in viral replication and immune evasion [12]. Retroviruses are distinguished by their replication mechanism, which involves reverse transcription of single-stranded (ss) RNA into double-stranded (ds) complementary DNA (cDNA) and integration of dsDNA into the host genome as a provirus. Figure 2 depicts the stages of HIV-1 replication which can be divided into two phases. The first of which is viral entry and integration into target cells (small arrowheads). The second phase includes the transcription and processing of viral RNA (dotted line with arrows), the translation and modification of viral proteins, and the budding of progeny virions through the cell plasma membrane (curved arrows).
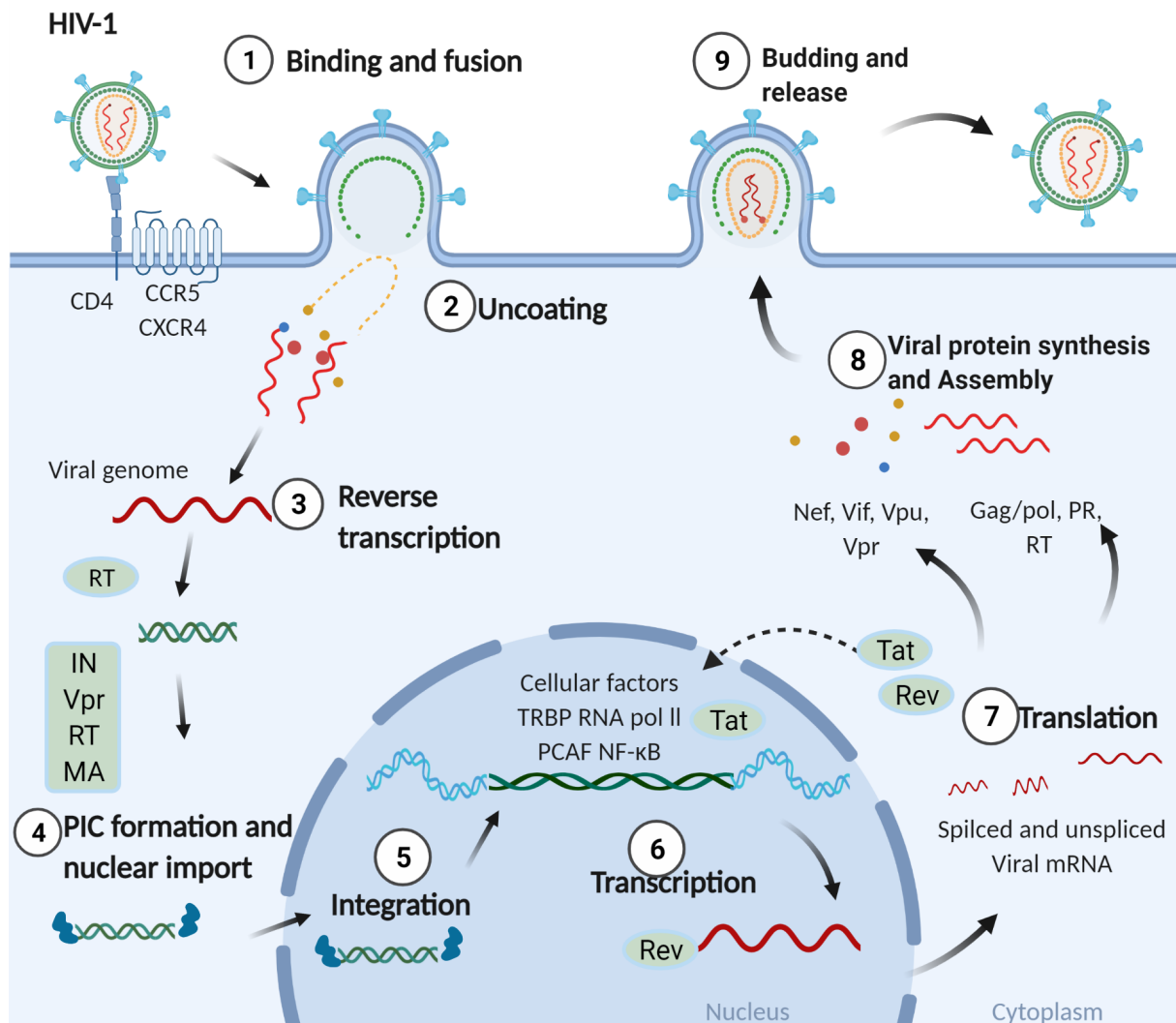
Figure 2: HIV-1 replication cycle
The infection of a target cell by HIV-1 begins with receptor-coreceptor interactions at the cell surface, followed by viral-cellular membrane fusion. The viral core enters the host cell through virus-cell membrane fusion (step 1). After gaining entry into a cell (step 2), the genomic ssRNA is reverse transcribed into dsDNA (step 3). The newly formed pre-integration complex (PIC, step 4) is then integrated into the host genome (step 5). Taking advantage of host RNA polymerase II (RNA pol II), viral RNA is transcribed from the provirus (step 6). Some viral mRNAs are spliced completely or partially and exported to the cytoplasm (step 7), where new viral proteins are translated and synthesized (step 8), followed by the release of mature virions (step 9). Figure modified from [13].

HIV-1 primarily replicates in CD4-positive immune cells, and the CCR5 coreceptor is used by the majority of sexually transmitted HIV-1 isolates [14]. The very first immune cells to encounter the virus during the early stages of HIV-1 infection are found on the mucosal surface of the genital or gastrointestinal tract [15]. Virions may pass through the mucosal barrier, particularly through mucosal lesions, where memory T cells, dendritic cells (DCs) and macrophages are constantly patrolling [16]. DCs residing in epithelial or mucosal tissue can capture virus in the periphery and thus carry the virus into a lymph node infecting CD4-positive T cells and macrophages [17]. The loss of

CD4-positive T cells is a result of several mechanisms such as direct killing by viral replication, HIV-specific cytotoxic T cells killing, bystander apoptosis and pyroptosis as well as a reduced regenerative capacity [18, 19]. CD4-positive T cells depletion is associated with impairment of cellular immunity and increasing susceptibility to opportunistic infections which are referred to as AIDS [19]. There is currently a decrease in disease progression and an increase in the longevity of people living with HIV (PLHIV) with combination antiretroviral therapy (ART) (Figure 1. D) [20]. Several large studies suggest that effective ART reduces the risk of sexual or perinatal transmission [21, 22]. However, there are no effective vaccines for HIV-1 prevention and treatment with ART is plagued with toxicity or virus drug-resistance [23-25]. With 1.7 million new infections and 0.7 million AIDS-related deaths in 2019 alone, there is global interest for the development of a cure in viral eradicating completely or a long-term viral remission therapy in the absence of ART [6].

1.1.2 Macrophages and their relevance in HIV-1 infection

Macrophage is one of the early targets of HIV-1 following sexual transmission and subsequently contributes to pathogenesis throughout the course of the disease [26]. Even though the exact mechanism for HIV-1 replication seems to be preserved, some features such as virion uptake [27-31], replication rate [32], integration [33], assembly [34], budding [35], maturation [36] and capacity to form viral reservoirs [37], differ significantly between CD4-positive T cells and macrophages. Infected macrophages have been believed to be a significant component of virus in the final stage of HIV-1 when CD4-positive T cells are depleted [38]. In this chapter, I aim to dissect the role of macrophages during HIV-1 transmission, to elucidate their contribution to AIDS progression, and to shed light on their significance as a viral reservoir in various anatomical sites.

As the first line of host defense, macrophages are a form of phagocyte that can be found in a variety of tissues with various names [39]. Because of their ability to migrate, HIV-1 infected macrophages are presumed to act as HIV-1 carriers and have been found in a variety of tissues and fluids *in vivo* [40, 41]. Via direct cell-to-cell interaction, macrophages can interact actively with other cell populations, providing a basis for virus spread [42]. HIV-1 may be transported to the mucosa of newborns from infected mammary macrophages during breast-feeding [43]. Although macrophages are

present in most organ systems and can disseminate the virus throughout the body, the relevance of macrophages for HIV-1 spread is complex. One explanation for this is that their ability to allow HIV-1 entry and promote replication varies greatly [44]. Intestinal macrophages in the mucosa, for example, which make up the body's largest single population of macrophages, the CD4, CXCR4 and CCR5 expression are low or non-existent, and tend to be relatively resistant to infection [45]. In contrast, vaginal macrophages express high levels of entry receptors as well as the innate response receptors (e.g., CD14, CD32 and CD46) and can be productively infected during sexual transmission [46]. Compared to colon-resident macrophages, higher HIV-1 susceptibility was demonstrated in rectal macrophages [47]. Alveolar, peritoneal, placental, perivascular macrophages and microglia are among the other types of resident tissue macrophages that are productively infected by HIV-1 *in vivo* [48]. Another explanation is that, based on the macrophages' function and localization, their lifespan vary from a couple of days to years [49-51] (Table 1). Compared to activated CD4-positive T cells, which are less resistant to HIV-1-induced cytopathic effects, infected macrophages have a longer lifespan despite low-level virion production [52, 53]. Because of macrophages widespread distribution across tissues and ability to infiltrate virtually all organs, they may act a crucial role in the spread of HIV-1 infected individuals [54].

Due to their heterogeneous population from various tissue locations, macrophages play a critical part in chronic immune activation and inflammation. There are proposed to be three kinds of activation states: M0 (deactivated macrophages), M1 (pro-inflammatory macrophages) and M2 (anti-inflammatory macrophages). In response to stimulants, monocytes can differentiate into either pro-inflammatory M1 (stimulated with TLRs, CD14 or G-MCSF) or anti-inflammatory M2 (stimulated with IL-4 and IL-13 or M-CSF) macrophages [55]. Apart from their obvious roles in AIDS progression, macrophage activation and deactivation are regulated in a complex manner that could have a significant impact on HIV-1 pathogenicity [56]. It is proposed that M1 macrophage stimulation predominates during the early stages of HIV disease; when these cells interact with TH1 cytokines, the release of pro-inflammatory cytokines and chemokines favors the viral reservoirs formation [57-60]. M1 macrophages facilitate the recruitment of monocytes and T cells on site at this time, causing tissue injury in lymph nodes specifically [61]. Additionally, IFN-I production is impaired with only

limited inhibition of viral assembly and egress. Macrophage-mediated inflammation is thought to be a key factor of HIV-associated liver disease, atherosclerosis and neurocognitive disorders [62-64]. As the systemic infection progresses, the M1 state fades out and an M2 activation state predominates. M2 macrophages tend to promote tissue repair and MHC-II-mediated antigen presentation, as well as the recruitment of neutrophils, monocytes and T cells [65]. M2 macrophages inhibit the reservoirs formation by modulating the TH2 response, which can be circumvented through Nef-induced phenotypic shift [56]. An imbalance in the TH1/TH2 shift has been proposed to contribute to immune dysregulation and AIDS progression [66]. In general, macrophage activation state influences early HIV-1 infection responses [67].

Because of HIV-1 persisting in reservoirs, current antiviral therapy that permanently suppresses viral loads is lifelong required [68-70]. Many cells *in vitro* are susceptible to HIV-1, however not all target cells are latency reservoirs (Table 1). For cells to constitute a reservoir, they have to fulfill the exact definition of latency which virions can be recovered from cells of ART suppressed patients [71]. Throughout the pre-ART era, macrophages were important HIV-1 cellular reservoirs in addition to resting CD4-positive T cells [72]. HIV-1 nucleic acid has been discovered in brain microglia, liver Kupffer, alveolar, penile urethral, vaginal mucosa, intestinal and duodenal macrophages in patients on antiretroviral therapy [46, 73-77]. Furthermore, replication-competent HIV-1 can be recovered from microglia, urethral macrophages and perivascular macrophages, which have been identified as important viral reservoirs [62, 78-80]. In contrast, HIV-1 proviral integration is not detected and infectious virus particles could not be recovered from intestinal macrophages or Kupffer cells from PLHIV under ART. As a result, it appears unlikely that these cells contribute to the HIV-1 reservoir of replication-competent cells [76].

During ART, HIV-1 persists regardless of viral loads in PLHIV [68]. These sanctuaries are located in deep tissue sites (e.g. brain, lymphoid and gut) with limited cytotoxic T cell surveillance, low neutralizing antibody titers, and reduced drug uptake, allowing HIV-1 to sustain in cells present within those sites [81]. The formation of so-called viral sanctuaries can be found different at anatomical sites since macrophages are present and disseminate the virus in every organ system [82]. Additionally, the presence of multidrug-resistance export pumps in macrophages reduces the concentration of

certain antiviral drugs, e.g., protease inhibitors, promoting the emergence of viral escape mutants [83]. Macrophages pose a major obstacle to virus eradication next to quiescent CD4-positive T cells. It has been demonstrated that ART-free remission is not feasible either in the "Mississippi Baby" [84]. Therefore, it is critical for cure strategies to target all potential reservoirs in patients. Based on a clear demonstration that macrophages are an important latent lentiviral reservoirs [85], a comprehensive evaluation of the biology and pathophysiology of viral latency in this cell type is required.

Table 1. Immune cells and their susceptibility to HIV-1 infection

Tissues	Hematopoietic								
Major cells	CD4 T lymphocytes	B lymphocytes	Monocytes	Macrophages	Natural killer	Megakaryocytes	Plasmacytoid dendritic cells	Myeloid dendritic cells	Follicular dendritic cells
Replication competent?	Yes	No	No	Yes	No	Yes	No	No	Yes
HIV presence?	Yes	No	Yes	Yes	Yes	Yes	No	No	Yes
Life span	1-3 years	1-3 years	4-7 days	2-24 months	14 days	8-9 days	ND	ND	2-14 days
Ref	[86, 87]	[88, 89]	[90, 91]	[90, 92]	[93, 94]	[95]	[90, 96]	[90, 97]	[98, 99]

Tissues	Brain				Skin	
Major cells	Capillary endothelial cells	Astrocytes	Microglial	Perivascular macrophages	Langerhans cells	Epithelial cells
Replication competent?	Yes	Yes	Yes	Yes	Yes	Yes
HIV presence?	Yes	Yes	Yes	Yes	Yes	Yes
Life span	Months	Months	3-10 years	Months	Months	Years
Ref	[100]	[101]	[80, 102]	[103]	[104]	[105]

Tissues	Reproductive tract				Lymph node	Bone marrow	Urethra	Liver	Lung	Kidney	Other
	Female		Male								
Major cells	Cervical cells	Vaginal macrophages	Prostate	Testis	Macrophages	Progenitor mast cells	Macrophages	Kupffer cells	Alveolar macrophages	Renal and tubular epithelial cells	Myocardium
Replication competent?	Yes	Yes	Yes	Yes	Yes	Yes	Yes	No	Yes	Yes	No
HIV presence?	Yes	Yes	Yes	ND	Yes	Yes	Yes	Yes	Yes	Yes	Yes
Life span	ND	ND	ND	ND	ND	Weeks	ND	3-4 days	2 month	ND	ND
Ref	[106, 107]	[46]	[108]	[109]	[77]	[110]	[77]	[76]	[111]	[112]	[113]

ND: Not determined

1.1.3 Herpes simplex virus

Herpes simplex virus (HSV) is a subfamily of human herpesviruses (HHV) and is responsible for various clinical manifestations, including cold sores, fever blisters, genital ulcers, blindness and encephalitis [114]. The two serotypes HSV-1 and HSV-2 are approximately 83% homologous and capable of causing lesions at either of these locations [115]. Both viruses are extremely common, and the prevalence of HSV infection varies greatly depending on geographical location, gender or ethnicity [116]. HSV-1 infection affects roughly 67% of the global population, outnumbering HSV-2 as the leading cause of infectious blindness and genital infection [117]. HSV-1 infection typically begins in the oral mucosa and spreads to neighboring nerve cells [118]. The virion is primarily transmitted via oral-oral contact, but it can also be transmitted via oral-genital contact, causing genital tract infection [119]. Infections with HSV-1 mainly occur after these viruses have gained contact with the mucosa or micro-lesions in skin epithelium [120]. The virus may also spread from infected pregnant mothers to infants *in utero* [121]. An important concern regarding HSV-1 genital infection is its association with susceptibility to acquiring HIV-1 [122]. Most of the time, HSV-1 causes asymptomatic latent infections that set up in the trigeminal and sacral nuclei for life. Usually the disease is self-limiting but sometimes it can cause symptoms like recurrent oral and genital lesions, or an over-active immune response which induces encephalitis and keratitis [123]. Overcoming HSV-1 infection continues to remain difficult in the absence of an HSV-1 vaccine and the existence of drug-resistant variants [124]. Potential treatment targets for HSV-1 infection-related diseases are desperately required.

The HSV-1 virion has a diameter of 100-200 nm and is composed of four parts: the CA, tegument, Env and linear dsDNA genome (153 kb) [125]. The genome is encased in an icosahedral CA that serves as a DNA core, and the tegument is encased in a host-derived lipid bilayer called the envelope, which contains ten viral glycoproteins [126]. In between CA and Env, an amount of tegument proteins participate in virus replication and host evasion in the nucleus. The virion has a broad cell tropism and predominantly infects epithelial cells and neurons [127]. HSV-1 is notable for its ability to establish latency infection, by which it is periodically activated to enter a lytic state, causing immunopathology [128]. Figure 3 depicts a schematic representation of the lytic replication cycle in detail.
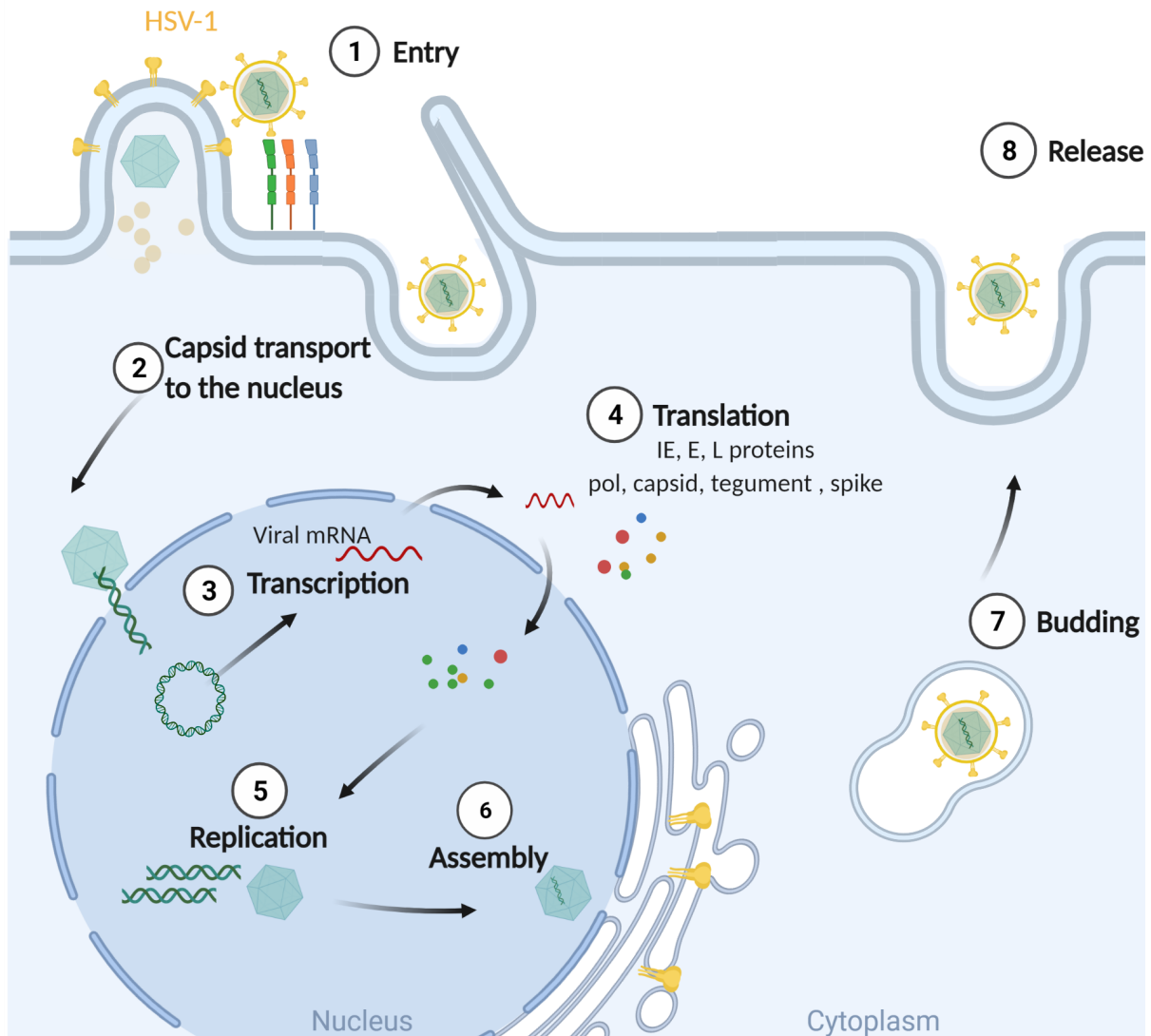
Figure 3: HSV-1 lytic replication cycle
HSV-1 infects cells via endocytosis or fusion (step 1). Once the viral and cell membranes have fused, DNA is further transported to the nucleus via interactions with the microtubule network after the tegument and nucleocapsid uncoating (step 2). HSV-1 starts up the lytic cycle as the immediate-early, early and late genes are expressed sequentially. The encoded immediate early (IE) proteins facilitate gene expression and evade the innate immune response (step 3). The early (E) and late (L) proteins are required in a regulated manner for viral genome replication and structural protein synthesis (step 4 and 5). New virus particles are assembled from late protein and DNA replication products (step 6). The developing virion moves through the endoplasmic reticulum and buds off the Golgi apparatus (step 7). After being released from exocytosis or cell lysis, the virus spreads and infects neighboring cells (step 8). Figure modified from [129].

1.1.4 Role of macrophages in restricting HSV-1

HSV-1 is a neurotropic herpesvirus with a wide range of cell tropisms, including the ability to infect macrophages. HSV-1 infects epidermal or epithelial cells at a peripheral site before invading sensory neurons in the trigeminal ganglion and establishing a latent infection [130]. Approximately 48 h upon initial infection, retrograde axonal transport transmits the virus to the sensory ganglia's neuronal cell bodies [131]. The

virus replicates briefly in the trigeminal ganglion, reaching peak levels in 3-5 days and then declining in 7-10 days [132]. HSV-1 replication in the trigeminal ganglion is modulated by innate immunity, and macrophages are the first responders around infected neurons, producing IL-1 and IL-18, which are critical for preventing severe HSV-1 disease [133]. Aside from chemokines and cytokines, macrophages produce secretome enhancing the early antiviral response [134]. Furthermore, macrophages can phagocytose antigens and present them to stimulate T lymphocyte proliferation. Macrophage depletion significantly increases viral titers, implying that macrophages play a role in constraining virulence within the trigeminal ganglion [135].

The antiviral activity of macrophages has typically been classified as intrinsic or extrinsic. The intrinsic antiviral activity is IFN-stimulated genes (ISGs) dependent, and resting macrophages have a high level of restriction factors, making them resistant to viral replication in general. Macrophages become activated and show greater antiviral potential during HSV-1 infection [136]. Extrinsic antiviral activity refers to macrophages' ability to inactivate extracellular viruses or to inhibit viral replication in bystander cells. In response to HSV-1 infection, infiltrating M1 macrophages contribute to IFN-I production, as well as secreting significant amounts of certain cytokines (e.g., TNFα, IFN-γ, IL-6 and IL-12) and chemokines (e.g., CXCL10, CCL2 and CCL3) [137]. These chemokines attract T lymphocytes, NK cells and other myeloid cells to cooperate in HSV-1 elimination. TNFα can synergize with IFN-γ to induce IFN-β, which suppresses HSV-1 replication in corneal fibroblasts and epithelial cells [138]. A TH0 immune response can be switched to a TH1 immune response by IL-12 [139]. Increased eye inflammation may be caused by M1 macrophages. To suppress inflammatory responses and facilitate tissue repair, M2 macrophages secrete a large amount of anti-inflammatory cytokines (e.g., IL-10, IL-1Ra and TGF-β) as well as the Arginase 1 [140]. These responses shape the progression of virus infection by activating appropriate defense mechanisms [141]. Thus, macrophages contribute crucially in many aspects of the immune response against HSV-1.

HSV-1 reactivates from latency in sensory neurons on a sporadic basis and is shed at peripheral sites, potentially causing neuroinflammation. Low levels of HSV-1, for example, are more frequently reactivated as the immune system deteriorates with age, leading to Alzheimer's disease [142]. Neuroinflammation, on the other hand, is closely

linked to an overactive innate immune response. Infiltrating macrophages producing pro-inflammatory cytokines have been associated with long-term neuroinflammation in the limbic system [143]. Microglia, as CNS-resident macrophage cells, produced multiple factors with both neurotoxic and neuroprotective effects and did not exhibit significant apoptosis after HSV-1 infection [144, 145]. Large amounts of circular HSV-1 DNA and latency-associated viral transcript have recently been detected in latently infected Mus musculus macrophages and neurons, indicating a role in HSV-1 latency; however, there have been few reports of latent infection in human myeloid cells [146-148]. HSV-1 replication is limited in resting macrophages, but the involved restriction factors remain uncertain. Given the importance of macrophages in innate immune responses to HSV-1 infection, further research into the complex role of macrophages in HSV-1 infection is required [149].

1.2 The innate immune response to HIV-1 and HSV-1 in macrophages
1.2.1 Macrophage sensing and intrinsic restrictions to viral replication
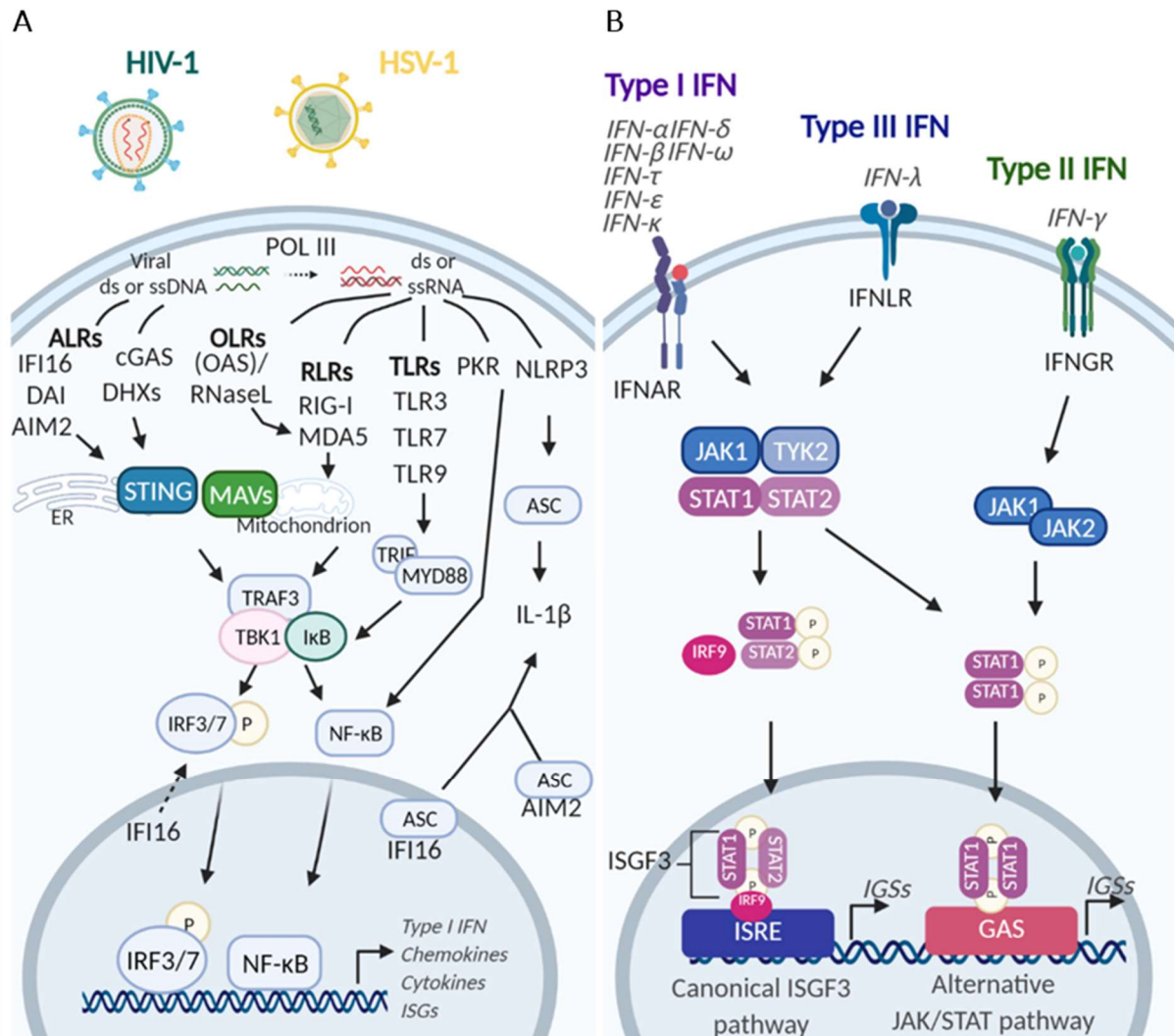
Figure 4: **Putative receptors recognise virus infection and restriction factors involved in innate immunity**
(A) The viral nucleic acid can be sensed by host PRRs. The activation of cytosolic PRRs causes downstream signalling through IRFs and NF-κB nuclear translocation, which contributes to the expression of chemokines, cytokines, IFNs and ISGs. (B) When IFN-I binds to IFNAR1/2, receptor-associated Janus kinases (JAKs) phosphorylate STAT1 and STAT2 proteins, causing them to dimerize and activate. ISGF3 transcription factor complex is formed by STAT1/2 heterodimers binding to IRF9 or STAT1 homodimers binding to gamma-activated sequence (GAS), which may promote antiviral and inflammatory responses. Figure modified from [150, 151].

Macrophages are immune cells that recognize pathogen-associated molecular patterns (PAMPs) or damage-associated molecular patterns (DAMPs) and respond by phagocytosing pathogens, presenting antigens and secreting immune mediators [152]. HIV-1 and HSV-1 have a replication cycle that involves the production of ssRNA, ssDNA, RNA-DNA hybrids and dsDNA, which can trigger PRRs to activate IRFs or transcription factors nuclear factor (NF-κB). IRFs and NF-κB then function together in

the nucleus to induce IFNs, ISGs and other cytokines, resulting in an antiviral effect (Figure 4. A) [153]. There is a network of PRRs specializing in the detection of distinct PAMPs. For instance, the Toll-like receptors (TLRs), RIG-I-like receptors (RLRs), DHX (DEAH-box) proteins, Oligoadenylate synthetase (OAS)-like receptors (OLRs), Absent in melanoma 2 (AIM2)-like receptors (ALRs), cyclic GMP-AMP synthase (cGAS), Nucleotide-binding oligomerization domain (NOD)-like receptors (NLRs) and several other cytosolic proteins are the ones in charge of detecting DNA [154]. Certain members of PRRs (AIM2, IFI16 and NLRP3) have been shown to form inflammasome to drive pyroptosis. The spectrum of PRRs recognizing a specific set of ligands is cell type dependent (Table 2) [155]. TLRs, RLRs, IFI16, DAI, Ku70, DDX60, DHX9, DHX36, and RNA pol III are constantly expressed in macrophages and HIV-1 is presumed to be detected at process of reverse transcription and integration [156, 157]. Although macrophage expresses a variety of cellular sensors, there appear to be a lack of profound ISG response. In contrast, incoming herpesviruses elicit a strong innate immune response by IFN-I production [158]. Macrophages are equipped with a panel of PRRs able to sense pathogens HSV-1 including TLRs, RLRs, IFI16, AIM2, cGAS, DAI, RNA POL III and DDX41 (Table 2). IFI16 can detect either cytoplasmic or replication-generated DNA from HSV-1 [148]. HSV-1 genome-derived DNA can be detected by cGAS, which triggers macrophages, DCs and fibroblasts to secrete IFN-I [159]. MDA5 detects HSV-1 replication-derived RNA structures in macrophages [160]. HSV-1 can activate the inflammasome producing in macrophages by interacting with the NLRP3 protein [161]. Despite the fact that multiple PRRs have been reported in the early anti-viral response, the ability of primary macrophages to detect exogenous or replicating viruses remains unknown [162]. When secreted IFNs bind to their cognate receptors, signaling cascades are activated, and ISGs are produced, which build an antiviral state in infected and adjacent cells (Figure 4. B) [163]. There are three main types of IFNs: IFN-I (α, β, ε, κ and ω), IFN-II (γ) and IFN-III (λ1, λ2, λ3) [164-166]. IFN-I constitutes an important class of IFNs which are bound to IFNAR1/2 that are expressed in all nucleated cells, amplifying cell antiviral state by promoting ISGs expression [163]. These ISGs have a wide range of antiviral activity and are collectively referred to as restriction factors. So far, more than nine groups of cellular restriction factors have been documented, including TRIM, SERINC, IFITMs, SAMHD1, APOBEC3, SLFN11, MARCH, MX and Tetherin, as well as nearly 200 other proposed ISGs [167]. A number of the PRRs described above, e.g., TLRs (TLR3 and TLR8),

RLRs (RIG-I), cGAS, IFI16 and PKR, are also known as ISGs since they are expressed at baseline levels but are upregulated in response to IFN [168]. IFN also upregulates a number of PRR downstream adaptors (e.g., MyD88, TRIF, TBK1 and IRF7) in addition to these PRRs, which are important in amplifying IFN response and the overall antiviral state [169]. The viral replication cycle can thus be disrupted at different stages by restriction factors. Although restriction factors can be upregulated by IFNs, many of them are constitutively expressed to high levels, allowing them to act very early during viral infection [170]. Restriction factors that exhibit anti-HIV and anti-HSV activity are characterized in table 3. Relative to CD4-positive T cells, macrophages represent a more restrictive environment for HIV-1 which may be due to differences in the expression of specific cellular factors. IFITM proteins have been shown to impair viral fusion and the effect of IFITM silencing was more pronounced in macrophages [171]. Tetherin and SAMHD1 are highly expressed in macrophages rather than CD4-positive T cells [172]. The viral envelope has recently been discovered to be targeted by MARCH8 and GBP5 in macrophages [173, 174]. Viperin [156], Visfatin [175], PAF1c [176] and p21 [177] are among the rest factors that restrain HIV-1 replication in macrophages. Despite the discovery of restriction factors induced by limited HIV-1 sensing, further investigating the role of their restriction in the HIV-1 replication cycle is warranted. Remarkably, some restriction factors that inhibit RNA viruses activity may also restrict DNA viruses. For instance, the MX1, MX2, ISG15, PKR, OAS/RNase L, APOBEC3, Tetherin and Viperin have been proposed as agonists of herpesvirus infection [178-180]. Although the body of literature generated through HTS studies has suggested that numerous host proteins inhibit viral replication *in vitro*, their full spectrum of action in immortalized cell lines remains to be expanded into primary macrophages.

1.2.2 Viral evasion of innate immune responses

The ability of PRRs to stimulate innate immune responses in macrophages to confer HIV-1 and HSV-1 restriction is well established. Given viruses' latent infections, their avoidance of PRR sensing are critical [150, 181]. It has been demonstrated that both viral infections can manipulate the sensing arm of IFN-I signaling. HIV-1 has evolved to circumvent the innate immune responses and establish disseminated infection [182]. To minimize viral recognition, HIV-1's low CG dinucleotide content genome is inaccessible to intrinsic PRRs. HIV-1 has been suggested to hijack the DC-SIGN

function to block mitochondrial antiviral signaling protein (MAVS) signaling [183]. HIV-1's Vif and Vpr, as well as protease-mediated sequestration of RIG-I and Vpu-dependent depletion of IRF3 and NF-κB, are capable of inactivating the cyclic GMP/AMP synthase-stimulator of IFN genes (cGAS-STING) pathway downstream [184-187]. In parallel, disruption of MHC-I by Nef [188], and Tat-mediated impairment of PKR [189] were also observed. Furthermore, HIV-1's mutations in the CA shielded reverse transcription product leaks, and HIV-1 exploited cellular exonuclease TREX1 to degrade excess viral DNA [190, 191]. Macrophages are targets of HSV-1 and express IFN-I and IFN-III, TNFα and the chemokines (CCL5 and CXCL10) to counteract infection [192]. While IFNs induce hundreds of ISGs, HSV-1 has numerous countermeasures to negate their anti-viral effects [193]. HSV-1 can directly constrain the cGAS and IFI16, as well as hijack multiple steps downstream of the RLRs and TLRs signaling pathways [194]. IFN signaling pathways are blocked by both HSV-1 IE (ICP0, ICP4 and ICP27) and L (ICP34.5, US3 and US11) proteins [195]. For example, the HSV-1 US3 and ICP0 proteins prevent IRF-3 from accumulating in the nucleus. ICP4 reduces the stability of host-cell mRNAs [196, 197]. The ICP27 and ICP34.5 interfere with STING signal and regulate the shutoff of host protein synthesis [198]. Restriction factors are usually less effective against viruses as a result of virus-host adaptation [199]. The CA of HIV-1 can employ cytoplasmic cofactors cyclophilin A (CypA) and CPSF (CPS6) to cloaks its cDNA or reduce its binding to TRIM5α without being detected by cytoplasmic cGAS [182, 200]. TRIM5α protein is lost during HSV-1 infection [201]. APOBEC3 family members have been implicated in the antiviral control but can be evaded by Vif of HIV-1 and by VP16 and ICP0 of HSV-1 [202, 203]. HIV-1 doesn't contain Vpx, which overcomes SAMHD1's restriction at the cost of avoiding triggering viral cDNA detection [204]. The Tetherin and SERINCs, which have been shown to limit HIV-1 release and infectivity, are inhibited by Vpu and Nef, respectively [205, 206]. HSV-1 contains a number of proteins that inhibit ISGs transcription as well as interfere with the restriction factors [207]. HSV-1 UL41 was demonstrated to evade the Ch25h antiviral function via its endonuclease activity [208]. Additionally, the HSV-1 US11 has been shown to inhibit both OAS/RNaseL and the PKR pathway [209, 210]. The main viral proteins engaged in circumventing the innate immunity are listed in Table 3. Though individual innate receptors and restriction factors have been demonstrated in different experimental models, the role of macrophages in restricting viruses hasn't been extensively explored.

Table 2. Cellular sensing of viral components

PRRs	PAMPs	Target cell	Signaling pathway	Counteraction by virus	Ref
TLR2	HIV-1 gp41, gp120 HSV-1 glycoproteins	CD4 T cells, Macrophages	MyD88→ NF-κB→ inflammatory cytokine	ND	[211, 212]
TLR3	HIV-1 or HSV-1 dsRNA	Innate immune cells except neutrophils and pDCs	TRIF→ IRF3→ IFN-α/β	ND	[213-215]
TLR7	HIV-1 ssRNA, HSV-1 dsRNA	Macrophages, DCs, B cells and fibroblasts	MyD88→ IRFs→ IFN-α/β and IFN-λ1	ICP0 (HSV-1)	[215-217]
TLR8	HIV-1 ssRNA	Monocytes, macrophages and DCs	MyD88→ IRFs→ IFN-α/β, Inflammatory cytokines	ND	[218-221]
TLR9	HIV-1 or HSV-1 CpG dsDNA	B cells, DCs and myeloid cells of murine origin	MyD88→ NF-κB→ IFN-α/β and IFN-λ1	gp120 (HIV-1)	[222-224]
RIG-I	HIV-1 or HSV-1 5'-PPP ssRNA, short dsRNA	All mammalian cell types	MAVS→ IRFs, STING→IFN-α/β, Inflammatory cytokines	Protease (HIV-1), US11 and UL37 (HSV-1)	[187, 225, 226]
MDA5	HIV-1 long dsRNA, HSV-1 RNA	All mammalian cell types	MAVS→ IRFs→ IFN-α/β, Inflammatory cytokines	US11, UL37 and UL41 (HSV-1)	[227, 228]
DDX3	HIV-1 abortive RNA	Macrophages, DCs	MAVS→ IRFs→ IFN-α/β	Tat (HIV-1)	[183]
DDX41	HIV-1 RNA/DNA hybrids, HSV-1 dsDNA	Macrophages, DCs	STING→ IRFs→ IFN-α/β, Inflammatory cytokines	ICP0, ICP27, ICP34.5 (HSV-1)	[229]
DDX60	HIV-1 or HSV-1 dsRNA	DCs	RLRs→ MAVS→ IRFs→ IFN-α/β, Inflammatory cytokines	ICP0, ICP27, ICP34.5 (HSV-1)	[230, 231]
DHX9-DHX36	HIV-1 or HSV-1 CpG DNA	pDCs	MyD88→ IRFs→ IFN-α/β, Inflammatory cytokines	ICP0, ICP27, ICP34.5 (HSV-1)	[231]
DDX1-DDX21	HIV-1 or HSV-1 DNA	DCs	TRIF→ IRF3→ IFN-α/β	VP16 (HSV-1)	[232, 233]
OAS-1/RNase L	HIV-1 or HSV-1 dsRNA	All mammalian cell types	RLRs→ MAVS→ IRFs→ IFN-α/β, Inflammatory cytokines	Tat (HIV-1), US11 (HSV-1)	[234-236]
IFI16	HIV-1 or HSV-1 dsDNA	CD4 T cells and macrophages	STING→ IRFs or NF-κB→ IFN-α/β, ASC→ procaspase-1→ IL1β→ Pyroptosis	Vpu (HIV-1), ICP0, ICP27, ICP34.5 and UL41 (HSV-1)	[207, 237]
DAI	HIV-1 or HSV-1 dsDNA	Macrophages and fibroblasts	IRF3 or NF-κB→ IFN-α/β, Inflammatory cytokines	Vif, Vpu and Vpr (HIV-1), VP16 (HSV-1)	[238, 239]
AIM2	HIV-1 or HSV-1 dsDNA	Macrophages	ASC→ procaspase-1→ IL1β→ Pyroptosis	VP22 (HSV-1)	[240, 241]
cGAS	HIV-1 or HSV-1 DNA	CD4 T cells, DCs and macrophages	STING→ IRFs→ IFN-α/β, Inflammatory cytokines	Vpr, Vpu (HIV-1), UL37, UL41 VP22 (HSV-1)	[229, 242, 243]
NLRP3	HIV-1 or HSV-1 dsRNA	Monocytes, DCs, Macrophages	ASC→ procaspase-1→ IL1β→ Pyroptosis	ICP0 (HSV-1)	[244, 245]
CARD8	HIV-1 protease	CD4 T cells, Macrophages	Protease /CARD8→procaspase-1→ IL1β→ Pyroptosis	ND	[246]
LRRFIP1	HSV-1 dsDNA, dsRNA	Monocytic Cell Lines	β-catenin→ IRF3→ IFN-β	US3 (HSV-1)	[247]
DNA-PK	HIV-1 DNA	Activated HIV-infected CD4 T cells	Caspase 3-apoptosis	ICP0 (HSV-1)	[248, 249]
MRE11	HIV-1 dsDNA	All mammalian cell types	STING→ IRF3	Vif, Vpu, Vpr (HIV-1)	[250]
RNA POL III	HSV-1 dsDNA	Macrophages	RLRs→ MAVS→ IRFs→ IFN-α/β	US11 (HSV-1)	[251]
PQBP1	HIV-1 dsDNA	DCs, Monocytic Cell Lines	cGAS-IRF3→ IFN-α/β	Vif, Vpu, Vpr (HIV-1)	[252]

ND: not determined

Table 3. Antiviral restriction factors

Step	Restriction factors	Viruses	Target cell	Restriction mechanism	Counteraction by virus	Ref
Entry and uncoating	SERINC3/5	HIV-1	CD4 T cells	Incorporates into virus particles and prevents target cell fusion	Nef	[206, 253]
	TLR2	HSV-1	DCs, macrophages	Produce proinflammatory cytokines such as IL-6, IL-12 and TNFα	ICP0 (HSV-1)	[212, 254]
	IFITMs	HIV-1, HSV-1	CD4 T cells, macrophages	Inhibits Env incorporation and/or fusion	Nef (HIV-1)	[255-257]
	Ch25h	HIV-1, HSV-1	CD4 T cells, DCs and macrophages	Produces 25-hydroxycholesterol to prevent membrane fusion	UL41 (HSV-1)	[258-260]
	Visfatin	HIV-1	Macrophages	Reduces HIV binding	ND	[260]
	PKC-delta	HIV-1, HSV-1	CD4 T cells, Macrophages	Cellular cofactor for entry	ND	[261]
	NONO	HIV-1	DCs, Macrophages	Binds cGAS and the CA to facilitate innate sensing	ND	[262]
Capsid transport to the nucleus and viral genome delivery	APOBEC3	HIV-1, HSV-1	CD4 T cells, DCs and macrophages	Interferes with reverse transcription processivity and causes lethal hypermutations during cDNA synthesis through cytidine deamination	Vif (HIV-1), VP16, ICP0 (HSV-1)	[262-265]
	SAMHD1	HIV-1, HSV-1	CD4 T cells, DCs and macrophages	Hydrolyzes cellular dNTPs	SAMHD1 phosphorylation by CDK2	[266-269]
	P21	HIV-1	CD4 T cells, macrophages	Suppresses RNR2 expression and phosphorylation of SAMHD1, and inactivates HIV-1 Integrase	USP18	[270, 271]
	TRIM5a	HIV-1, HSV-1	CD4 T cells, DCs and macrophages	Interferes with cDNA synthesis by binding and fragmentize the capsid	ND	[200, 201]
	MX1	HSV-1	Fibroblasts, DCs	limits genome replication and viral CA transport	ND	[272]
	MX2	HIV-1, HSV-1	CD4 T cells, macrophages	Reduces viral cDNA nuclear abundance by inhibiting uncoating, nuclear import, and/or PIC integrity	ND	[273-276]
	TRIM28	HIV-1	CD4 T cells, macrophages	Induces deacetylation of integrase	ND	[277]
	MOV10	HIV-1	CD4 T cells, PBMCs	Interacts with HIV-1 nucleocapsid and is packaged into virions, reduced proteolytic processing of HIV-1 Gag	ND	[278]
	PAF1c	HIV-1	CD4 T cells, macrophages	Interacts with RNA polymerase II	ND	[279]
	Hili	HIV-1	CD4 T cells	Binds to tRNA	ND	[280]
	ADAR	HIV-1	CD4 T cells	Upregulate gag expression and viral production	ND	[281]

Step	Restriction factors	Viruses	Target cell	Restriction mechanism	Counteraction by virus	Ref
Viral replication and transcription	G3BP1	HIV-1	CD4 T cells, macrophages	Binds cytosolic RNA transcripts thus preventing translation or packaging	ND	[282]
	Tetraspanin	HIV-1, HSV-1	CD4 T cells, DCs and macrophages	Incorporates into HIV-1 virions and inhibit budding	Vpu (HIV-1)	[283]
	TRIM22	HIV-1	CD4 T cells, macrophages	Interferes with the LTR's transcriptional activation by Sp1	ND	[284-286]
Viral protein synthesis and assembly	ZAP	HIV-1, HSV-1	CD4 T cells, macrophages	Degrades multiply spliced viral mRNAs	UL41 (HSV-1)	[287, 288]
	EIF2AK2	HIV-1, HSV-1	CD4 T cells, macrophages	Blocks translation by phosphorylating eIF2α	Tat (HIV-1) ICP34.5, US11 (HSV-1)	[210, 289, 290]
	SLFN11	HIV-1	CD4 T cells, DCs and macrophages	Inhibits the synthesis of viral proteins in a codon-usage-specific manner	ND	[291, 292]
	IFITM	HIV-1	CD4 T cells	Inhibits HIV-1 protein synthesis	Nef (HIV-1)	[171]
	OAS-1/RNaseL	HIV-1, HSV-1	Monocytes, macrophages	2-5A is produced by OAS1 to activate RNaseL, causing viral mRNA to be cleaved.	ICP0, US11 (HSV-1)	[235, 236, 293]
	HERC5	HIV-1	Macrophages	Increases ISGylation of Gag to inhibit assembly	ND	[294]
	CNP	HIV-1	Macrophages	Inhibits particle assembly by binding Gag	ND	[295]
	GBP5	HIV-1	CD4 T cells, macrophages	Inhibits Env maturation and incorporation, which reduces the infectivity of progeny virions	ND	[296, 297]
	MARCH2/8	HIV-1	DCs, macrophages	Env is downregulated from the cell surface	ND	[173, 298]
	90K	HIV-1	CD4 T cells, macrophages	Reduces the amount of mature gp120 and gp41 that is incorporated into progeny virions	ND	[299]
Viral egress and budding	Tetherin	HIV-1, HSV-1	Macrophages	Tethers budding virions to the plasma membrane	Vpu (HIV-1) gM, gD, UL41 (HSV-1)	[300-302]
	Viperin	HIV-1, HSV-1	Macrophages	Inhibits isoprenoid biosynthesis to prevents HIV-1 virus budding	UL41(HSV-1)	[303] [156]
	BCA2/Rabring7	HIV-1	CD4 T cells, macrophages	Co-factor of Tetherin	Vpu (HIV-1)	[304]
	ISG15	HIV-1, HSV-1	CD4 T cells, macrophages and neurons	Induce proteins post-translational modifications and inhibits assembly and release	ICP27 (HSV-1)	[305-307]

ND: not determined

1.2.3 The role of MX2 and SAMHD1 in viral restriction

A

B
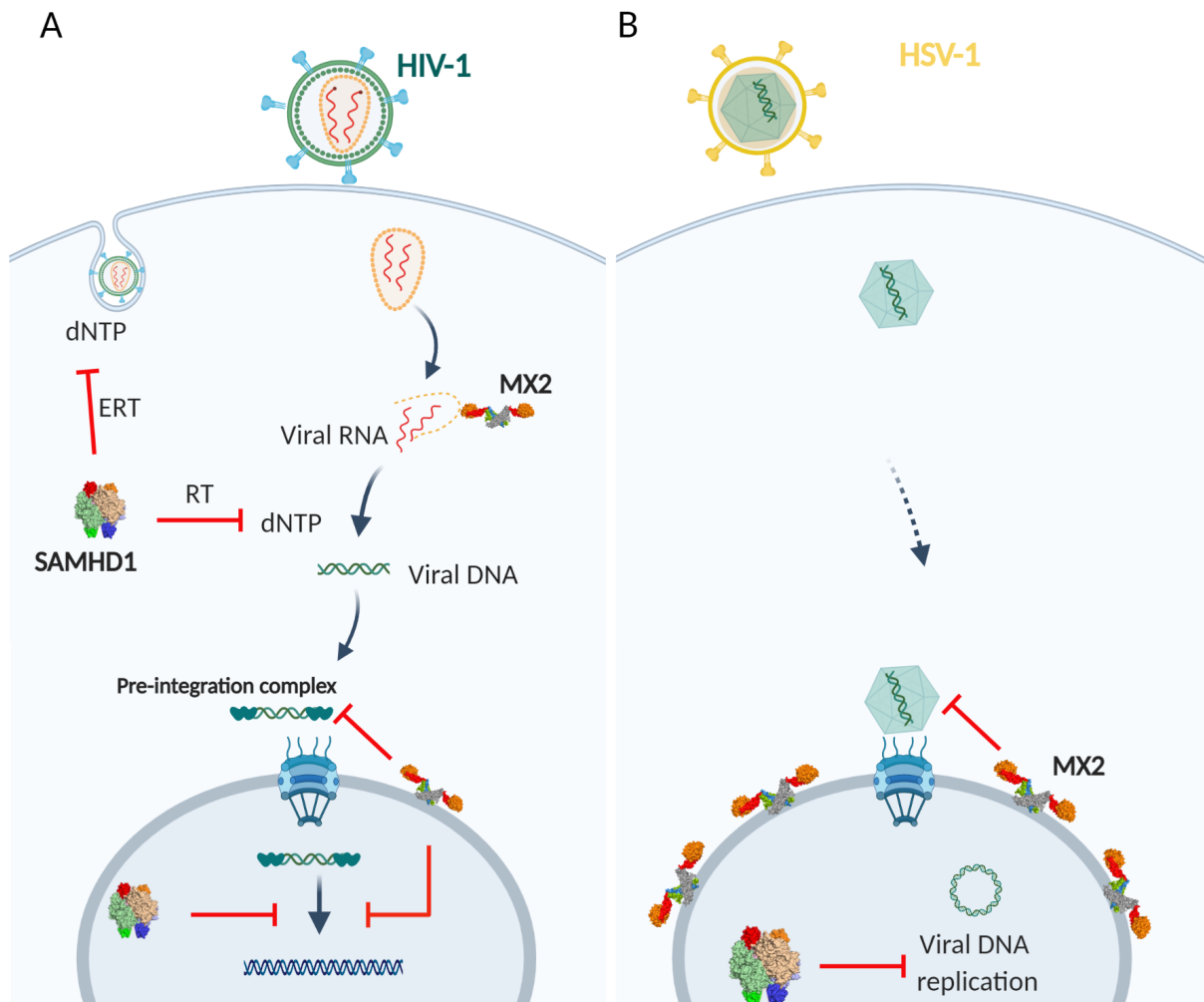
Figure 5: MX2 and SAMHD1 inhibit post entry steps of the replication cycles of HIV-1 and HSV-1
(A) MX2 restricts HIV-1 PIC nuclear import and proviral DNA integration. SAMHD1 blocks HIV-1 RT, endogenous reverse transcription (ERT), and proviral DNA incorporation by limiting the amount of intracellular dNTPs. (B) MX2 inhibits nuclear delivery of HSV-1 dsDNA. SAMHD1 cleaves dNTPs, which are necessary for HSV-1 DNA genome amplification. Figure modified from [308, 309].

Nearly a thousand candidate host factors that limit viral infection have been identified through large-scale RNA interference (RNAi)-based screens. MX2 together with SAMHD1 are found to show potent activities against HSV-1 in regards to anti-HIV-1 activity.

1.2.3.1 MX2: a potent HIV-1 and HSV-1 post-entry inhibitor induced by IFN

The MX proteins, MX1 and MX2 (also known as MXA and MXB), are dynamin-like large guanosine triphosphatases (GTPases) which are IFN-inducible in human cells [310], yet are important for two global-scale infectious diseases, influenza and AIDS [273]. Both proteins fold into similar structures, with an oligomerization stalk and a

GTPase activity domain [311]. Despite the similarity in architecture, the orientation of individual domains differs between MX1 and MX2 [312]. However, the formation of oligomers is indispensable for both MX1 and MX2 to restrict their target viruses [313, 314]. MX2 has two isoforms, the long one of which contains a nuclear localization signal (NLS) and preferentially localizes to the cytoplasmic face of nuclear pores, while the short form is found in the cytoplasm [315]. MX2 was previously thought to regulate nucleocytoplasmic transport and the cell cycle but to be antiviral inactive [316]. Recently, it was identified as being involved in the HIV-1 replication cycle wherein its ectopic overexpression potently reduce while knockdown rescue HIV-1 permissiveness [273]. MX2 suppresses HIV-1 and, to a lesser extent, HIV-2, as well as SIV, but not other retroviruses like feline immunodeficiency virus or murine leukemia virus [276]. The expression of MX2 prevented infection of both primary HIV-1 strains and pseudotyped vesicular stomatitis virus glycoprotein (VSV-G) reporter viruses, implying that MX2 inhibition occurred after HIV-1 entry. Further experiments revealed that MX2 can reduce viral PIC accumulation by lowering viral two-long terminal repeat (2-LTR) circle levels and the distribution of DNA integration sites in the nucleus [317]. The mechanism, which most likely occurs near the host cell nucleus and involves the viral CA [275]. Mutagenesis studies and viral escape assays indicate that MX2's viral target is the HIV-1 CA. MX2 attaches to the HIV-1 core inhibiting the uncoating process, which NLS sequence was involved in the CA recognition [273, 318]. However, MX2's binding to HIV-1 CA is insufficient for antiviral activity. A variety of CA mutants known to interact with cellular CypA allow partial escape from MX2 restriction, suggesting MX2's indirect effects in restricting HIV-1 [319]. CypA is a host factor that guides viral CA to nucleoporins (Nups) and facilitates PIC nuclear import [320]. CypA silencing increases HIV-1 resistance to MX2, implying that CypA and HIV-1 CA binding are required for MX2 restriction. Furthermore, MX2's anti-HIV activity appears to be dependent on Nups, as Nups levels can affect MX2's binding to the HIV-1 CA [321]. Unlike MX1 which is GTP-binding and GTP-hydrolysis dependent for antiviral activity, MX2 mutants lacking GTP binding or hydrolysis still have anti-HIV-1 activity, which suggests that MX2 GTPase activity is not involved in HIV-1 restriction [273, 276]. MX2 uses an NLS-like sequence to target the HIV-1 CA core, whereas MX1 identifies viral nucleoproteins with its unstructured loop 4 [322, 323]. It has been proposed that the short MX2 isoform which lacks antiviral activity can interact with CA, thereby modulating the antiviral function of the long MX2 isoform [324]. Thus, MX2 and MX1

appear to employ distinct mechanisms to restrict virus replication with regard to GTP hydrolysis.

In addition to HIV-1, MX2 has also been shown to be a novel IFN-induced restriction factor that prevents HSV-1 lytic infection [325]. IFN-treated cells become vulnerable to HSV-1 if MX2 is silenced. Correspondingly, the early replication of HSV-1 dramatically reduced when MX2 is overexpressed [274]. MX2 interferes with HSV-1 from entering the nucleus after tegument dissociation but no interactions with HSV-1 CA proteins have been demonstrated so far [274, 309]. Early research found that only the full-length form of MX2 has full anti-HSV activity, a feature shared in the inhibition of HIV-1 [318]. Inactivation of MX2's triple-arginine motif at positions R11-13A still restricts HSV-1 but not HIV-1, indicating that the N-terminal determines antiviral specificity [323]. Moreover, MX2 mutants lacking oligomerization or GTPase function lost anti-HSV-1 activity, indicating that proper GTP hydrolysis is essential [325]. MX2 blocks initial HSV-1 genome synthesis, however HSV-1 can conquer MX2 during replication, probably indicating the presence of a bona fide viral MX2 antagonist. Although lentiviruses and herpesviruses are evolutionarily unrelated, they share nuclear entry mechanisms, at least in terms of using nuclear pore complexes (NPCs) as a portal into the nucleus [326]. Both HIV-1 and HSV-1 are blocked at or before the uncoating of viral genomes at an early post-entry stage. Recognizing and affecting the stability of viral CA to the nuclear entry pore appears to be a common feature (Figure 5). MX2 binds to the HIV-1 CA affecting the its interaction with Nups. However, a number of HIV-1 CA mutants allow them to avoid MX2 restriction [325]. Although MX2 inhibits HSV-1 DNA delivery to the nucleus, it's unclear whether MX2 targets HSV-1 CA or Nups and no MX2 escape mutations have yet to be discovered [327, 328]. Both NLS and oligomerization are required for antiviral activity [325, 329]. Additionally, the anti-HSV but not anti-HIV effects are dependent on both GTP binding and hydrolysis which is reminiscent of MX1 [329]. Taken together, the exact mechanism by which MX2 suppresses HIV-1 and HSV-1 is unspecified.

1.2.3.2 SAMHD1 restricts HIV-1 and HSV-1 by limiting dNTPs pool

SAMHD1 is a 65-kDa GTP-dependent deoxynucleotide (dNTP) triphosphohydrolase containing an N-terminal NLS, a sterile alpha motif, a catalytic histidine-aspartate domain essential for dNTPase function, followed by a C-terminal phosphorylation site

of T592 and subsequent Vpx-binding site [330, 331]. SAMHD1 was initially discovered to be the human homolog of Mus musculus MG11, an IFN-γ induced GTP-binding protein earlier described [332]. SAMHD1 is able to bind and hydrolyze dNTPs when it is tetramerized [333-335]. As a NLS-containing protein, SAMHD1 is partially cytosolic and predominantly nuclear [336]. SAMHD1 expression levels vary by cell cycle and cell type, IFNs downregulate miR-181 and miR-30a in monocytes, microglia, and astrocytes, triggering SAMHD1 expression [337, 338]. SAMHD1 is abundantly expressed in resting CD4-positive T cells, nondividing DCs and macrophages, regardless of IFN treatment [266]. Furthermore, SAMHD1 gene expression is also governed by promoter methylation [339, 340].

SAMHD1, in collaboration with cellular ribonucleotide reductase (RNR) and thymidine kinase (TK), can serve as a vital controller of intracellular dNTP homeostasis due to its dNTPase activity [341]. In the G1-like phase, CDK-mediated phosphorylation at amino acid T592 is thought to affect SAMHD1 activity, and T592 phosphorylation impairs SAMHD1 tetramerization, resulting in decreased dNTP hydrolysis capacity [269, 342]. Thus, SAMHD1 can facilitate (e.g. dividing T cells) or impede (e.g. nondividing macrophages) viral replication depending on its level and state [343, 344]. In cycling CD4-positive T cells which SAMHD1 is phosphorylated, HIV-1 is efficient in infecting dividing cells [332, 345]. Only under its dephosphorylated state in non-cycling cells, e.g. macrophages, SAMHD1-mediated low dNTP pools effect HIV-1 cDNA synthesis and delay DNA integration [346, 347]. Interestingly, in cultured primary macrophages there is a spontaneous G1-like state in which SAMHD1 is temporarily inactive, allowing HIV-1 to circumvent restriction [348]. Furthermore, dephosphorylated SAMHD1 induced by host DNA damage during viral integration appears to block HIV-1 2-LTR and provirus formation [349]. In addition to T592 phosphorylation, arrest-defective protein 1 can acetylate SAMHD1, resulting in increased dNTPase activity [350]. However, since the phosphomimetic SAMHD1 mutants loss HIV-1 restriction yet are effective in depleting dNTPs, an additional dNTPase-independent mechanism has been proposed [351-353]. In addition to its dNTP hydrolase function, SAMHD1 possesses RNA and DNA binding capability and exhibits RNase activity towards single ssRNA *in vitro* [354-356]. However, this putative RNase activity may be attributed to contamination during enzyme purification [357]. SAMHD1 phosphorylation has been shown to inhibit RNase activity while having no effect on dNTPase activity, thus

resulting in a loss of anti-HIV-1 function [269]. Although the histidine-aspartate domain is responsible for SAMHD1's dNTPase and RNase activities, SAMHD1's RNase activity does not require tetramerization [354]. SAMHD1 is thought to function in a dGTP-dependent manner, it tetramers into an active dNTPase enzyme at high dGTP levels and exists as monomers or dimers with only active RNase activity at low dGTP levels [358].

HIV-1 replication can be boosted in resting CD4-positive T cells, DCs and macrophages by infecting the cells with extracellular dNTPs, Vpx-containing virions or virus-like particles (Vpx-VLPs) of HIV-2 and certain SIV strains (SIVsm/SIVmac) [336, 359]. dNTP precursors, i.e. deoxynucleosides (dN), which are converted via the salvage pathway to replenish the intracellular dNTP pool. Vpx proteins recruit the CUL4A-DCAF1 E3 ubiquitin ligase complex by binding to the SAMHD1 C-terminus via the (NLS)-like sequence [360]. SAMHD1 cytoplasmic NLS variant is resistant to Vpx-mediated degradation and potently block lentiviral infection [361, 362]. SAMHD1 deficiency causes a significant increase in dNTP levels, allowing for a rapid HIV RT process [363]. Even though the antiviral state has been fully established, delivery of Vpx-VLPs enables a complete rescue of HIV-1 infection in DCs [364]. SAMHD1 has been shown to prevent IFN induction and to constrain consequent innate and adaptive immune responses in myeloid cells [204]. In contrast, SAMHD1 deficiency is thought to result in an accumulation of nucleic acids derived from prematurely terminated RT products, which triggers cGAS to inhibit HIV-1 [365, 366]. HIV-1 encodes Vpr instead of Vpx and is unable to counteract SAMHD1, thus avoiding an immune response [172]. Vpr has also been demonstrated to dysregulate the TANK-binding kinase, which prevents activation of IRF3 in DCs [185]. During early stages of infection, HIV-1 is thought to prevent innate sensing via cGAS-STING or IFI16 pathway through lower viral replication in the presence of SAMHD1 in macrophages [237, 367]. SAMHD1-mediated suppression of HIV-1 gene expression has a negative impact on HIV-1 latency reactivation, implying a new role for SAMHD1 in HIV-1 latency regulation [368].

Recent research suggests that SAMHD1 suppresses inflammation by interfering with immune signaling and DNA damage repair pathways [369]. SAMHD1 interferes with IRF7 thereby negatively regulating IFN-I production [370]. SAMHD1 may also function as a ssRNA-binding protein that inhibits RIG-I/MDA5 or TLRs mediated immune

responses, but this activity has yet to be confirmed due to contradictory nuclease activity [357, 371]. Therefore, SAMHD1 acting as a suppressor of intercellular antiviral responses, analogous to TREX1, may be advantageous in HIV-1 latency [191, 370]. Given SAMHD1's role in HIV-1 infection, its catalytic activity indicates that dNTP depletion may have an impact on DNA virus replication since intracellular dNTPs are most often required [267, 372, 373]. SAMHD1 appears to be sufficient in inhibiting HSV-1 replication by depleting dNTPs in resting myeloid cells and infection can be partially overcome by exogenous dN and Vpx [267]. Unlike HIV-1, HSV-1 restriction is unaffected by SAMHD1 phosphorylation status and sterile alpha motif domain deletion [374]. Furthermore, SAMHD1 can reduce the size of the dNTP pool even though HSV-1 has an excess of dNTP biosynthesis machinery (e.g. TK, RNR), implying that the antiviral mechanisms are not identical [267].

Taken together, as a multifunctional protein, SAMHD1 links cell-cycle progression, virus replication and innate immune responses. SAMHD1 lowers intracellular dNTP levels to a point where viral DNA synthesis is prevented. Interestingly, no HIV-1 or HSV-1 countermeasure has yet been described for restriction of MX2 or SAMHD1. Although SAMHD1 restriction may become deficient in non-dividing cells that did not co-express MX2 [375], SAMHD1 is unlikely to interact directly with MX2. MX2 interacts with HIV-1 core and inhibits uncoating while having no effect on SAMHD1's cellular localization, dNTPase activity, or phosphorylation state, implying that MX2 is merely a co-factor. However, due to the lack of a MX2 or SAMHD1-deficient primary cell model, it is still unknown how they function *in vivo*. The aim of this study was to see if MX2 and SAMHD1 affect HIV-1 and HSV-1 replication in primary macrophages.

1.3 Macrophage models for viral infection

1.3.1 Commonly used macrophage cell line in viral infection

Macrophages play an important role in innate and adaptive immunity by expressing a variety of PRRs and participating in the initiation and regulation of these responses. Since macrophage phenotypes are tissue-specific and diverse, a macrophage model with relevance for investigation of viral infection is necessary [376]. Explants of human tissue have been used to study macrophages from the lung, tonsils, urethra, foreskin and cervix adipose tissue [73, 377-380]. Although these tissues contain mature macrophages, their isolation and recovery from the infected tissue without inducing adherence-mediated activation and differentiation is difficult. One option would be generating macrophage cell lines with the benefit of unlimited expansion, easy to synchronize and genetically manipulated. THP-1, U937 and HL-60 are among the myeloid cell lines that can be differentiated into a macrophage-like morphology [111]. Their chronically infected derivatives, such as U1 and OM-10, have broadened the macrophage platform [381-383]. HSV-1 infection has been studied primarily in macrophage cell lines such as murine J774A.1, RAW264.7 [384]. Although these experimental systems allowed rapid progress towards macrophage's role against viral infection, the information obtained was misleading. Widely used models, for example, THP-1 hardly resemble the immunobiology of human primary myeloid cells. It was found that monocytic cell lines are heterogeneous with regards to expression of the HIV-1 entry receptors, their phenotype are unstable and their anti-HIV-1 activity is varied [385, 386]. HSV-1 proliferation and macrophage phenotypes are different between the RAW 264.7 and J774.1. Another issue with these cell lines is their multi-faceted species differences which lead to variances in pathogenic outcome. For example, the MX2 orthologue was lost during rodent evolution, and the MX2 gene of modern mice and rats actually codes for an MX1-like GTPase that is from an ancient MX1 gene duplication [387]. More importantly, the defects in IFN responsiveness were observed [388]. Several signalling pathways that are active in primary immune cells are either partially or completely absent in these cell lines (e.g., U937 cells) [389]. For example, IFN-induced MX2 expression did not alter HIV-1 infectivity in Jurkat T cells. It has been reported that U937 cells express MX2, but this expression has only limited impact on HIV-1 infection. Some host factors, such as CPSF6, are necessary for HIV-1 replication in primary macrophages but not required in cell lines [182]. Although transgenic mouse models may be useful, some of these critical issues will not be

resolved currently by low cost and less time-consuming procedures. To fully understand the host response to virus infection, research using an infection model of a clinically relevant pathogen and cell-type is essential. We therefore characterized monocytic cell line BLaER1 as well as primary macrophages in the context of viral infections. The two models collaborating together are likely to highlight complementary aspects of virus replication in macrophages.

1.3.2 Modeling macrophages with the *trans*-differentiated BLaER1 cell line

The majority of innate immune sensing and signaling pathways have traditionally been studied using monocytic cell line-derived macrophages. Here, we sought to establish more relevant macrophage models to overcome this limitation. By heterologous expression of C/EBPα, human B cells can be *trans*-differentiated into post-mitotic monocytes and acquire myeloid properties, allowing viral infection and intracellular replication [390, 391]. The BLaER1 cell line is an estradiol-inducible B-cell leukemia that has been artificially created to express C/EBPα fused with the estrogen receptor hormone binding domain [392]. *Trans*-differentiation can be initiated by β-estradiol mediated C/EBPα translocating and driven by IL-3 and M-CSF [393, 394]. *Trans*-differentiated BLaER1 cells resemble primary macrophages in terms of transcriptome and immune response sensitivity [393]. So far, *trans*-differentiated BLaER1 cells have helped to identify TLR4's role in activating NLRP3 inflammasome in BLaER1 cells and primary macrophages but not in THP-1 cells or murine macrophages [389]. TLR8 recognizes specific RNA products and activates the NLRP3 inflammasome in response to arch aeons [395, 396]. In the field of viral infection, it was recently demonstrated that USP18 mediated downregulation of p21 enhances HIV-1 replication in BLaER1 cells [397]. Moreover, BLaER1 cells are competent for cGAS→ STING-mediated sensing of HIV-1 cytoplasmic [398]. Thus, BLaER1 is a promising macrophage model for characterizing the host-virus interaction that could not have been uncovered in commonly used human macrophage cell line systems.

1.3.3 Generating CRISPR/Cas9-targeted genetic ablation in monocyte-derived macrophages

Macrophages typically are tissue-resident cells of the innate immune system that have different origins: yolk sac-progenitors, fetal liver-derived monocytes and infiltrating

blood monocyte-derived cells [399, 400]. Monocytes are widely distributed in the bloodstream, they continuously differentiate from bone marrow precursors to macrophages in tissue and microglia in the nervous system. Primary human monocyte-derived macrophages (MDMs) from peripheral blood, which resemble tissue macrophages, are vulnerable to HIV-1 infection *in vitro* and the viral replication kinetics are comparable in tissue macrophages [401, 402]. MDMs may be more responsive to stimuli since aberrantly active NF-κB has been reported in transformed cell lines [403]. For these reasons, MDMs are more likely to accurately reflect *in vivo* HIV-1 infection of macrophages. Attempts have been made in the past to render monocytes genetically tractable. One approach is to edit fully differentiated macrophages by RNAi. RNAi is a eukaryotic cell technique based on a system that exists in mammalian cells to degrade mRNA and thus prevent translation [404]. The ability of harnessing the RNAi pathway to silence virtually any gene in any organism, either by delivering synthetic small interfering RNA (siRNA) or vectors expressing short hairpin RNA (shRNA) into cells, holds great potential [405]. Editing hematopoietic stem cells (HSCT) and differentiating them into macrophages is yet another alternative, although it is challenging and consuming [406].

Primary monocyte genetic modification is an appealing strategy for producing gene-modified macrophages and has yielded promising results. Despite technical challenges, several studies have actually modified CCR5 in primary CD4-positive T cells using zinc-finger nucleases (ZFNs) and transcription activator-like effector nucleases (TALENs) [407, 408]. However, both ZFNs and TALENs have had potential drawbacks and limitations [409]. More recently, the CRISPR/Cas system has become a very popular endonuclease due to its superior simplicity. The CRISPR/Cas system does not require de novo protein engineering for each genomic target, making it more efficient in a range of cell types [410, 411]. CRISPR/Cas was first discovered in bacteria and archaea, and it has since been implemented to antiviral research [412]. This system has two components: a short guide RNA (sgRNA) and an endonuclease. Instead of the protein-DNA interactions required by ZFNs and TALENs, the CRISPR/Cas system relies on sgRNA to target gene base-pairing [413]. Depending on the endonuclease sequence and structure, the CRISPR/Cas system is generally divided into three categories: type I, II and III [414]. The most common CRISPR/Cas system is a type II that was developed from Streptococcus pyogenes (spCas9) and

can be targeted towards any 5-NGG target gene sequence to create a precise double strand break (DSB) [411, 415]. The DSB is then repaired via cellular DNA repair mechanisms such as the non-homologous end joining (NHEJ) and homology directed repair (HDR) in eukaryotes. Since NHEJ is more efficient and error prone than HR, it may produce deletions and insertions (indels) or substitution. If these indels are placed inside an exon, frameshift mutations are thus introduced [416, 417]. Previously efforts utilize CRISPR/Cas9 for gene editing relied on sgRNA and Cas9 expression constructs being transfected [418]. Despite the success of genetic manipulation in HSCT and primary T cells, transfection's application has been limited due to MDMs' *in vitro* inability of proliferation and genes expression. Recent studies have shown that nucleofection of Cas9 ribonucleoproteins (RNPs), the complexes of recombinant Cas9 and synthetic sgRNA, has high targeting efficiencies and low toxicity [419]. CRISPR-mediated knockout monocytes may represent a promising strategy to complement genetically altered BLaER1 cells. Thus, a number of the key targets screened by performing large scale knockouts (KO) in BLaER1 cell studies can be subsequently validated in CRISPR-mediated knockout MDMs.

1.3.4 Hypotheses and Aims

To elucidate cell type-specific host responses to pathogenic viruses, including HIV-1 and HSV-1, experimental model systems that allow screening approaches, genetic manipulation and are that physiologically relevant, we hypothesized that complementary cell systems resembling macrophage biology could be developed and experimentally exploited.

In this thesis we examined two model systems to address this need and perform experimental validations:

A) BLaER1 cells

(i)   Do human BLaER1 cells, that can be *trans*-differentiated into macrophage-like cells, resemble key aspects of primary macrophage biology?

(ii)   Which phenotype do the established viral restriction factors SAMHD1 and MX2 display in this cell model in the context of HIV-1 or HSV-1 infection?

(iii)   Can gene knockouts at a larger scale be readily accomplished in BLaER1 cells and used for an educated screening of cellular factors regulating virus susceptibility?

B) Primary monocyte-derived macrophages

(i)   Can efficient gene knockouts be established in primary human macrophages based on the CRISPR/Cas9 technology, while preserving cells' basic physiology?

(ii) What is the impact of SAMHD1 or MX2 knockouts on HIV-1 and HSV-1 infection?

(iii) How does this model system and *trans*-differentiated BLaER1 cells compared?

2. Material and methods

2.1 Materials

2.1.1 Chemicals and Kits

Chemical	Vendor	Chemical	Vendor
Ammonium sulfate	Sigma-Aldrich #A4418-500G	Nucleobond Xtra Midi plasmid DNA purification	Macherey-Nagel #740410.100
Agarose	Carl Roth #3810.3	NuPAGE™ LDS-Sample Buffer (4×)	Thermo Fisher Scientific #NP0007
Accutase® solution	Sigma-Aldrich #A6964-100ML	Opti-MEM™ I Reduced Serum Medium	Thermo Fisher Scientific #31985070
Albumin Fraction V (BSA)	Carl Roth #8076.3	Pancoll human	PAN-Biotech #P04-60500
Aminobenzyl penicilline	Carl Roth #K029.4	PAN MONOCYTE ISOLATION KIT	Miltenyi Biotec #130-096-537
Bolt Bis-Tris Gel 4-12%	Thermo Fisher Scientific #NW04120BOX, #NW04127BOX	Paraformaldehyde (PFA)	Applichem #A3813.1000
β-Gal Staining	Thermo Fisher Scientific #K146501	Penicillin-Streptomycin	Thermo Fisher Scientific #15140-122
Calcium chloride	Carl Roth #A119.1	Perm/Wash Buffer	BD Biosciences #554723
Clarity Western ECL Substrate	Biorad #1705061	Phusion High Fidelity DNA Polymerase	Thermo Fisher Scientific #F530LPM
D(+)-Saccharose	Carl Roth #4621.2	Phusion HF Buffer	NEB #B0518S
DharmaFECT Transfection Reagent	Dharmacon #T-2001-03	Pierce bicinchoninic acid (BCA) protein assay kit	Thermo Fisher Scientific #23227
Dimethylsulfoxide (DMSO)	Carl Roth #4720.2	Polyethylenimine (PEI, linear)	Polysciences #23966
Dimethylformamide (DMF)	Sigma-Aldrich #227056-100ML	Potassium Ferricyanide	Sigma-Aldrich #02587-250G
DNeasy Blood & Tissue Kit	Qiagen #69506	Potassium Chloride	Carl Roth #6781.3
dNTPs (10mM)	Thermo Fisher Scientific #R0192	Prestained Protein Ladder 10 to 250 kDa	Thermo Fisher Scientific #26619
dN mix (Purines and pyrimidines)	Sigma-Aldrich #D0776-250MG; D7145-100MG; D7400-250MG; T9250-1G	Proteinase K	Thermo Fisher Scientific #EO0491
Dulbecco's Modified Eagle Medium (DMEM) high glucose, GlutaMAX™	Thermo Fisher Scientific #31966047	Protran® Nitrocellulose Membranes	Sigma-Aldrich #GE10600000
Efavirenz	Sigma-Aldrich #SML0536-10MG	P3 Primary Cell 96-well Kit (96 RCT)	Lonza #V4SP-3096
Estradiol	Sigma-Aldrich #E8875-250mg	Recombinant Human M-CSF	Peprotech #300-25-50µg
Ethylenediaminetetraacetic acid disodiumsalt-dihydrate	Chemsolute, Th. Geyer #2216.1000	Recombinant Human IL3	Peprotech #300-03-50µg

Chemical	Vendor	Chemical	Vendor
EDTA-free protease inhibitor cocktail complete, Mini	Roche #11836170001	RiboLock RNase-Inhibitor	Thermo Fisher Scientific #EO0381
FcR blocking reagent	Miltenyi Biotec #130- 059-901	ROFERON-A	Roche #SAP-10131273
Fetal bovine serum (FBS)	Sigma-Aldrich #F7524	Roswell Park Memorial Institute Medium 1640 (RPMI)	Thermo Fisher Scientific #64870-010
Glycerin	TH.Geyer #2050.1011	RNeasy Mini Kit	Qiagen #74106
GoTaq Hot Start DNA Polymerase	Qiagen #203203	Sodium dodecyl sulfate (SDS)	Carl Roth #CN30.3
Hard shell 96 well PCR plate	BioRad #HSP9601	Sodium hydroxide	Carl Roth #8655.1
High-Capacity RNA-to-cDNA Kit	Thermo Fisher Scientific #4387406	Sodium Chloride	Carl Roth 9265.2
HiPerFect Transfection Reagent	Qiagen #301704	Sodium azide	Carl Roth #4221.1
Invitrogen Novex NuPAGE MOPS SDS Running Buffer (20×)	Thermo Fisher Scientific #NP0001	Sodium chloride	Carl Roth #3957.1
Invitrogen Novex NuPAGE Transfer Buffer (20×)	Thermo Fisher Scientific #NP00061	Sodium pyruvate	Thermo Fisher Scientific #11360070
Kalium choride Hydrochloride acid (HCl, 32%)	Carl Roth #P074.3	SYBR Green Master Mix	Thermo Fisher Scientific #A25779
Live cell imaging solution	Thermo Fisher Scientific #A14291D	SuperSignal™ West Pico PLUS Chemiluminescent Substrate	Thermo Fisher scientific #34577
Lysogenic broth powder	ChemSolute #8885.0500	Stericup-HV sterile vaccum filtration system 0.45 µm; 0.22 µm	Sigma-Aldrich #S2HVU05RE; #S2GPU05RE
Magnesium chloride	Carl Roth #KK36.3	TaqMan Fast Advanced Master Mix	Applied Biosystems via Thermo Fisher Scientific #44-449-64
Mercaptoethanol	Carl Roth #4277.3		
Methanol	CHEMSOLUTE #1437.2511	TaqMan™ RNase P Control Reagents Kit	Thermo Fisher Scientific #4316844
Milk powder	Carl Roth #T145.3	Triton X-100	Serva #39795.01
MS2 RNA	Sigma #10165948001	Tris	Sigma-Aldrich #T1503-1KG
Nonidet P40	PanReac Applichem #A1694	Terrific Broth Medium	TH.Geyer #8077-500G
NucleoZOL	Macherey-Nagel #740404.200	Tween	Carl Roth #9127.1
Nuclease-Free Water	Qiagen #129114	X-Gal staining	Thermo Fisher Scientific #R0404

2.1.2 Plasmids

BLaER1 CRISPR/Cas9 plasmids

Table 2.1.2.1 CRISPR/Cas9 plasmids for electroporation

Plasmids	Constructs
gRNA	pLKO.1-gRNA-CMV-GFP
Cas9	pRZ-BFP-T2A-Cas9

Transfer vectors for Lentivirus production

Table 2.1.2.2 Proviral plasmids

Vector	Plasmids
Vpx-containing virus-like particle (Vpx)	pMD2G VSV-G-encoding plasmid, pSIV3$^+$
Lentiviral vector BFP	pCMV △8.9, pMD2G VSV-G-encoding plasmid, pCDH-EF1α-mtagBFP
HIV-1$_{NL4-3\ \Delta Env\ VSV-G\ GFP}$	pNL43-E-CMV-GFP, pVSV-G
HIV-1$_{NL4-3\ NLENG1-IRES\ GFP}$	pNLENG1-IRES-70

2.1.3 Oligonucleotides

Primer sequences were purchased from Eurofins Genomics.

Table 2.1.3.1 Primers for quantitative real-time polymerase chain reaction (qRT-PCR)

Primer name	Sequence
SG-PERT	Fw 5'-TCCTGCTCAACTTCCTGTCGAG-3'
	Rv 5'-CACAGGTCAAACCTCCTAGGAATG-3'
IFIT1	Fw 5'-GATCTCAGAGGAGCCTGGC-3'
	Rv 5'-AGACTATCCTTGACCTGATGATC-3'
CXCL10	Fw 5'-TATTCCTGCAAGCCAATTTTGTC-3'
	Rv 5'-TCTTGATGGCCTTCGATTCTG-3'
GAPDH	Fw 5'-GATCATCAGCAATGCCTCCT-3'
	Rv 5'-TGTGGTCATGAGTCCTTCCA-3'
2-LTR	Fw 5'-GTGCCCGTCTGTTGTGTGACT-3'
	Rv 5'-CTTGTCTTCTTTGGGAGTGAATTAGC-3'
2-LTR probe	(FAM)-TCCACACTGACTAAAAGGGTC TGGGGATCTCT-(TAMRA)

The siRNA oligonucleotides were purchased from Dharmacon.

Table 2.1.3.2 siRNAs for transfection

Target name	Sequence
ON-TARGETplus siRNA-CD32 (Dharmacon #L-015650-00-0005)	GGGCAGCUCUUCACCAAUG, GAAUGUAUGUCCCAGAAAC, GGUCAUUGCGACUGCUGUA, CAUUAAGUCUCCAUUGUUU
ON-TARGETplus Non-targeting Pool (Dharmacon #D-001810-10-05)	UGGUUUACAUGUCGACUAA, UGGUUUACAUGUUGUGUGA, UGGUUUACAUGUUUUCUGA, UGGUUUACAUGUUUUCCUA

The sgRNA oligonucleotides were purchased from Integrated Device Technology.

Table 2.1.3.3 sgRNAs for nucleofection

Target	sgRNA	Primers for amplifying edited loci
SAMHD1	TATTCCACTTGCTCGCCCGG	Fw 5'-ACACTCTTTCCCTACACGACGC TCTTCCGATCTCAGATGTTTTTCTTGTTCT AAGGCTGCT-3' Rv 5'-GACTGGAGTTCAGACGTGTGCT CTTCCGATCTAGACTACTGTGAGAACCAA ACAAAAGC-3'
CD32	TGGAGCACGTTGATCCACGG	Fw 5'-ACACTCTTTCCCTACACGACG CTCTTCCGATCTTTGAGGACTGACGACAG CTGC-3'
Syn CD32	GCACAGTGCTGGGATGACTA; ATTGACAGTTTTGCTGCTGC; TTTCAGACACTCCTACTGCC	Rv 5'-TGACTGGAGTTCAGACGTGTG CTCTTCCGATCTCAGGGTCCTCTCTCCTC TTTC-3'
MX2	GGCACTGTGCCGAATGGCGGTGG	Fw 5'-GGCAAAAGTGCCAACTCAGG-3'
Syn MX2	AAUUGACUUCUCCUCCGGUA; GCACUGUGCCGAAUGGCGG; GGACGCUGCUUUCCUCGCCA	Rv 5'-GGTTGGCTCCTGTTTCCTGG-3'
Syn CD46	TCGTTCACCAATCTCATAGT; TTTGTGATCGGAATCATACA; AAATGTTGGTGGCTCCTCAC	Fw 5'-GTTTATTCCCAAACAAACCA AAAGCTAATAGG-3' Rv 5'-GCCAGGAAAATGATTTCTTGGAG-3'

2.1.4 Antibodies

Table 2.1.4.1 Primary antibodies

Antibody	Clone	Vendor	Dilution
CD11b APC	Ms mAb [ICRF44]	BD Bioscience #561015	FC 1:50
CD206 BV421	Ms mAb [19.2]	BD Bioscience #566281	FC 1:50
CD86 BV421	Ms mAb [IT2.2]	BD Bioscience #305411	FC 1:50
CD79a APC	Ms mAb [HM47]	BD Bioscience #551134	FC 1:50
CD14 APC	Ms mAb [M5E2]	BD Bioscience #561708	FC 1:50
CD19 BV421	Ms mAb [HIB19]	BD Bioscience #562441	FC 1:50
CD20 BV421	Ms mAb [H1 (FB1)]	BD Bioscience #563346	FC 1:50
CD68 BV421	Ms mAb [Y1/82A]	BD Bioscience #563346	FC 1:50
CD32 PE	Ms mAb [FUN-2]	Sony Biotech #2116030	FC 1:50
CD46 BV421	Ms mAb [E4.3]	BD Bioscience #563346	FC 1:50
HLADR FITC	Ms mAb [L243]	BD Biosciences #347400	FC 1:50
MAPK	Ms mAb	Santa Cruz sc1647	WB 1:500
Vinculin	Ms mAb	Sigma-Aldrich V9264	WB 1:5000
MX1	Rb PAb	Proteintech #13750-1-AP	WB 1:1000
MX2	Rb PAb	Novus Biologicals #NBP-1-81018	WB 1:200
HIV core p24	Ms mAb [KC57-RD1]	Beckman Coulter #6604667	FC 1:100
HIV core p24	Ms PAb [MA183]	Lab-made antibodies from mouse hybridoma	WB 1:200
HSV CA ICP5	Ms mAb [3B6]	Abcam #ab6508	WB 1:500; FC 1:200
SAMHD1	Ms mAb	Eurogentec EGT986-11G6E8	WB 1:250 FC 1:200

Mouse monoclonal antibody, Ms mAb; Rabbit polyclonal antibody, Rb PAb; FC, Flow cytometry; WB, Western blot

Table 2.1.4.2 Secondary antibodies

Antibody	Clone	Vendor	Dilution
Anti-mouse-HRP	Goat mAb [ICRF44]	SeroTec #STAR7	WB 1:1000
Anti-rabbit-HRP	Goat PAb	Bethyl #A120-101P	WB 1:1000
Anti-mouse-Alexa Fluor ®647	Goat PAb [Y1/82A]	Invitrogen # A-21236	FC 1:200

Goat monoclonal antibody= Goat mAb, Goat Polyclonal antibody = Goat PAb

2.1.5 Drugs

Name	Vendor	Stock	Diluted in
β-estradiol	Sigma-Aldrich	100 mM	β-estradiol was dissolved in 100% ethanol and subsequently diluted in order to receive a 10 mM solution of 50% ethanol. The 10 mM stock was then diluted to 1 mM in water and sterile filtered (0.22 µm). The 1 mM stock was used for further serial dilutions.
dN	Sigma-Aldrich	20 mM	dN was diluted in appropriate medium and the pH was adjusted to 7.0.
M-CSF, IL-3	Peprotech	10 µg/mL	Add an appropriate volume of PBS to the lyophilized cytokine stock and mix thoroughly at room temperature. For long-term storage, the cytokine stocks should be kept at -80°C.
Efavirenz Dolutegravir	Sigma-Aldrich	10mg/ml	Drugs for HIV infection assays were dissolved in DMSO and the aliquot were stored at -20°C.
SIK0001	Oliver T. Keppler, Max Von Pettenkofer-Institute, Munich	50 mM	The SAMHD1 inhibitor was diluted in DMSO for a working solution of 25 µM (0.05% DMSO).
IFN-α (2a)	ROFERON-A	6.0×10^6 IU/mL	The stock was diluted at the indicated concentrations in cell culture medium

2.1.6 Buffers and media

2.1.6.1 Standard buffers and solutions
SG-PERT lysis buffer (2×)

Kalium chloride (KCl)	50 mM
Tris-HCl (pH 7.5)	100 mM
Glycerol	40% [v/v]
Triton X-100	1% [v/v]
RiboLock	1:100 added to lysis buffer (2×) before use

SG-PERT PCR dilution buffer (10×)

Ammonium sulfate (($NH_4)_2SO_4$)	50 mM
Kalium chloride (KCl)	200 mM
Tris-HCl (pH 8.3)	200 mM

SG-PERT PCR reaction buffer (2×)

SG-PERT PCR dilution buffer	1×
BSA	2×
SYBR Green	1×
Magnesium chloride ($MgCl_2$)	10 mM
dNTPs	400 µM
RT-Assay-primer	1 pM
MS2 RNA	8 ng

Deep sequencing PCR lysis buffer

Tris (pH 7.5)	10 mM
Proteinase K	0.2 mg/mL
Calcium chloride (CaCl$_2$)	1 mM
Magnesium chloride (MgCl$_2$)	3 mM
EDTA	1 mM
Triton X-100	1% [v/v]

RIPA lysis buffer (1×)

Tris-HCl (pH 7.5)	50 mM
Sodium chloride (NaCl)	150 mM
EDTA	0.5 mM
NP-40	1% [v/v]
SDS	1% [w/v]
Protease Inhibitor	1×

SDS sample buffer (1×)

NuPAGE LDS Sample Buffer (4×)	1×
Cell lysis	3×
β-mercaptoethanol	5% [v/v]

Running buffer (1×)

NuPAGE MOPS SDS Runnifng Buffer (20×)	50 mL
Distilled water	950 mL

Transfer buffer (1×)

NuPAGE Transfer Buffer (20×)	50 mL
Methanol	100 mL
Distilled water	850 mL

Tris Buffered Saline (TBS, 10×)

Potassium Chloride (KCl)	0.027 M
Tris-HCl	0.25 M
Adjusted pH to 7.4 with HCl	

Washing buffer TBS-T (1×)

TBS	1×
Tween	0.1% [v/v]

Blocking buffer

TBS-T	1×
Non-fat dry milk powder or BSA	5% [w/v]

Antibody dilution buffer

TBS	1×
BSA	1%
Sodium azide	0.09%
Adjusted pH to 7.2	

Flow cytometry staining buffer (1×)

PBS	1×
Inactivated FBS	1% [v/v]

| EDTA | 2 mM |

Flow cytometry Perm/Wash buffer (1×)

| Perm/Wash Buffer (10×) | 10 mL |
| Distilled water | 90 mL |

Flow cytometry fixation buffer (1×)

| PBS | 1× |
| Paraformaldehyde (PFA) | 4% [v/v] |

MACS buffer (1×)

PBS	1×
Inactivated FBS	0.5% [v/v]
EDTA	2 mM

Prepared freshly and kept cold at 4 °C

2.1.6.2 Virus preparation
PEI transfection reagent

| PEI | 250 mg |
| Distilled water | 250 mL |

Adjusted to pH 7.0 via HCl and sterile filtered, aliquoted and stored at -20°C.

Sucrose solution

| Sucrose | 25% [w/v] |
| PBS buffer | 1× |

Sterile filtered by 0.22 μm vacuum filtration system

2.1.6.3 Blue cell assay
β-gal reaction solution

PBS	1×
Potassium ferricyanide ($K_3[Fe(CN)_6]$)	3 mM
Magnesium chloride ($MgCl_2$).	1 mM

X-Gal solution

| X-Gal | 20 mg |
| Dimethylformamide (DMF) | 100 mL |

stored at -20 °C, protected from light

2.1.6.4 Media for cell culture
BLaER1 suspension culture media

RPMI-1640 without phenol red

charcoal stripped FBS	3% (v/v)
P/S	1% [v/v]
Sodium pyruvate	1% [v/v]
Glutamine	2 mM

BLaER1 *trans*-differentiation culture media

RPMI-1640

FBS	10% [v/v]
P/S	1% [v/v]
Sodium pyruvate	1 mM

Glutamine	2 mM
β-Estradiol	100 nM
M-CSF	10 ng/mL
IL-3	10 ng/mL

Primary MDMs differentiation culture media

RPMI-1640	
FBS	10% [v/v]
P/S	1% [v/v]
M-CSF	100 ng/mL

HEK 293T cell culture media

DMEM	
FBS	10% [v/v]
P/S	1% [v/v]

Freezing medium

FBS (heat-inactivated)	90% [v/v]
DMSO	10% [v/v]

2.1.6.5 Media for bacterial culture

LB-broth medium

Lysogenic broth powder	25 g
Distilled	1000 mL

After autoclaving, the media was supplemented with 50 µg/mL ampicillin

Terrific broth medium

Terrific Broth powder	50.8 g
Distilled water	900 mL
Glycerin	4 mL

Adjust pH to 7.2 and make final volume to 1000 mL. 50 µg/mL ampicillin is supplemented after autoclaving

2.1.7 Cells

Cells	Characteristics
HEK 293T cells (ATCC no.: CRL-11268)	Human cell line derived from embryonic kidney cells. The cells grow adherent with an epithelial morphology and are cultivated in complete DMEM.
BLaER1 cells (DSMZ no.: ACC 548)	BLaER1 (Veit Hornung, Gene Center Munich, Germany) stably expressing C/EBPα-ER-IRES-GFP construct was kept at 1×10^5 to 2×10^6 cells/mL in suspension culture media.
Human primary monocytes	CD14-positive cells were isolated from blood cones that were obtained from the Hospital of the University of Munich, Dept. of Immunohematology, infection screening and blood bank. The request for ethics approval for the proposed studies has been submitted.
TZM-bl (NIH AIDS reagent program)	The Hela cell-derived cell line contains HIV Tat-dependent expression cassettes for luciferase and β-galactosidase. The cells grow adherent and are cultivated in complete DMEM.

In general, cells were cultivated at 37°C, 5% CO_2, 95% humidity and were frequently tested for mycoplasma contamination

2.1.8 Machines and software

Machines

Laboratory equipment	Vendor
BD FACS Lyric	BD Biosciences
BD FACS Fortessa	BD Biosciences
BD FACS Aria III	BD Biosciences
Quantstudio 3 Real-Time PCR-system, 96-Well 0.1-mL Block	Thermo Fisher Scientific
Mini Gel Tank A25977	Thermo Fisher Scientific
Mini Blot Module B1000	Thermo Fisher Scientific
Nanodrop One	Thermo Fisher Scientific
FUSION FX - Western Blot & Chemi imaging	VILBER
Sorvall WX+ Ultracentrifuge and Rotor SW28	Beckman Coulter
Vi-Cell XR cell viability analyzer	Beckman Coulter
Eclipse Ti2 microscope with DS-Qi2 camera	Nikon
Mastercycler Vapo.protect	Eppendorf
4D-Nucleofector Core Unit and X Unit	Lonza AAF-1002B, 1002X
Gene Pulser electroporation device	Bio-Rad Laboratories
UV DNA gel imager UVP UVsolo Touch	Analyst Jena
Microplate Reader CLARIOstar Plus	MGG Labtech

Software

GraphPad Prism v6.01

Quantstudio Design & Analysis Software v1.5.1

CFX Manager Software

NIS Elements Software

FlowJo v10.6.1

All Figures were created with BioRender.com

2.2 Methods

2.2.1 Cell culture

2.2.1.1 *Trans*-differentiation of BLaER1 into macrophage-like cells

Prior to BLaER1 *trans*-differentiation, cells are grown in suspension culture media. The cell divides on average every 24 h and have a density of no more than 2×10^6 cells/mL. *Trans*-differentiation was induced by cultivating 0.5×10^5 cells in 200 µL BLaER1 *trans*-differentiation culture media in a 96-well flat bottom plate for 7 days. The 36 wells at the edge of the 96-well plate should be loaded with blank media to prevent inter-well differences from medium osmotic evaporation. In order to boost *trans*-differentiation, 1.25 mM dN were added at day 5 and incubated with cells for 24 h. dN were then removed before experiments that allowed cellular dNTPs return to normal level. The *trans*-differentiation process was evaluated utilizing flow cytometry for myeloid surface marker expression on a routine basis. After *trans*-differentiation, the cells must be treated with caution when subjecting to stimulation assay, as they may be negatively affected by the sudden change of temperature.

2.2.1.2 Primary monocytes isolation and macrophage differentiation

Blood from healthy blood donors is obtained from the Immunohematology, Infection screening and Großhadern blood bank of the LMU Klinikum München. And a request for ethics approval of the proposed studies has been approved by the ethics committee of the LMU München, Munich, Germany. Peripheral blood mononuclear cells (PBMCs) were collected by 2-step gradient centrifugation. In brief, 15 mL was overlaid with 35 mL blood (1:3 diluted in PBS). A mononuclear cell layer containing leucocytes was collected after centrifugation (700×g without brake, 40 minutes). The leucocytes were washed with PBS (350×g, 10 minutes) twice to remove residual pancoll and then the cell count was determined with a Vi-Cell XR cell viability analyzer (Beckman Coulter). Monocytes were later purified using a pan monocyte isolation Kit (Miltenyi Biotec, #130-096-537) by negative selection. Firstly, up to 1×10^7 PBMCs in 30 µL MACS buffer were incubated with 10 µL FcR-Receptor blocking reagent together with the 10 µL biotinylated antibody cocktail for 10 minutes at 4°C. Next, cells were mixed with 30 µL cold MACS buffer, 20 µL of Streptavidin conjugated micro beads were added and incubated for a further 10 minutes at 4°C. The appropriate MACS Separator and MACS Columns were chosen according to the number of labeled cells. The column was placed in the magnetic field of a suitable MACS Separator (Miltenyi Biotech) and the

column was rinsed with the appropriate amount of buffer. Labeled cells were proceeded to a magnetic separator. Flow-through containing unlabeled cells was collected, representing the enriched monocyte fraction. Cells collected without beads were incubated on ice with an additional 5 mM EDTA (Sigma) to inhibit phagocytic uptake. The monocyte fraction in this type of preparation is on average 90-95% CD14-positive by single staining. Monocytes are differentiated for 7 days with RPMI-1640 supplemented with 10% [v/v] FBS, 1% [v/v] P/S, and 100 ng/mL M-CSF. The cultures were refed with fresh medium every 2 days by adding half the volume into each well.

2.2.1.3 Cells freezing and thawing

For long-time storage, cells were cryopreserved in liquid nitrogen. Up to 5×10^6 cells were pelleted by centrifugation and suspended in 1 mL freezing medium. Cells were frozen for 24 h at -80°C with a cooling rate of 1°C per minute and afterwards transferred into liquid nitrogen. Thawing of frozen stocks was performed rapidly at 37°C in a water bath. Cells were diluted in complete medium, centrifuge at 500×g for 5 minutes, medium was removed and then suspended in an appropriate volume of fresh medium.

2.2.2 Nucleic acid methods

2.2.2.1 Plasmid large scale amplification and preparation

To amplify plasmid DNA, 50 μL freshly thawed STAB-II cells were mixed with 1 μg plasmid DNA and incubated on ice for 20 minutes. The mix was subjected to heat shock at 42°C for 2 minutes and transferred immediately on ice for 5 minutes. Plasmid-transformed STAB-II cells were cultured in 500 μL LB medium at 37°C for 0.5 h. Then cells were expanded into 300 mL TB medium containing 50 μg/mL ampicillin over night at 37°C. Plasmid DNA was isolated through NucleoBond® Xtra Midi EF (Macherey-Nagel # L0T1607/004) based on the manufacturer's instructions. Finally, plasmid DNA was dissolved in PCR-grade water as well as the concentration was quantified with a Nanodrop spectrometer (Thermo Fisher Scientific).

2.2.2.2 Cell mRNA extraction and subsequent qRT-PCR

For total cellular mRNA isolation, the NucleoSpin RNA Kit (Qiagen #74106l) was used according to the supplier's manual. The isolated RNA was then reverse transcribed to cDNA using the high capacity RNA-to-cDNA kit (Thermo Fisher Scientific #4387406)

according to manufacturer's instruction. The reverse transcription included extending at 37°C for 1 h and then inactivating reverse transcriptase at 95°C for 5 minutes.

Table 2.2.2.2.1 High capacity RNA-to-cDNA master mix components

Component	×1 reaction (µL)
2× RT buffer	10
20× RT enzyme mix	1
RNase-free H_2O	4
RNA	5
Total	20

The mRNA expression levels of CXCL10 and IFIT1 cDNA were quantified via qRT-PCR in a Quantstudio Real-Time PCR-system (Thermo Fisher Scientific) as following:

Table 2.2.2.2.2 Master mix worksheet for ISGs set

Component	×1 reaction (µL)
2× SYBR Green Mix	5
10 µM Fw and Rv primer	1
Nuclease-free H_2O	2
cDNA	2
Total	10

Transcript levels were evaluated using the corresponding Quantstudio Design & Analysis Software. To analyze ISGs mRNA expression levels, the normalizer used was GAPDH and fold modulations were calculated using the $2^{-\Delta\Delta Ct}$ method. Data is analyzed as a log or an n-fold change when comparing to control samples, as shown in the figure.

2.2.2.3 Quantitative evaluation of CRISPR genome editing

Genomic DNA was isolated from 0.5×10^5 of cells using 30 µL PCR MiSeq lysis buffer. After incubation for 10 minutes at 65°C and 15 minutes at 95°C, the very first PCR I reactions were carried out with a 1 µL lysate template.

Table 2.2.2.3.1 PCR I reaction mix, all primers are provided in section 2.1.3.1

Component	×1 reaction (µL)
5× HF Buffer	5
10 µM Fw and Rv primer	1.2
dNTPs	0.5
Nuclease-free H_2O	15.85
Phusion Polymerase	0.25
DNA	1
Total	25

Table 2.2.2.3.2 Mastercycler PCR reaction

Stage	Temperature (°C)	Time	Repeats
Pre-denaturation	95	5 min	1

Denaturation, annealing and extension	98	20 sec	18
	60	30 sec	
	72	40 sec	
Final	72	3 min	1

Of this reaction, 6 µL PCR I products were added into cycling system using barcoding.

Table 2.2.2.3.3 PCR II reaction for genotyping of genomic DNA

Component	×1 reaction (µL)
2× HF Buffer	4
Primer Bar Code	4
dNTPs	0.4
Nuclease-free H_2O	5.4
Phusion	0.2
PCR I	6
Total	20

The thermal cycling conditions were set as follows

Table 2.2.2.3.4 PCR II program

Stage	Temperature (°C)	Time	Repeats
Pre-denaturation	95	5 min	1
Denaturation, annealing and extension	98	20 sec	25
	60	30 sec	
	72	40 sec	
Final	72	3 min	1

To separate right DNA fragments, a 1.5% agarose gel was run at voltage of 80 for 40 minutes to size-separate 5 µL PCR II products. After ethidium bromide being visualized under UV light, PCR products with the right size DNA bands were pooled for deep sequencing according to the manufacturer's protocol using the MiSeq (Illumina) benchtop sequencing system. Data were obtained in FASTQ format and analyzed at the website evaluation tool OutKnocker (www.OutKnocker.org) or ICE (ice.synthego.com).

2.2.3 Protein methods

2.2.3.1 SDS-PAGE and immunoblotting

In general, cells were lysed in RIPA lysis buffer with a protease inhibitor for 30 minutes at 4°C and centrifuged at 10,000×g for 10 minutes. Protein concentration was determined based on the Pierce bicinchoninic acid protein assay. Cell lysates were

denatured in SDS sample buffer (10% [v/v] β-mercaptoethanol) for 5 minutes at 95 °C. Protein samples were stored at -20°C. To determine the expression of the proteins of interest, cell lysates were separated by SDS-PAGE using 4-12% Bolt Bis Tris gels. 20 µg of protein from total cell lysates was loaded onto a SDS-polyacrylamide gel. Electrophoresis was performed at 80 V for 20 minutes and afterwards at 100 V until the lower hinge was reached. Separated proteins were then transferred onto nitrocellulose membranes in a wet transfer process of 20 V for 60 minutes. Depending on the protein of interest, immunoblot analysis was performed (antibodies list in section 2.1.4.1). Initially, membranes were incubated in blocking buffer for 30 minutes to avoid unspecific antibody binding, followed by rinsing 3 times with TBS-T for 10 minutes and incubation with different primary antibodies at 4°C. Following an overnight incubation, the membranes were rinsed with TBS-T 3 times before being incubated with the corresponding specific antibody at room temperature for 1h. After rinsing 3 times with TBS-T for 10 minutes, the membranes were developed with the Clarity™ western ECL substrate. Detection was performed by digital imaging of chemiluminescence with the Vilber Fusion FX.

2.2.3.2 Flow cytometric staining and analysis

For flow cytometry, the macrophages were washed and detached from the dish using accutase solution. For cell surface marker staining, cells were collected into a 96-well conical bottom plate and washed with cold FACS buffer. To improve the specificity of immunofluorescent staining, cells were incubated with FcR blocking reagent for 15 minutes at room temperature. Following centrifugation at 300×g for 5 minutes, the pellets were stained with fluorophore-conjugated antibodies for 30 minutes at 4°C in 50 µL FACS staining buffer. After incubation, cells were washed with FACS buffer and fixed with 4% PFA for 10 minutes at room temperature. Then the supernatant was removed and the cells were suspended in 200 µL of FACS buffer and analyzed by flow cytometry. For detection of intracellular proteins, cells were first fixed with 4% PFA for 90 minutes and permeabilized using flow cytometry Perm/Wash buffer for 20 minutes at 4°C. Cells were washed twice and stained with the directly (fluorophore conjugated) or indirectly corresponding antibodies for 30 minutes at 4°C. For the non-conjugated primary antibodies, secondary antibody incubation was performed for another 30 minutes at 4°C in the dark accordingly. Cells were suspended in 200 µL FACS buffer and subjected to flow cytometry analysis using BD FACS Lyric and Fortessa (BD

Biosciences). The gating strategy was determined by using unstained cells as negative controls and single antibody staining as positive controls. For each cell line and condition, 10×10^3 cells were acquired and the median fluorescent intensity (MFI) of stained proteins or the percentage of positive cells were analyzed by FlowJo.

2.2.4 Microscopy and quantitative analysis of phagocytosis

Macrophages were washed to remove non-adherent cells and 50 μL of pHrodo Red *Zymosan* BioParticles (0.5 mg/mL) were layered onto MDMs at 37°C for 1 h. Cells were washed twice with warm RPMI medium and re-suspended in colorless live image buffer. The uptake of particle conjugates was visualized using the Eclipse Ti2 microscope with DS-Qi2 camera (Nikon). For the phagocytosis quantitative assay, pHrodo Red MDMs were detached and fixed using 4% PFA for 30 min at room temperature. The percent uptake of pHrodo was detected by BD FACS Fortessa (BD Biosciences).

2.2.5 CRISPR/Cas9 mediated gene editing in BLaER1

CRISPR/Cas9 technology was utilized to generate knockout gene variants in proliferating BLaER1 cells [420]. Initially, sgRNAs specific for the indicated genes were designed to target an coding exon. In a 0.4 cm cuvette, 2.5×10^6 BLaER1 cells were mixed with 5 μg U6-sgRNA and CMV-mCherry-T2A-Cas9 expression plasmids of 250 μL Opti-MEM, and the Gene Pulser (Bio-Rad Laboratories) was set at an exponential pulse at 250 V and 950 μF. After 48 h transfection, the recovered mCherry positive cells were sorted and plated under limiting dilution conditions. Cells were plated at a density of 0.8 cells per well in 96-well round-bottom plates and grown for 2-3 weeks. The grown single-cell clones were picked and duplicated, one half was used for further cell culture and the other half was genotyped via sequencing or immunoblotting. For the following experiments, only cells carrying frameshift mutations from both target alleles were considered.

2.2.6 Primary MDMs knockout generation using CRISPR/Cas9 technology

In general, freshly isolated monocytes were nucleofected with the related Cas9-gRNA RNP complex before differentiating them into macrophages (Table 2.1.3.3 lists all of the gRNA sequences in this research). All gRNA sequences were pre-designed and RNP complex was prepared in advance as previously described. The gRNAs were

annealed to complex with *Streptococcus pyogenes* Cas9 (IDT Cas9 V3) at a molarity of 2.5:1 at room temperature for 15 min in a sterile 1.5 mL tube. The RNP complex mixture was then kept on ice or frozen in aliquots at -80°C. For the nucleofection of RNPs, 2×10^6 freshly isolated monocytes per reaction were suspended in 20 µL of P3 primary nucleofection solution with supplement buffer. The harvested cells were washed and suspended in polypropylene tubes to prevent adhesion to the tubes. The 20 µL cell/P3 nucleofection solution was then added to the 5 µL Cas9-RNP complex in a sterile PCR strip and triturated to mix. The mixture was then transferred into the Lonza cassette strip and electroporated under the condition of P3, EH-100. The cassette strip was then expelled and each well was immediately provided with 100 µL of pre-warmed RPMI-1640 (without additives). After 15 minutes recovering at 37°C, the mixture in primary MDMs culture media was seeded into suitable tissue culture plate. The cells were cultured for 7 days into mature macrophages. Deep sequencing, flow cytometry, or immunoblotting were performed to determine the knockout effectiveness.

2.2.7 siRNA-mediated knockdown in primary MDMs

CD14-positive monocytes were isolated from PBMCs as described above (method 2.2.1.2) and 0.8×10^6 cells were seeded in a 24-well plate containing 0.5 mL differentiation media for 7 days. For stable transfections, cells were transfected continually on day 5 and day 7. Mature MDMs were transfected with either specific siRNAs or a non-targeting control siRNA pool. Two available transfection reagents DharmaFECT™ and HiPerFect were included in transfection optimization experiments.

Table 2.2.7.1 Amounts of siRNA and DharmaFECT™ transfection reagents

Tube 1	Tube 2
0.625 µL 20 µM siRNA + 49.375 µL Opti-MEM, mix gently	2 µL DharmaFECT + 48 µL Opti-MEM, mix gently and incubate at room temperature 5 minutes

Table 2.2.7.2 Amounts of siRNA and HiPerFect transfection reagents

Tube 1	Tube 2
0.25 µL 20 µM siRNA + 3.75 µL RPMI 1640, mix gently	11 µL HiPerFect + 110 µL RPMI-1640, mix gently

On the day of transfection, MDMs were seeded in the media without antibiotics. The lipid-siRNA complexes were prepared by mixing Tube 1 and 2 in medium and

incubated at room temperature for 30 minutes, then added to cell culture as indicated above. MDMs were treated with dropwise additions of siRNA-liposome complexes. After 6 h, the medium was replaced with fresh warm medium to avoid cytotoxicity and cells were further incubated for 48 h at 37°C. 2 days post last transfection, cells were detached by non-enzymatic cell dissociation solution Accutase and harvested for flow cytometry analysis.

2.2.8 Virus preparation

2.2.8.1 Lentivirus and virus-like particles production

For lentiviral vector production, PEI (1 µg/mL) transfection methods are described in table 2.2.8.1. In general, 24 h before transfection, 293T cells were seeded in 15 cm^2 dishes at a density of 6×10^6 cells/dish. The plasmid mixture was diluted in 2 mL DMEM (no additives) and incubated with PEI at room temperature for 45 minutes. The plasmids used are listed below.

Table 2.2.8.1 Amounts of plasmid for virus preparation

Component	×1 plate (µg)
BFP Lentiviral vector (64.17)	
DMEM (no additives)	2 mL
pCMV△8.9	7 µg
pMD2G VSV-G	8 µg
pCDH-EF1a-BFP	11 µg
PEI	10 µL
Vpx-VLP	
DMEM (no additives)	2 mL
pcDNA-Vpx SIVmac 239	16.5 µg
pMD2G VSV-G	4.5 µg
PEI	751 µL
HIV-1 NL4-3 ΔEnv VSV-G GFP	
DMEM (no additives)	2 mL
pNL43-E-CMV-GFP	15 µg
pMD2G VSV-G	5 µg
PEI	60 µL
HIV-1 NLENG1-IRES GFP (CCR5-tropic,R5)	
DMEM (no additives)	2.5 mL
NLENG1-IRES GFP	37.5 µg
PEI	112.5 µL

Cell culture supernatant was harvested two days post-transfection, passed through 0.45 µm pore size filters and concentrated by ultracentrifugation. Therefore, 28 mL supernatant was layered over 6 mL of 25% sucrose solution. Centrifuge tubes were balanced with medium solution in pre-chilled buckets (Rotor SW28, Beckman Coulter).

Virus particles were concentrated by ultracentrifugation at 28,000×g at 4°C for 2 h. After centrifugation, supernatant was discarded, viral particles were dissolved in PBS (100 µL/tube) and aliquots were stored at -80°C. For lentiviral vector, the infectivity was determined on target cells by flow cytometry. To summarize, a series of stock dilutions were incubated with cells for 48 h, and the volume producing 5-10% reporter cells were determined ideally. For HIV lentivirus, the virus titers were determined by TZM-bl blue cell assay. Briefly, 2.5 µL HIV-1 virus stock was 1:10 seriously diluted, then 100 µL of each dilution was added to TZM-bl cells ($5×10^3$ cells/well) in a 96 well flat bottom plate. 48 h after infection, cells were stained for β-galactosidase activity using X-gal. TZM-bl cells were fixed with 4% PFA (200 µL/well) at room temperature for 5 minutes. After fixation, PFA was replaced with 100 µL blue cell assay solution (10 mL β-gal solution + 100 µL x-gal solution). The plate was then incubated at 37°C for 4 h until blue cells (infected) were visible. Plaques were counted and titers were calculated based on the infectious units per mL (IU/mL) of the stock.

2.2.8.2 HSV-1 propagation

HSV-1 was kindly provided by Dr. Barbara Adler (Max Von Pettenkofer-Institute, Germany). The HSV-1 based on strain SC16 expressing CA protein VP26 fused at its C terminus to YFP was constructed. Viral titers were calculated as the number of positive centers produced by an infection rate of 5-10% reporter cells per microliter of viral stock.

2.2.9 Infection assays

2.2.9.1 Lentiviral transduction and HIV-1 infection of BLaER1 and primary MDMs

For BLaER1 infection, $5×10^4$ cells/well were seeded in 200 µL *trans*-differentiation or proliferating medium prior to adding virus. For primary MDMs, $2.5×10^5$ cells/well were seeded in 200 µL cell primary MDMs culture media. The cells were incubated with the virus at 37 °C for 48 h. Vpx-VLPs were added to adherent cells for 24 h at sufficient volume in order to degrade SAMDH1 but not cause cell cytotoxicity. Single-round infections with replication-competent HIV-1 were carried out by adding the dN, SIK0001 and Vpx-VLPs. Efavirenz (EFV) and dolutegravir (DTG), a well-characterized noncompetitive inhibitor and integrase inhibitor of HIV-1, were added during the HIV-1 infection and maintained throughout the culture. Subsequently, the cells were harvested in 300 µL Accutase 48 h post infection (p.i.). The cell suspension was

transferred into 96-well conical bottom plate and fixed with 4% PFA . Positive cells were analyzed by flow cytometry.

2.2.9.2 HSV-1 infection of BLaER1 and primary MDMs

For infection experiments using HSV-1 YFP, the BLaER1 cells and primary MDMs were plated as described above. Before infection, the medium was removed and replaced with 190 μL of the respective medium with 2% FBS. Next, virus dilutions at the indicated multiplicity of infection (MOI) were performed in medium and added at a volume of 10 μL to the target cells. After incubation at 37°C for 3 h, the cell culture medium was changed and supplemented with fresh medium containing 10% FBS. The infection levels were checked via CA ICP5 expression by flow cytometry analysis 18 h p.i. Briefly, fixed cells (4% PFA for 90 minutes) were permeabilized and stained with a primary antibody against HSV-1 ICP5 (1:200) at 4°C for 0.5 h, and the cell pellets were washed and then probed with an Alexa Fluor 647-conjugated anti-mouse antibody (1:200) at 4°C for another 0.5 h (see section 2.2.3.2). The infected cells were analyzed by flow cytometry.

2.2.9.3 Quantification of retroviral reverse transcriptase activity by SG-PERT

An estimation of RT in the viral sample was quantitatively estimated by using SG-PERT assay [421]. Theoretically, the RT enzymes derived from retroviral particles should theoretically convert the bacteriophage MS2 RNA into cDNA in a one-step reaction, with the amount of synthesized cDNA representing the level of RT activity and thus a measure of the amount of retroviral particles. Briefly, the samples were prepared by lysis with virus containing supernatant and an equal volume of lysis buffer (in section 2.1.6). After 10 minutes at room temperature, samples can be transferred outside the P3 laboratory or kept at -80°C. For quantification of HIV RT activity, a known virus stock pCHIV#528 (T107VIII from 293T) was taken as standard and diluted with 1× PCR dilution buffer as 10-fold serial dilutions (10-10^6 molecules). Also, a non-target control (NTC, supernatant of un-transfected HEK 293T cells) was used. Both standard and NTC were lysed in the same way as the samples before. During the lysis period, the pre-mixed 2× reaction buffer (supplemented with the GoTaq Hot Start DNA Polymerase) and 10 μL per well were plated in a 96-well PCR plate (BioRad). Next, 10 μL of standard, NTC and samples were added to the reaction buffer polymerase mix.

All measurements were performed in duplicates. Plates were sealed and SG-PERT analysis was performed using the C1000/CFX96 system.

Table 2.2.9.3.1 SG-PERT PCR mix

Component	×1 reaction (µL)
2× reaction buffer	10
GoTaq Hot Start DNA Polymerase	0.01
Supernatant lysis	10
Total	20

Table 2.2.9.3.2 BioRad CFX96 parameters

Stage	Temperature (°C)	Time	Repeats
RT Reaction	42	20 minutes	1
GoTaq Hot Start	95	2 minutes	1
Denaturation, Annealing, Extension and acquisition	95	5 secs	40
	60	5 secs	
	72	15 secs	
	80	7 secs	

Following the run, data was analyzed using BioRad's CFX Manager Analysis software. Starting dilution of the standard was set to 1.06×10^8 RT Units/µL and based on the titration steps, a standard curve was generated. The standard curve was used to estimate RT activity of the different samples.

2.2.9.4 Quantitation of HIV-1 2-LTR circle by qPCR

The cell genomic DNA was extracted 48 h p.i. using the DNeasy Blood and Tissue Kit (Qiagen #69506). In brief, at least 0.5×10^6 cells were collected and lysed by adding 200 µL Buffer ATL (10% Proteinase K) at 56°C for 10 minutes. The disinfected lysate was then mixed with 1 volume of 100% ethanol and transferred to a DNeasy Mini spin column, washed twice at 6000×g for 1 minute with 500 µL Buffer AW1 and AW2 respectively. The DNA extracts were eluted by 50 µL Buffer AE by centrifuge at 6000×g for 1 minute and kept at -20°C for future use. To determine 2-LTR copies, a real-time PCR system was developed from TaqMan probe-based assay. The standard method with $\log_{10}$ serial dilutions ($10-10^6$ molecules) of the 2-LTR expression plasmid pU3U5 (1 µg/µL pU3U5 diluted 1:1.92 contains 1×10^{11} copies/µL) was used. These samples were run along with known dilutions and 2-LTR copies were evaluated by a

corresponding standard curve. A negative control lacking the template was also included. NIC was added only for 2-LTR standard amplification.

Table 2.2.9.4.1 Master mix worksheet for HIV 2-LTR primer/probe set

Component	×1 reaction (µL)
2× TaqMan Universal Master Mix	12.5
10 µM 2-LTR Fw and Rv primer	1.5
10 µM 2-LTR FAM probe	1
DNA	2.5
Total	20

Host genomes were quantified utilizing genomic RNaseP to normalize viral genome counts. The RNaseP standard was prepared from uninfected cells, a serial dilution was initiated from known DNA concentration as well as 2-LTR standards. All measurements were performed in duplicates. Plates were sealed and PCR analysis was performed using the Quantstudio 3, Real-Time PCR-system.

Table 2.2.9.4.2 Master mix worksheet for RNaseP primer/probe set

Component	×1 reaction (µL)
2× TaqMan Universal Master Mix	12.5
20× RNaseP VIC probe	1.25
Nuclease-free H_2O	5.85
DNA	2.5
Total	22.5

Table 2.2.9.4.3 The qRT-PCR reaction set

Stage	Temperature (°C)	Time	Repeats
Pre-denaturation	50	2 minutes	1
Taq activation	95	10 minutes	1
Denaturation, annealing and extension	95	15 secs	40
	60	1 minute	

The data was analyzed by the relevant Quantstudio Design & Analysis Software. The numbers of copies of 2-LTR circles relative to the amount of genomic DNA were then calculated.

2.2.10 Statistical analysis

For all data analysis and visualization, mean ± SD are depicted in scatterplots and bar graphs by GraphPad Prism 6. When experimental values were normalized, the mean of free virus or mock were set to 1. Two sample unpaired t-tests were used for independent sample comparisons. If two genotypes or stimuli were to be compared, pairwise statistical analyses were performed using a two-way ANOVA ($p < 0.05$) test .

3. Results

3.1 Workflow for screening of virus restriction factors/sensors using the BLaER1 cell line
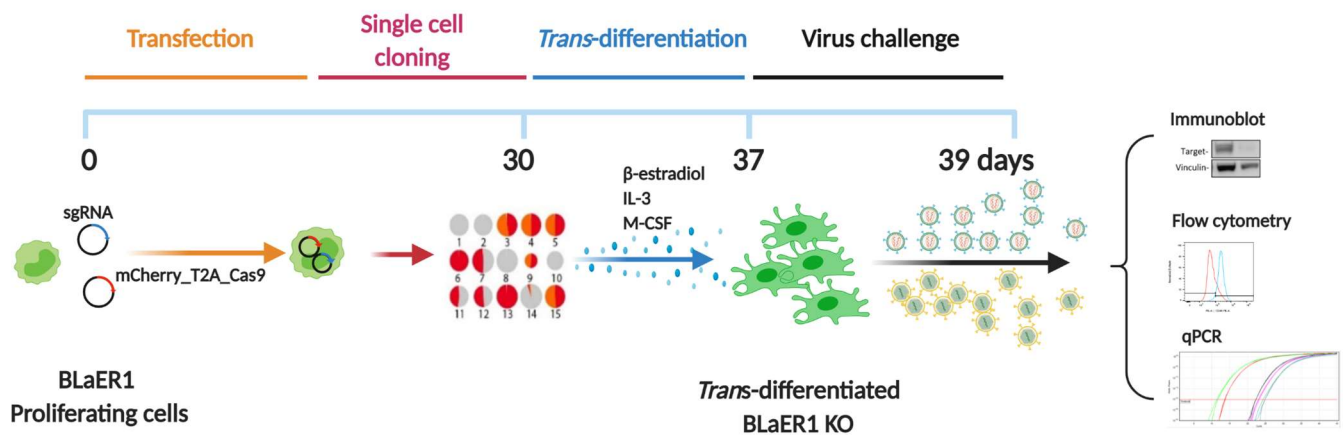

Figure 6: Graphical outline for BLaER1 cell knockout generation and setup for a restriction factor screening
Initially, proliferating BLaER1 cells were electroporated with sgRNA and Cas9 vectors to generate gene of interest deficiencies polyclones. After transfection, mCherry-positive cells are sorted and diluted into monoclone for expanding. 3-4 weeks later, the frequency of Indels mutations in various monoclones was examined, and clones with indels from both alleles were chosen for further investigation. The gene effects on restricting viral infection were studied in *trans*-differentiated BLaER1 KO cells in comparison to WT cells. Figure modified from [420].

Because of the heterogeneity and lack of efficient editing strategies in primary macrophages, we sought to develop a *trans*-differentiated macrophage-like cell model that is easily amendable to complex genetic studies. BLaER1 cells can be *trans*-differentiated and have been suggested to be used to model macrophages for fast identification of critical cellular factors [422]. To exploit this system for loss-of-function studies, a workflow was established to perform CRISPR/Cas9-mediated genome editing in their proliferative stage, and applied to viral challenge following *trans*-differentiation (Figure 6). Gene-deficient BLaER1 cells were created using an earlier described approach that enables for single-cell gene editing and corresponding sequencing [393]. BLaER1 cells were transfected with two different vectors from the CRISPR/Cas9 system to perform functional knockout screens *in vitro* by expressing sgRNAs and the Cas9 nuclease. The sgRNA successfully transfected cells were then selected for the desired genotype starting from a polyclonal cell culture via sorting. To collect monoclones with the intended gene disruption, single-cell cloning and resultant sequencing of the genetic locus were performed. To this end, cells were plated in round-bottom 96-well plate at a density of 0.8 cell/well and cultured for 2-3 weeks. The genetic knockout verification of individual sub-cloned monoclonal was then carried out

by a streamlined workflow to analyse deep sequencing via the evaluation tool OutKnocker (Method section 2.2.2.3) [420]. And though deep sequencing is usually applied to assess knockout efficiency, flow cytometry or western blotting are also used to further examine the cell membrane or cellular cytoplasmic targets. This workflow eliminated the need to subclone PCR products for single alleles sequencing, allowing multiple clones to be analyzed simultaneously. To learn more about the antiviral activity of MX2 and SAMHD1 of this macrophage model, we generated a series of MX2 or SAMHD1 KO monoclones in which both genetic loci were disrupted. It was speculated that these genes, whose editing alters the infection rate considerably, might be candidate host factors that require more mechanistic investigation.

The CRISPR/Cas9 system was used to transiently transfect BLaER1 cells using a guide RNA that targeted exon 2 of MX2 and exon 6 of SAMHD1, respectively. By sequencing genomic DNA from single-cell clones, the integrity of exons was determined. We looked at 34 clones for MX2 and 96 clones for SAMHD1 genome editing in total (Figure 7.). At least one edited allele was found in 19 out of 34 MX2 clones and 90 out of 96 SAMHD1 clones. Two distinct edited regions of nearly similar frequency which can be viewed as two edited alleles were found in the majority of clones (Figure 7. A, e.g., clones B3, C6, C10. Figure 7. B, e.g., clones A2, A3, A5). However, clones that include only one specific mutation and cannot be distinguished by sequencing have also been detected (Figure 7. A, e.g., clone C4. Figure 7. B, e.g., clones C1, C7, C10). This could be attributable to a certain indels mutation over all alleles or the clone having lost another allele. If Cas9-mediated genetic modification was active during clone replication, various edited sequences were most likely derived from other clones expanding (Figure 7. A, e.g., clone B11. Figure 7. B, e.g., C5, F3). All-allelic frameshift mutations without WT reads were found in 4 of 34 (MX2) and 26 of 96 (SAMHD1) clones, indicating functional KO clones (represented by pie charts in red color). Overall, this cost-effective methodology produces stable knockout phenotypes while allowing redundant pathways to be turned off at the same time, which implies a wider range of high-throughput screening options than siRNA.
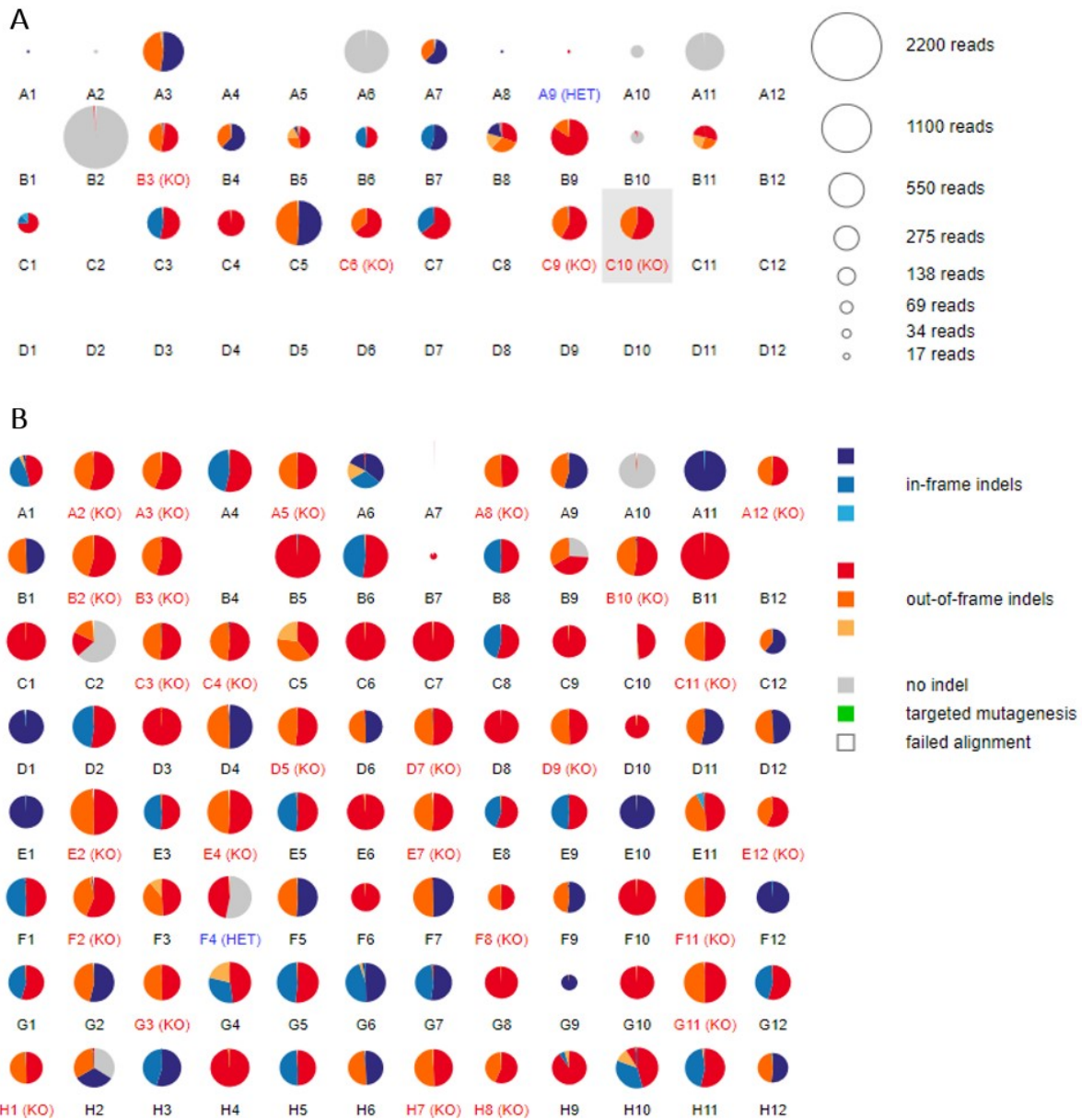
Figure 7: Evaluation of BLaER1 cell clones targeted by CRISPR/Cas9
Shown are the (A) MX2 and (B) SAMHD1 gene deletion analysis performed by OutKnocker of BLaER1 cells. The pie-charts were depicted with the corresponding barcode number indicated below. The size of the pie charts indicates the number of successfully aligned reads, whereas a legend is given on the right side. Grey pie chart areas indicate reads without an observed indels event, whereas blue and red areas indicate alleles with in-frame (blue) or out-of-frame (red) indels events. The identified indels mutations of clone are depicted as KO.

3.2 *Trans*-differentiated BLaER1 cells become quiescent and highly phagocytic, resembling primary macrophages

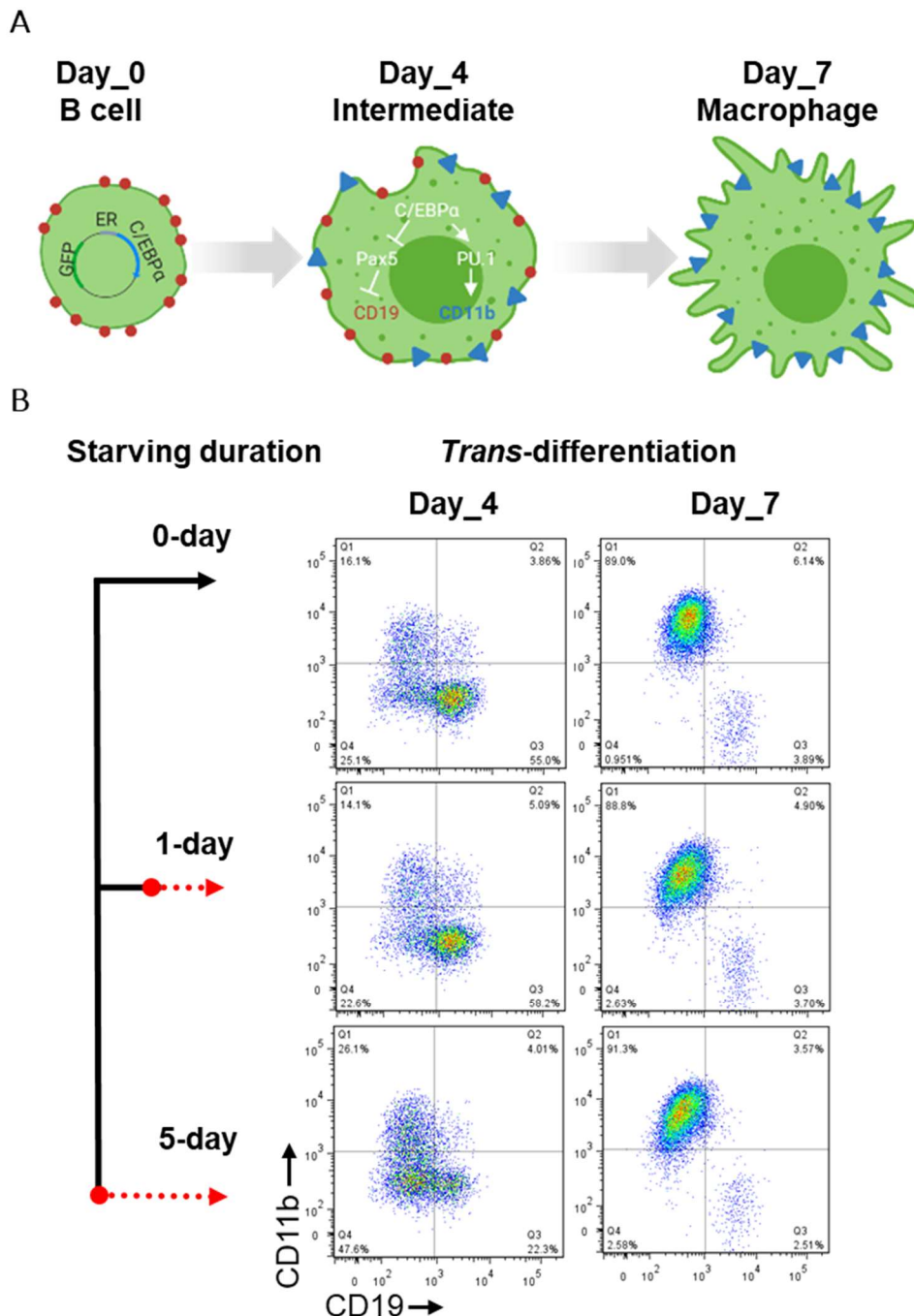### 3.2.1 Serum starvation increases the transient *trans*-differentiation efficiency

Figure 8: **Serum starvation increases the transient *trans*-differentiation efficiency**
(A) The transcription factor Pax5 is inhibited by forced C/EBPα expression, which synergizes with endogenous myeloid PU.1, resulting in a reciprocal regulation of CD19 (red) and CD11b (blue). Figure modified from [393]. (B) Cells were cultured in BLaER1-starving culture media for 5 days, 1 day or without prior starving in advance to the *trans*-differentiation. The duration of serum starvation is indicated in the red dot line. Expression of cell lineage markers CD19 and CD11b was analyzed by flow cytometry on day 4 and day 7.

BLaER1 is an estrogen steroid hormone-inducible cell line and can be *trans*-differentiated following cytokine- and C/EBPα-activation (Figure 8. A) [393]. With a

transcriptome similar to that of primary macrophages, BLaER1 cells can be efficiently converted into cells with increased adherent, phagocytic, and quiescent properties [392]. To increase the effects of the estrogen steroid hormone β-estradiol mediated *trans*-differentiation, we explored the impact of a preceding serum starvation. BLaER1 cells were first cultured in hormone "low level" medium for 5 days, 1 day, or not starved at all before *trans*-differentiation (Figure 8. B, dotted red line). To selectively remove endogenous hormones and growth factors in medium from supplementation, the reduced-serum media was prepared by phenol red-free media containing charcoal treated FBS. We found starved cells to be more sensitive to *trans*-differentiation, with a higher percentage of CD11b-positive cells following pre-starvation for five days (26.6%) compared with cells pre-starved for one day only (13.3%), or non-starved cells (15.3%) when analyzed at day 4 post *trans*-differentiation (Figure 8. B). Of note, there was no difference between CD11b-positive cells among the starved and non-starved cells at the end of *trans*-differentiation, while cells pre-starved had reduced viability. We concluded that for high viability and a high *trans*-differentiation rate, starving of cells before *trans*-differentiation is not necessary.

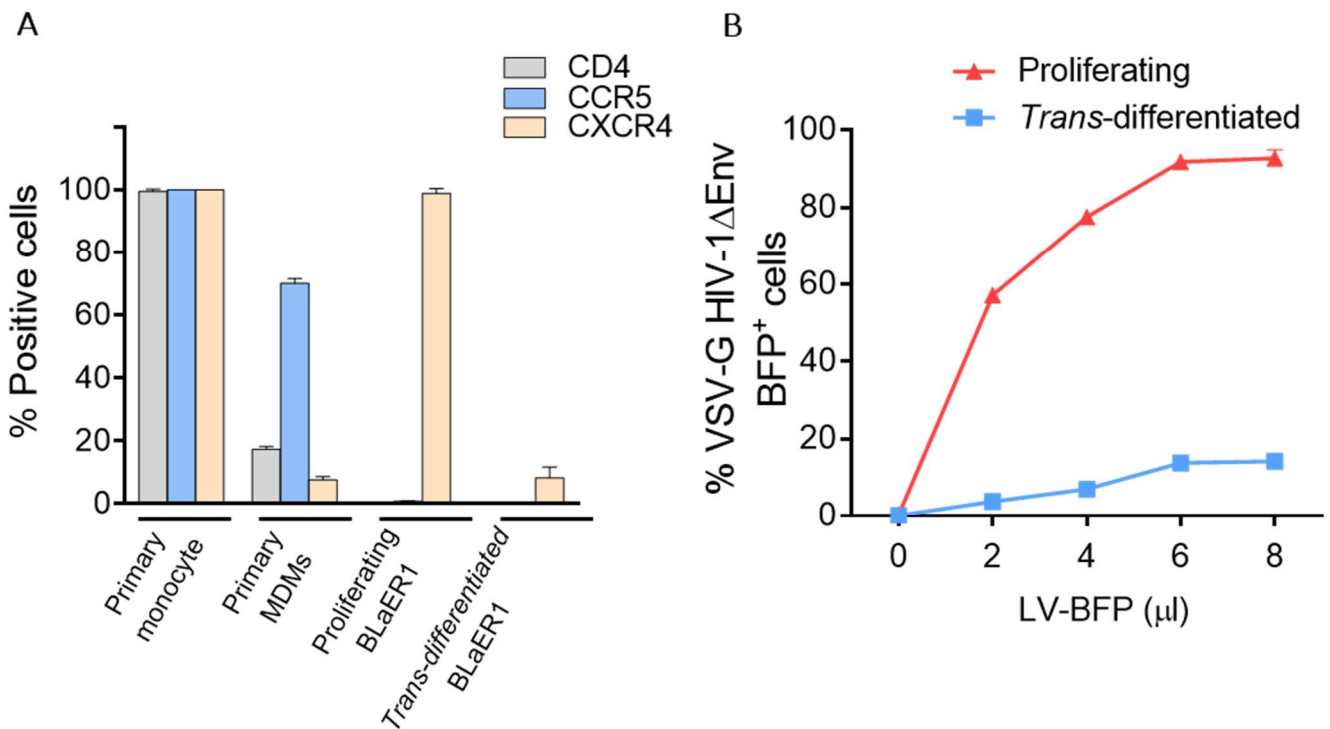### 3.2.2 BLaER1 cells have no functional HIV-1 entry receptor complex

Figure 9: **BLaER1 cells have no HIV-1 entry receptor complex**
(A) Measurements of CD4, CCR5 and CXCR4 levels on the surface of BLaER1 cells. Compared with MDMs, BLaER1 cells express CD4 and CCR5 at background levels, but do express CXCR4. (B) HIV-1 lentiviral vectors expressing BFP as a reporter were used to titrate and compare transduction efficiencies of *trans*-differentiated BLaER1 cells with proliferating non-differentiated BLaER1 cells. Proliferating and *trans*-differentiated BLaER1 cells were incubated with increasing titers of lentiviruses and BFP-positive cells were measured by flow cytometry at 48 h p.i. Data from one of three biological replicates is presented.

The attachment and fusion of virions to host cells are crucial to infection. Whether HIV-1 replicates permissively in *trans*-differentiated BLaER1 cells is unknown. First, we tested expression of the HIV-1 entry receptor complex on the cell surface of BLaER1 cells, and primary monocytes were included as controls. The CXCR4 co-receptor was readily detectable on the surface of both BLaER1 B cells and freshly isolated monocytes. However, CD4, CCR5 and CXCR4 surface expression were down-regulated following primary monocyte differentiation into macrophages, but CCR5 was still highly expressed compared to CD4 and CXCR4 (Figure 9. A). In contrast, CD4 or CCR5 were exposed on the surface of *trans*-differentiated BLaER1 cells at background levels, i.e. no expression of these receptors was evident. Cell surface expression of CXCR4 was further decreased in BLaER1 macrophages. Thus, BLaER1 cells do not express a functional HIV-1 entry receptor complex and WT HIV-1 strains are incapable of infecting cells productively. As a consequence, the VSV-G pseudotyped HIV-1ΔEnv

(VSV-G HIV-1 ΔEnv) was used to infect *trans*-differentiated BLaER1 cells. The virus can be endocytosed by binding to the low-density lipoprotein receptor via VSV-G, bypassing the membrane fusion which CD4, CXCR4 or CCR5 are required [423]. Thus, a HIV-1-based lentiviral vector expressing blue fluorescent protein (LV-BFP) as a reporter of infection, rather than GFP, was generated to overcome the issue of inherently GFP-positive BLaER1 cells. Lentiviral vector were added to proliferating and *trans*-differentiated BLaER1 cells in a dose-increasing manner. At 48 h p.i., the percentage of BFP-positive cells, which indicates successful transduction to monitor viral infection, was determined by flow cytometry (Figure 9. B). Notably, the infection rate of *trans*-differentiated BLaER1 cells was generally lower than that of proliferating cells. With proliferating cells reached nearly 90% infection, only 20% of non-dividing BLaER1 cells were successfully transduced. The resting state of *trans*-differentiated BLaER1 suggested the existence of restriction factors. Human monocytic THP-1 and U937 cells become resistant to HIV-1 due to endogenously expressing SAMHD1 when differentiated to a non-cycling state. Similarly, noncycling cells macrophages and DCs that express SAMHD1 are also effective at preventing HIV-1 infection [353]. We first investigated how SAMHD1 protein levels were affected in different cell states of BLaER1 to learn more about its role in HIV-1 infection.

3.2.3 SAMHD1 acts as an HIV-1 restriction factor within the *trans*-differentiated BLaER1 cells
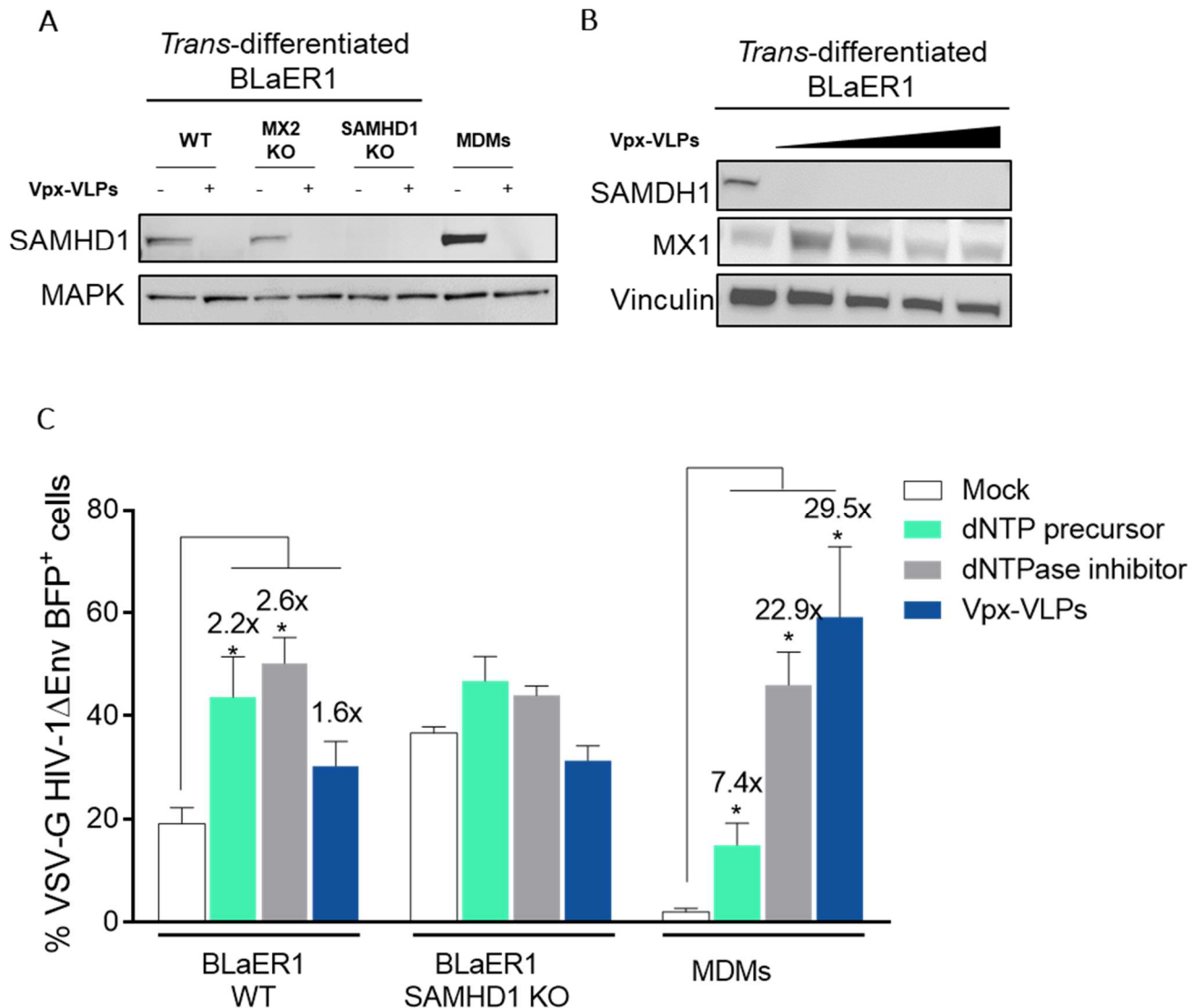

Figure 10: SAMHD1 acts as an HIV-1 restriction factor within the *trans*-differentiated BLaER1 cells
(A) *Trans*-differentiated BLaER1 cells together with primary MDMs were transduced with Vpx-VLPs for 24 h. Immunoblotting was used to examine SAMHD1 protein levels in Vpx-VLP-treated and untreated cells. MAPK acted as a loading control. (B) Vpx-VLPs treatment in BLaER1 cells induced MX1 expression. Vinculin served as housekeeping proteins. (C) *Trans*-differentiated BLaER1 cells and primary MDMs were pre-treated with dN (MDMs: 2.5 mM, BLaER1: 1.25 mM) for 0.5 h, 25 µM of the SAMHD1 inhibitor SIK0001 or Vpx-VLPs for 24 h respectively, prior to transduction with LV-BFP. Cells were analyzed by flow cytometry at 48 h p.i. To avoid cytotoxicity of dN to BLaER1 SAMHD1 KOs, a lower concentration of dN (0.31 mM) was used as shown in the figure. Bars indicate relative means ± S.D., each dot depicts a biological replicate.

Many monocytic cell types (e.g. THP-1 and U937) become resistant to HIV-1 after differentiation, and SAMHD1 is suggested to be a key player for this restriction [266]. It was discovered that infecting differentiated THP-1 cells with Vpx-VLPs increased their susceptibility to HIV-1 infection [360]. Remarkably, SAMHD1 was upregulated

following BLaER1 *trans*-differentiation (Figure 10. A). That's in accordance with previous that *trans*-differentiated BLaER1 cells express myeloid genes, although they generally expressed lower levels of SAMHD1 compared to MDMs. Since Vpx proteins encoded by SIVmac/HIV-2 deplete SAMHD1 [424]. We examined the susceptibility of *trans*-differentiated BLaER1 cells in which SAMHD1 had been depleted using Vpx-VLPs. To test whether SAMHD1 can be depleted by Vpx-VLPs in this system, *trans*-differentiated BLaER1 cells and primary MDMs were pretreated with Vpx-VLPs for 24 h. Immunoblotting confirmed that SAMHD1 depletion was efficient (Figure 10. A). Following Vpx-VLPs treatment, SAMHD1 in MDMs, as well as BLaER1 WT and MX2 KO cells were depleted and resulted in enhanced lentiviral transduction (Figure 10. C), confirming the functionality of the interaction of the accessory viral protein and the restriction factor in different cellular contexts, in particular the BLaER1 cell model. Additionally, the Vpx-VLPs treatment induced MX1 expression for unknown reasons. To our knowledge, this is the first demonstration that SAMHD1 function can be modulated through *trans*-differentiation in BLaER1 cells.

SAMHD1 has been linked to low dNTP levels in resting CD4 T cells and macrophages [268]. Usually, dividing cells harbor a higher dNTPs concentration than non-dividing cells. It turned out that *trans*-differentiated BLaER1 cells were largely resistant to lentiviral transduction, likely due to SAMHD1, which had been upregulated during *trans*-differentiation. Exogenous administration of dNTP precursors dN or depletion of SAMHD1 (genetically or via Vpx-VLPs treatment) can rescue macrophage HIV-1 infection [425]. Here, we examined whether exogenous dN treatment or depletion of SAMHD1 affects HIV-1 infection/lentiviral transduction of macrophages. Once dN have diffused into the cell, they are quickly converted to dNTPs [268]. As illustrated in Figure 10. C in primary MDMs, adding dN to the medium significantly improved transduction (7.4-fold increase). SAMHD1's dNTPase activity has been reported to be inhibited by a number of drugs [426]. SIK0001 is a small molecule proven to inhibit SAMHD1 dNTPase activity (provided by Dr. Paul R. Wratil, Keppler laboratory), also drastically increased the transduction efficiency (22.9-fold increase). Depleting SAMHD1 by Vpx-VLPs resulted in the highest rescue of lentiviral transduction, i.e. 29.5-fold relative to control. Thus, Vpx-VLPs treatment was able to elevate lentiviral transduction levels in primary MDMs more effectively than dN and, to a lesser extent, SIK0001 treatment. The next step was to see if SAMHD1 performs the role of restricting HIV-1 in BLaER1.

In *trans*-differentiated BLaER1 cells, SAMHD1 deficiency resulted in a 2-fold higher infection level compared to untreated BLaER1 wild-type (WT) cells. The percentage of cells expressing BFP rose by up to 2.2-fold and 2.6-fold in the presence of dN and SIK0001 treatment, respectively (Figure 10. C). Although LV-BFP transduction efficiencies were less effectively augmented by Vpx-VLPs treatment than by dN or SIK0001 adding, the basal transduction of BLaER1 WT cells was increased to levels comparable to BLaER1 SAMHD1 KO cells, demonstrating that the SAMHD1 restriction is active in this cell model. Since the expression level of SAMHD1 in BLaER1 cells is not as high as that in primary MDMs (Figure 10. A), the rescuing effects of Vpx-VLPs are not as profound as that in MDMs. Most importantly, the Vpx-VLPs are able to induce ISGs, suggesting an antiviral state is established which may restrict lentiviral transduction indirectly (Figure 10. B). Generally such findings suggest that *trans*-differentiation of BLaER1 cells limits lentiviral transduction as seen in primary MDMs [266], and SAMHD1 is an important host factor constituting an important macrophage-like property of this cell model.

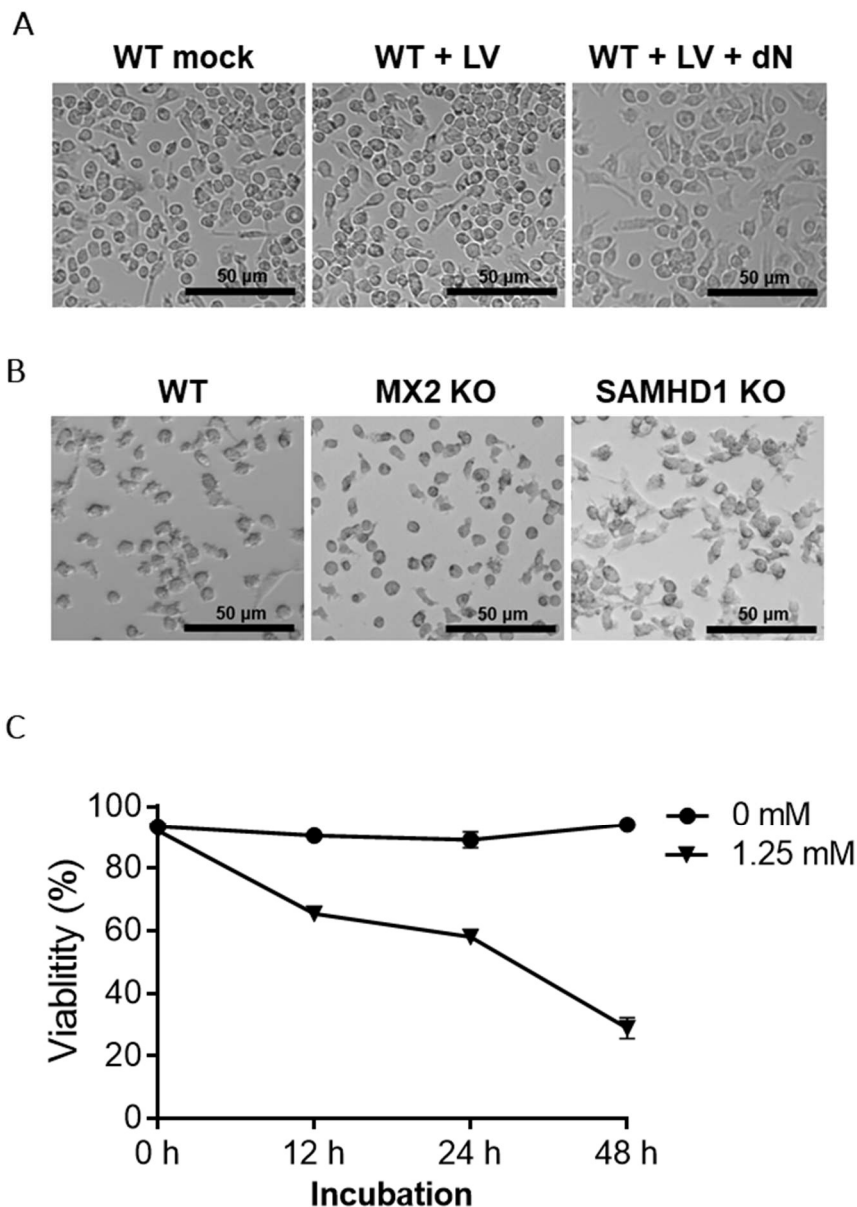## 3.2.4 Increased dNTP levels are a reprogramming booster in BLaER1 cells

Figure 11: Effects of dN treatment on BLaER1 viability and *trans*-differentiation
(A) dN treatment enhanced BLaER1 cell differentiation during lentiviral vector transduction. *Trans*-differentiated BLaER1 cells were mock or pre-treated with dN. (B) SAMHD1 KO BLaER1 cells have a more mature macrophage-like morphology. BLaER1 WT, MX2 and SAMHD1 KO cells were *trans*-differentiated without dN treatment. Morphology were recorded compared and the scale bar indicates 50 µm. (C) dN treatment showed cytotoxicity to proliferating BLaER1 cells. Proliferating BLaER1 cells were incubated with 1.25 mM dN for 2 days and cell viability was recorded.

Beyond the finding that enhanced dNTP levels appear to be essential for reverse transcription and lentiviral infection, the morphology of *trans*-differentiated BLaER1 cells can also be influenced by the addition of extracellular dN (Figure 11. A). BLaER1 cells cultivated together with dN during *trans*-differentiation displayed a more pronounced macrophage-like polarization. Despite this observation is beyond the

focus of this research to investigate the molecular mechanisms underlying these effects, it suggests that increasing dNTP levels during maturation from B cells to macrophages results in a boost for lineage reprogramming. To validate the dN's effect on BLaER1 cell *trans*-differentiation, we firstly examined dN toxicity on proliferating BLaER1 cells. Due to the presence of a GFP marker, reduction of GFP positivity can accompany BLaER1 viability. We thus monitored dN's effect on cell viability by the amount of GFP-positive cells. Proliferating BLaER1 cells were treated with 1.25 mM dN for 48 h and cell viability was subsequently recorded. After two days, the dN-induced cytotoxicity in proliferating BLaER1 cells reduced viability down to about 30% compared to untreated cultures (Figure 11. C). It is tempting to speculate that dN treatment can limit the proliferation of "non-macrophage-like cells", thus increasing the relative abundance of *trans*-differentiated BLaER1 cells in cultures and improving the culture's overall myeloid morphology. In support of this is the observation that dN treatment during *trans*-differentiation can convert more BLaER1 B cells to an M2-type macrophage phenotype. We also found that *trans*-differentiated BLaER1 SAMHD1 KO cells had a similar cell morphology compared to dN-treated BLaER1 WT cells. The SAMHD1 KO cells have increased cell polarization than BLaER1 WT or MX2 KO control (Figure 11. B). This effect is likely due to an increase in cellular dNTP levels, which boosts BLaER1 *trans*-differentiation by overcoming SAMHD1's inhibition of the cell cycle.

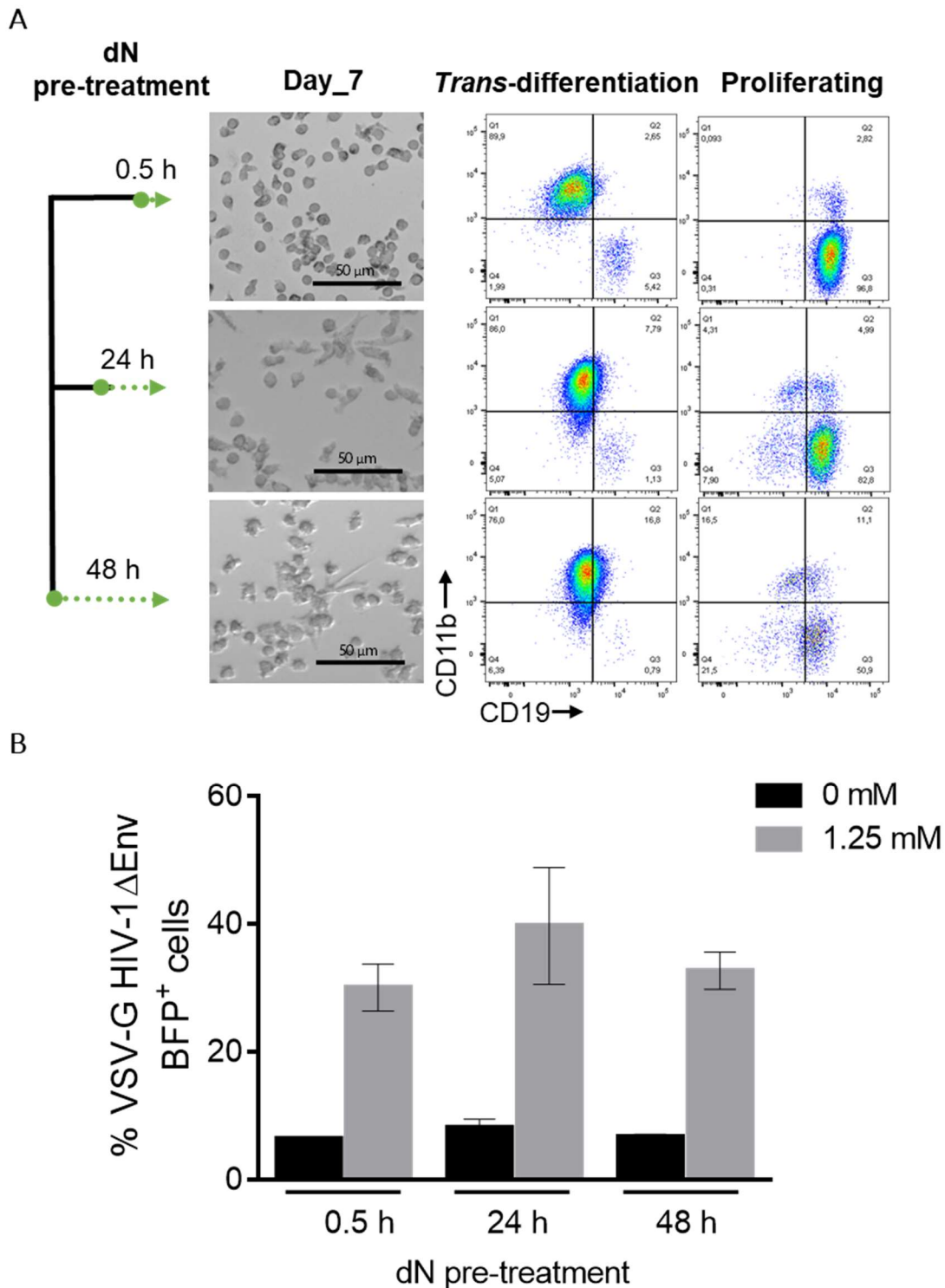## 3.2.5 dN treatment enhances *trans*-differentiation of BLaER1 cells

Figure 12: dN incubation enhances BLaER1 *trans*-differentiation
(A) BLaER1 cells were treated with 1.25 mM dN at time points 0.5, 24 or 48 h before infection (green dotted line). Cells provided with extracellular dNTPs for 24 h minimum resembled the morphology of primary MDMs. The scale bar indicates 50 µm. Flow cytometry analysis indicates that dN can boost *trans*-differentiation through enhanced killing of B cells. (B) Flow cytometry analysis indicates that the duration of dN pre-treatment has no major influence on the final transduction efficiency. Flow cytometry analysis of BLaER1 cells transduced with a LV-BFP, with and without dN pre-treatment. The experiment shown is representative of three. Histogram bars indicate relative means ± S.D.

To test whether the long duration of dN pre-treatment would affect lentiviral transduction, we performed dN pretreatment at different time points during a 7-day *trans*-differentiation period. Prior to lentiviral vector transduction, BLaER1 cells were cultivated with 1.25 mM dN for 48 h (from day 5-7), 24 h (from day 6-7) or 0.5 h (at day 7) (Figure 12. A, dotted green line). After dN pre-treatment, cells were cultivated with BLaER1 *trans*-differentiation medium without dN for another day to let cellular dNTPs fall back to normal level. As shown in Figure 12. A, dN's temporary pre-treatment (0.5 h) of BLaER1 macrophage-like cells resulted in them being only moderately attached to the cell plate and easily detachable. In contrast, following dN pre-treatment for 24 or 48 h, BLaER1 cells were markedly more adherent to the culture plate. In addition, only 1.13% and 0.79% of proliferating B cells existed after 24 and 48 h of dN pre-incubation, respectively, compared to 5.42% of BLaER1 cells undergoing regular *trans*-differentiation in the absence of dN pre-treatment. To test whether dN can overcome SAMHD1's restricting effect, dN treatment was resumed during transduction. We noticed that these well *trans*-differentiated BLaER1 were more resistant to LV-BFP transduction, yet dN addition subsequently yielded comparable transduction rates, suggesting that the duration of dN pre-treatment has no marked influence on the final transduction efficiency (Figure 12. B). Taken together, BLaER1 cells cultivated with dN for at least 24 h before biological experiments can improve the efficiency of macrophage reprogramming.

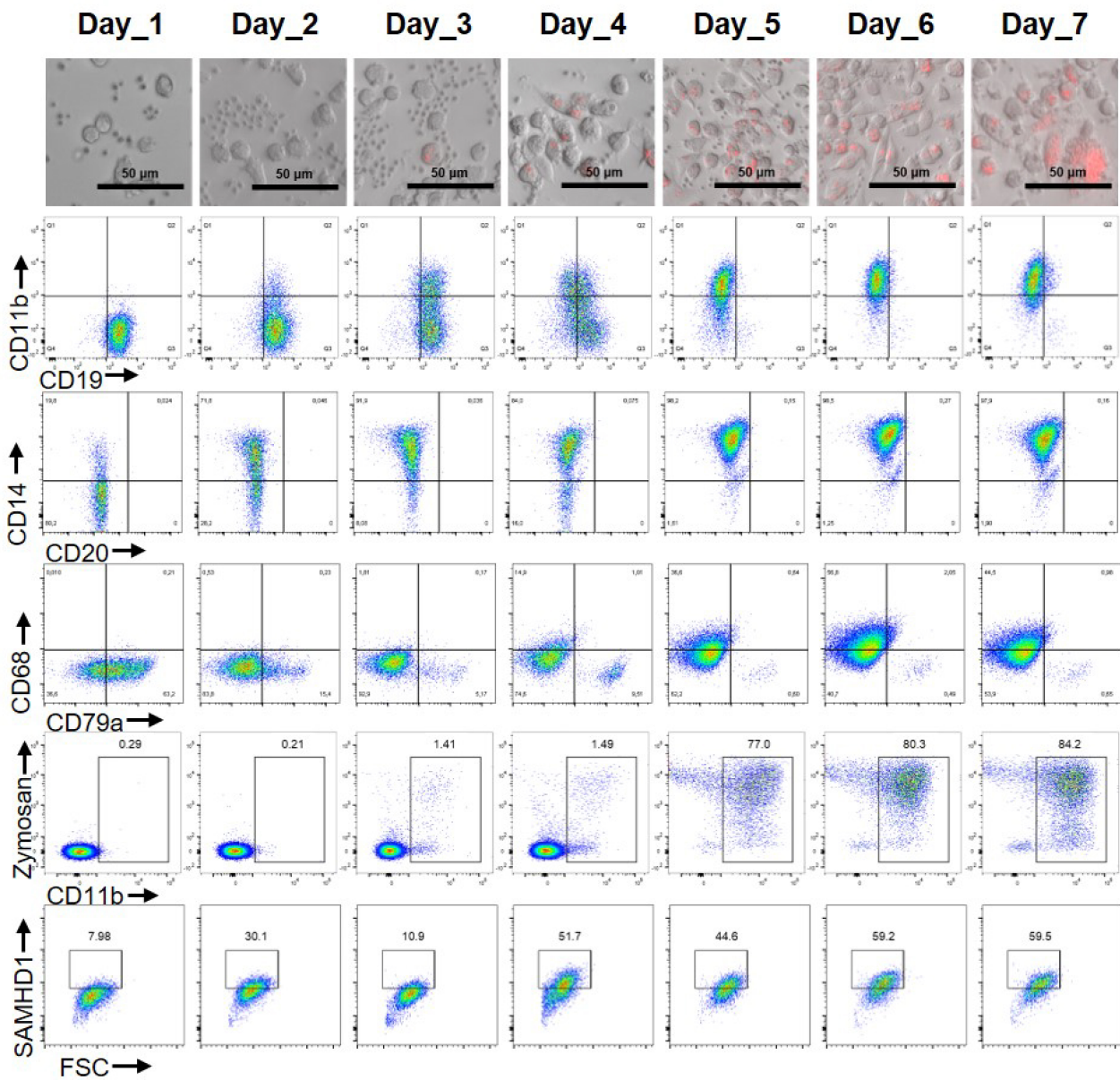### 3.2.6 *Trans*-differentiated BLaER1 cells express myeloid surface markers and are highly phagocytic

Figure 13: *Trans*-differentiated BLaER1 cells adopt a macrophage-like morphology, lose B cell marker CD19 and upregulate the macrophage marker CD11b
Overview of morphology and myeloid surface marker expression CD11b, CD14 and CD68 as well as Zymosan levels and SAMHD1 protein expression levels. 50,000/well of BLaER1 cells were seeded into 96-well plate with a flat bottom, cultivated in *trans*-differentiation medium and treated with dN for 24 h before experiment. Expression of myeloid cell markers CD19, CD79a, CD11b, CD14, SAMHD1 as well as phagocytosis were defined by flow cytometry. The scale bar indicates 50 μm.

Based on the above results, we established a protocol, in which BLaER1 cells were cultured in *trans*-differentiation medium and pre-treated with dN for at least 24 h before infection. We characterized the *trans*-differentiation of BLaER1 by flow cytometry and microscopy. The images in Figure 13 depict the morphology of BLaER1 cells during the 7-day differentiation. The phenotypic transition from entirely round B cells to

monocytic/macrophage-like cells with extrusions is triggered by *trans*-differentiation. *Trans*-differentiated BLaER1 cells ceased to proliferate and adopted a macrophage-like morphology. Dynamic changes in myeloid gene expression and phagocytosis functionality were characterized in order to identify specific myeloid cell populations after *trans*-differentiation. CD11b and CD14 have often been used as general markers of myeloid cell types, while CD19 and CD79a are expressed during all stages of B cell maturation. As shown in Figure 13, BLaER1 cells became CD19 negative during 7 days of *trans*-differentiation. Besides, they gradually upregulated the monocytic markers CD11b and CD14, while downregulating B cell marker CD79a. Interestingly, SAMHD1 was upregulated gradually following *trans*-differentiation.

Activated primary macrophages become highly phagocytic and responsive to pathogens [427]. *Trans*-differentiated BLaER1 cells were incubated with Zymosan for 1 hour at 37°C to see if the reprogrammed cells acquired these properties. Induced cells ingested bioparticles tagged with a pH-sensitive fluorescent dye, allowing for phagocytosis quantification. An index based on the pHrodo™ red percentage indicating comparable levels of phagocytosis was assessed. The quantitative analysis by flow cytometry showed that 80% of the induced cells became phagocytic (Figure 13). When monocytes mature into macrophages, they develop an adherent cell phenotype, which is characterized by a strong adhesion to culture plates that requires a lot of force to remove. To this end we found that Accutase, a proteolytic and collagenolytic enzyme, was better suited for detachment than a Trypsin-EDTA solution.

3.2.7 *Trans*-differentiated BLaER1 cells resemble MDMs in their response to IFN-α
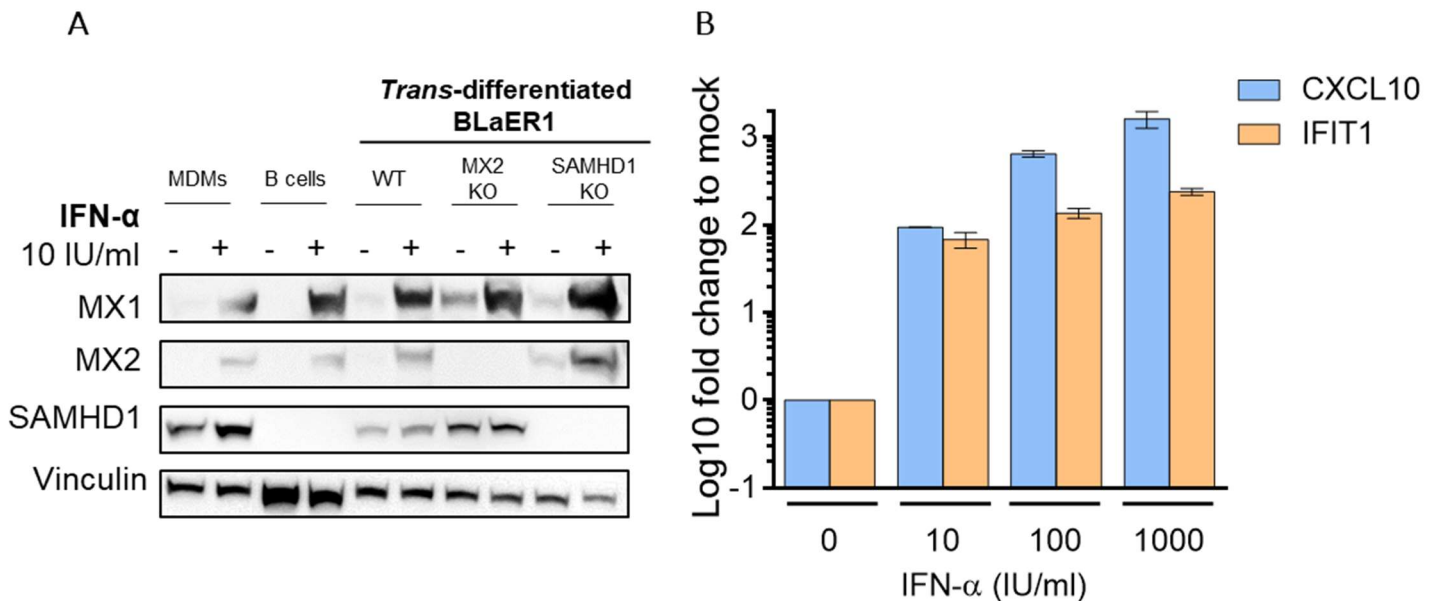

Figure 14: *Trans*-differentiated BLaER1 cells resemble MDMs in their response to IFN-α
(A) Immunoblotting was used to determine MX2 and SAMHD1 expression levels in extracts from cells treated with IFN-α for 24 h and anti-Vinculin antibody served as a loading control. (B) *Trans*-differentiated BLaER1 WT cells were exposed to amount of IFN-α for 24 h. CXCL10 and IFIT1 mRNA expression levels were measured in comparison to the reference gene GAPDH using qRT-PCR. Data is presented as mean ± SD of two measurements.

Intracellular restriction factor MX2 is stimulated by IFN which inhibits HIV-1 replication. To test whether BLaER1 cells are responsive to IFN-α stimulation, three MX2- or SAMHD1-KO BLaER1 cell clones were generated and *trans*-differentiated (Figure 7). Primary MDMs, BLaER1 WT, MX2 KO and SAMHD1 KO were treated with 10 IU/mL IFN-α for 24 h. Similar to primary MDMs, MX2 basal expression was low and showed differential upregulation following IFN-α treatment, i.e. only WT and SAMHD1 KO clones displayed increased MX2 expression (Figure 14. A). In contrast, MX2 KO clones did not express MX2 under basal cultivation conditions and, expectedly, failed to upregulate the restriction factor in response to IFN-α while the reference ISG MX1 was highly induced. Collectively, the absence of MX2 or SAMHD1 KO cells confirmed efficient knockout of the target gene. SAMHD1 is considered to be a modulator of the innate immune response, and IFN-I does not stimulate its expression in macrophages or CD4-positive T cells [428, 429]. We found no SAMHD1 expression in proliferating BLaER1 B cells. SAMHD1 was only upregulated following *trans*-differentiation, while not being further affected by IFN-α treatment (Figure 14. A). BLaER1 macrophage activation was also characterized by production of the IFN response gene CXCL10

and IFIT1. As shown in Figure 14. B, mRNAs of CXCL10 and IFIT1 were readily induced and shown to be dependent on the IFN-α dose. Thus, BLaER1 knockouts can be easily established and *trans*-differentiated, they resemble MDMs, and most importantly they are IFN-responsive.

3.3 *Trans*-differentiated BLaER1 cells are productively infected by pseudotyped HIV-1
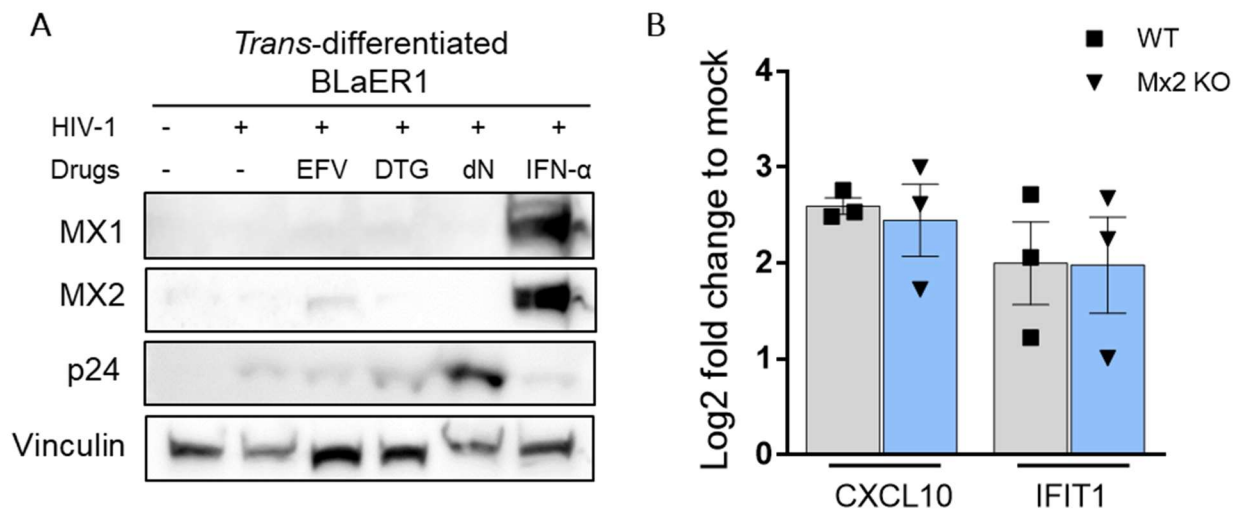

Figure 15: *Trans*-differentiated BLaER1 cells support post-entry steps of HIV-1 replication
Trans-differentiated BLaER1 cells with or without IFN-α treatment were challenged with VSV-G HIV-1ΔEnv at low MOI (0.75). The reverse transcriptase inhibitor efavirenz and integrase inhibitor dolutegravir at 10 µM each were used as controls. dN-treated cells served as an infection control. Cells were harvested and either analyzed by immunoblotting for (A) intracellular HIV-1 p24 expression and ISGs induction, or (B) extracted for ISGs CXCL10 and IFIT1 quantification by qRT-PCR 48 h p.i., as well as the housekeeping gene GAPDH. The results of two separate experiments were normalized using GAPDH and matched to non-infected cells as calibrators. The experiment shown is representative of three. Histogram bars indicate relative means ± S.D. Biological replicates are represented by dots, and statistical test was carried using a two-way ANOVA.

Professional antigen-presenting macrophages in mucosal tissues are critical for detecting HIV-1 at the initial site of infection. Previously, we established that BLaER1 cells do not express the HIV-1 entry receptors and are incapable of being productively infected by wild-type HIV-1 strains. Here, we used a VSV-G HIV-1ΔEnv virus to allow synchronized single-round infections. HIV-1 replication in macrophage has been shown to either evoke an IFN-I response or not [157, 182]. To gain first insight into the immune activation following HIV-1 infection, reverse transcriptase inhibitor efavirenz (EFV) and integrase inhibitor dolutegravir (DTG) were used as specificity controls to evaluate different stages of the HIV-1 life cycle for triggering the IFN-I response. To eliminate the possibility that the weak HIV-1 replication from low MOI infection was unable to induce ISGs, dN were added to enhance VSV-G HIV-1ΔEnv infection. *Trans*-differentiated BLaER1 cells were less susceptible to HIV-1 infection mostly because of host restriction factors that prevent viral infection from establishing or spreading. As shown in Figure 15. A, immunoblotting indicated that a very weak infection corresponding to the p24 CA protein and both EFV and DTG inhibited infection or suppressed ISG induction. Furthermore, HIV-1 does not trigger MX1 and MX2

induction at all despite high levels of viral replication within dN treated cells. In contrast, BLaER1 cells pre-treated with IFN-α showed strong MX1 and MX2 expression and no concurrent HIV-1 p24 signal suggesting IFN-I had restricted HIV-1 replication. Our findings clearly show that HIV-1 could indeed reproduce in *trans*-differentiated BLaER1 cells without inducing MX2. Despite poor replication, induction of a weak but detectable ISG has been observed in VSV-G HIV-1ΔEnv-infected BLaER1 macrophages, CXCL10 and IFIT1 gene expression were determined using qRT-PCR (Figure 15. B). It's no surprise that HIV-1 is a poor IFN inducer because it's sensitive to ISGs and the antiviral response induced by IFN [430]. These low or even non-existent innate responses are consistent with previous research displaying that HIV-1 can inhibit the production of proinflammatory cytokines and antiviral IFN-I in both *trans*-differentiated BLaER1 and primary macrophages.

3.4 HIV-1 infection is restricted by IFN-I response in *trans*-differentiated BLaER1 cells through MX2 at the level of nuclear import of the pre-integration complex
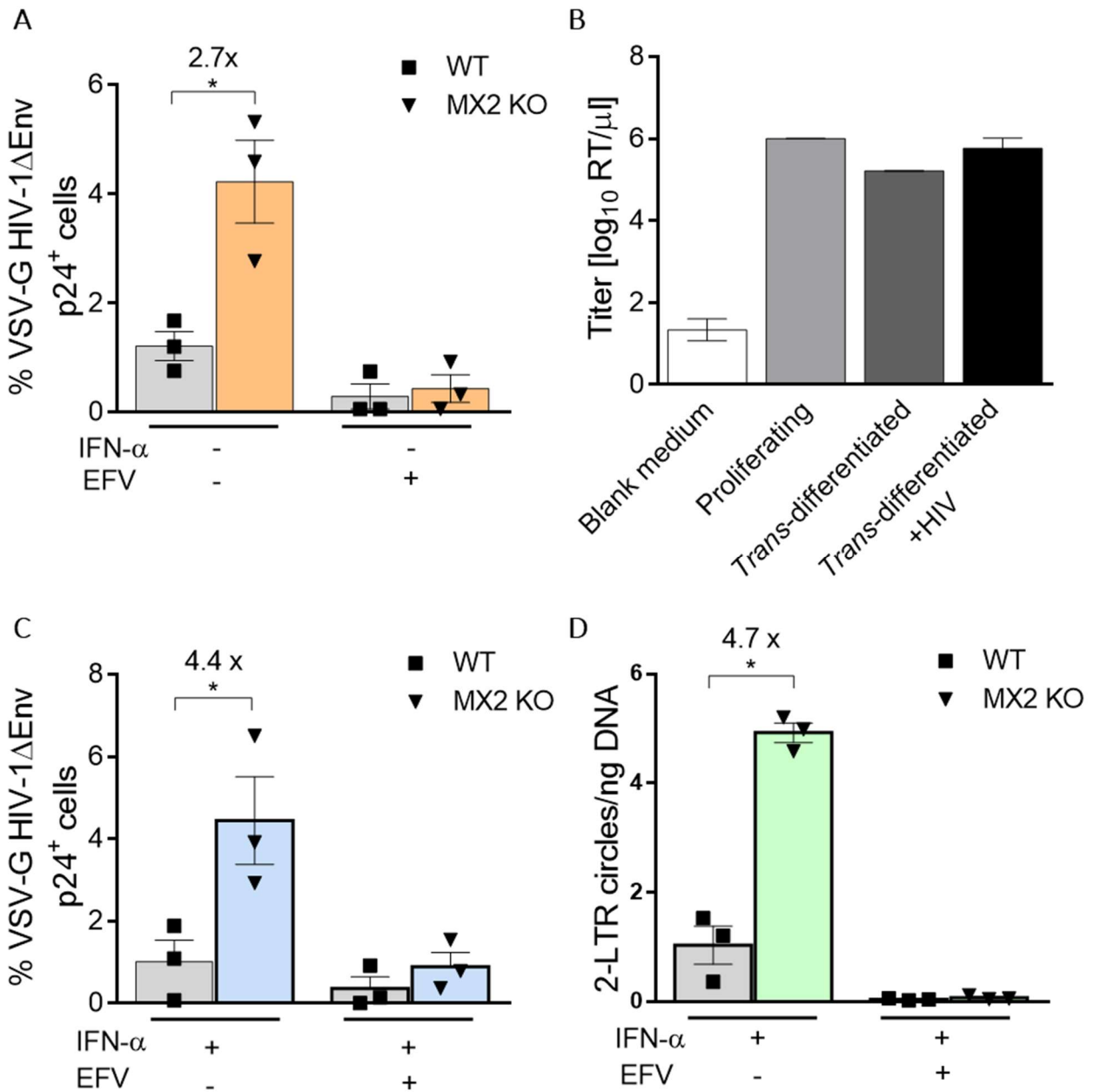
Figure 16: IFN-α induced MX2 restricts HIV-1 infection in *trans*-differentiated BLaER1 cells
Trans-differentiated BLaER1 cell clones without IFN-α treatment were incubated with VSV-G HIV-1ΔEnv at low MOI (0.75) or pretreated with low dose IFN-α (10 IU/ml for 24 h) then challenged with virus at high MOI (2). The reverse transcriptase inhibitor EFV at 10 µM served as an infection control. 48 h p.i. (A, C) Cells were harvested and examined for the presence of HIV-1 p24 or (D) extracted for episomal 2-LTR circle quantification. (B) The released replication-defective lentiviruses in the supernatant of BLaER1 cells were measured by SG-PERT assay. The experiment shown is representative of three. Histogram bars indicate relative means ± S.D. Biological replicates are represented by dots, and statistical test was carried using a two-way ANOVA.

As shown in Figure 15, challenge of macrophage-like BLaER1 cells with VSV-G HIV-1ΔEnv resulted in a robust infection indicated by p24 positivity, suggesting that *trans*-differentiated BLaER1 cells support post-entry steps of HIV-1 replication. To test whether a lack of the HIV-1 restriction factor MX2 enhances HIV-1 infection, a set of BLaER1 clones carrying *MX2* knockouts were generated (Figure 14 and 15). Although HIV-1 infection per se did not strongly induce MX2 (Figure 15. A), *trans*-differentiated BLaER1 MX2 KO clones were incubated with VSV-G HIV-1ΔEnv at low MOI initially to avoid excessive ISGs. Importantly, the BLaER1 MX2 KO clones showed 2.7-fold higher infection compared with BLaER1 WT cells (Figure 16. A). Conversely, EFV-treated BLaER1 cells could not be productively infected, representing the background of viral input. The absence of MX2 modestly enhanced infection, demonstrating a restrictive role of this cellular factor in HIV-1 replication in the BLaER1 cell model. Since MX2 basal expression is low in BLaER1 cells as well as MDMs, and MX2 expresses robustly only after IFN-α activation (Figure 14. A), *trans*-differentiated BLaER1 cells were firstly pretreated with IFN-α at a low dose (10 IU/mL) for 24 h to induce MX2 expression without strongly inducing all ISGs that would block infection completely. The latter results showed that MX2 ablation resulted in a 4.4-fold increase of HIV-1 infection compared to WT cells (Figure 16. C). Other mechanistic study showed that MX2 had little impact to HIV-1 cDNA synthesis but did decrease the amount of 2-LTR circles in infected cells [273]. In the current study, HIV-1 2-LTR circle formation was analyzed using quantitative TaqMan PCR and a plasmid standard for 2-LTR circles. Likewise, 2-LTR circles were also found to be enhanced (4.7-fold) in *trans*-differentiated BLaER1 MX2 KO cells compared to WT cells, while not being detected in EFV-treated cells (Figure 16. D). Our findings support the notion that MX2 induced by IFN limits HIV-1 PIC nuclear import.

In IFN-treated THP-1 cells, MX2 gene disruption had no restorative effect on HIV-1 infectivity [431]. In addition to analyses of intracellular p24-positivity comparing VSV-G HIV-1ΔEnv-infected WT and MX2 KO BLaER1 cells, we also analysed the RT activity in culture supernatants, as a measure of virus production and release using the PCR-enhanced reverse transcriptase (PERT) assay [432]. This assay was originally developed by Pizzato *et al*. to detect all sorts of human and non-human retroviruses in different types of biological samples. The real-time detection system based on SYBR

Green enables a cost and time-effective one-step PERT assay, referred to as SG-PERT assay. To this end, we collected supernatants from HIV-1-infected, *trans*-differentiated BLaER1 cells. Cell-free culture without dilution was commonly taken as an input for the assay. The supernatants from blank medium and uninfected cells were taken as controls. Surprisingly, high RT activity was observed in cells that had not been exposed to HIV-1, and cross-contamination between samples was ruled out in subsequent experiments (Figure 16. B). The qRT-PCR confirmed high concentrations of reverse transcriptase activity in the supernatant of up to 10^6 RT/µL irrespective of the BLaER1 cells' HIV infection status. In the BLaER1 cell, the depth of RNA-sequencing reads mapping to SMRV (GenBank: M23385.1) was abundant. Complete copies of SMRV proviral genome were discovered after gene cloning and sequencing of the RT gene. Moreover, in the supernatant replication-compentent SMRV was detected. It has previously been documented that therapeutic medical products derived from cell cultures can be contaminated with SMRV, resulting in contamination of vertebrate cell lines [433]. Despite the presence of SMRV in this model cell line, it is known to be non-pathogenic, as opposed to exogenous simian retroviruses [434]. Therefore, it is possible to use BLaER1 cells to screen for potential HIV restriction factors and sensors. In summary, macrophage-like properties of *trans*-differentiated BLaER1 cells as well as first insights into their post-entry HIV-1 permissivity and basic innate responses to infection, make them a genetically versatile and easily accessible infection and screening model. According to our findings, SAMHD1's restriction to HIV-1 is a primary macrophage-like property of this cell model. In addition, MX2 is IFN-inducible that prevents HIV-1 PIC from entering the nucleus.

3.5 MX2 and SAMHD1 restrict post-entry steps of HSV-1 infection in BLaER1 macrophages
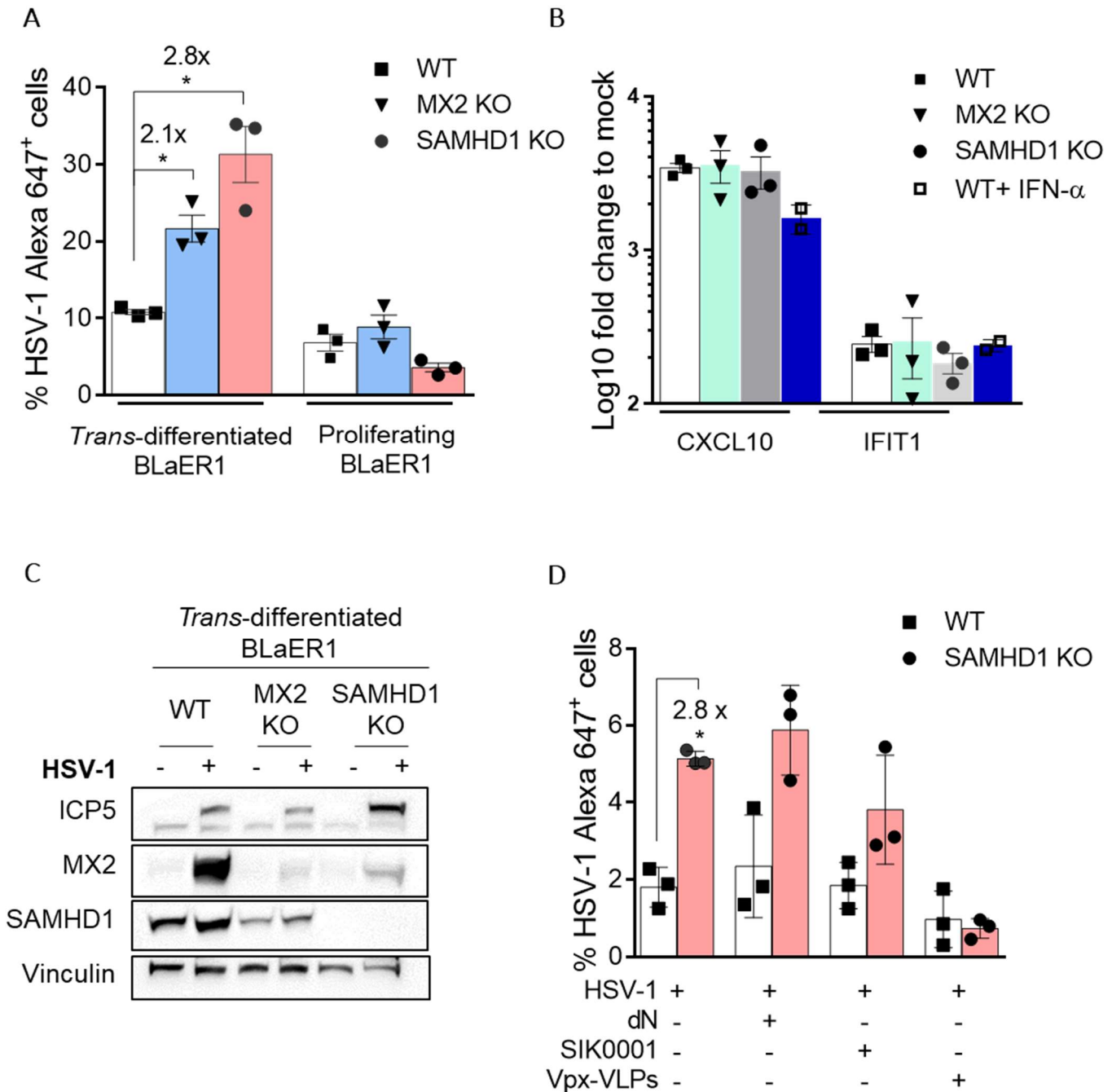
Figure 17: MX2 or SAMHD1 KOs rescue HSV-1 replication in non-dividing BLaER1 macrophages
BLaER1 cells were either mock infected or infected with HSV-1 for 18 h at 37°C. (A) HSV-1 reproduction was determined by quantification of the HSV-1 CA protein ICP5 by flow cytometry. (B) ISGs induction by HSV-1 replication was detected by qRT-PCR. *Trans*-differentiated BLaER1 cells treated with 100 IU/mL IFN-α for 24 h were taken as ISGs induction control. (C) HSV-1 replication in *trans*-differentiated BLaER1 cells induced MX2 expression. Using immunoblotting analyses, MX2 and HSV-1 CA protein ICP5 were detected in cell lysates. (D) Prior to infection of HSV-1, *trans*-differentiated BLaER1 cells were pre-treated with either dN for 0.5 h or Vpx-VLPs for 24 h, respectively. The fold changes between control groups are displayed. One representative experiment out of three is shown. Bars indicate relative means ± S.D., each dot depicts biological replicates. Statistical analysis was performed via two-way ANOVA.

MX2 prevents the HSV-1 genome from entering the nucleus, as per mechanistic studies [274]. In addition, SAMHD1 is known to regulate cellular dNTPs, which have been connected to HSV-1 genome replication [373]. However, these studies were performed exclusively in cell lines and the studies of MX2 and SAMHD1 inhibition of HSV-1 replication remain to be confirmed. In the current thesis, we studied the potential inhibitory effect of MX2 and SAMHD1 for HSV-1 in both BLaER1 macrophage-like cells and primary human MDMs.

To assess the activity of MX2 and SAMHD1 against herpesviruses, we first investigated whether BLaER1 cells are at all permissive to HSV-1 infection. BLaER1 cells were either mock or infected with HSV-1 for 18 h at 37°C. The viral core protein ICP5, a virus late gene-encoded protein that is synthesized mainly at late stages during HSV-1 infection, was detected intracellularly by flow cytometry using a sensitive staining method (method section 2.2.3.2). Both proliferating and *trans*-differentiated BLaER1 WT cells could be readily infected by HSV-1 (Figure 17. A). In *trans*-differentiated BLaER1 cells, both MX2 and SAMHD1 KOs enhanced HSV-1 infection as assessed by flow cytometry, by 2.1-fold and 2.8-fold, respectively, compared to WT cells (Figure 17. A). HSV-1 genome synthesis was delayed by SAMHD1 in *trans*-differentiated BLaER1 cells. In contrast, in proliferating BLaER1 cells, knockouts of MX2 or SAMHD1 had either no or only a minor effect on the percentage of HSV-1 ICP5-positive cells, supporting that SAMHD1 restricts HSV-1 in differentiated mechanism. These results showed B cell pattern is limited in HSV-1 the study. Remarkably, in all *trans*-differentiated BLaER1 cell clones, HSV-1 infection triggered a pronounced innate immune response, assessed by induction of CXCL10 and IFIT1, that was even stronger than IFN-α (100 IU/mL) treatment in BLaER1 WT cells (Figure 17. B). MX2 expression increase modestly during HSV-1 infection, possibly as a result of the virus-induced IFN response. Increased HSV-1 CA ICP5 were also observed in BLaER1 SAMHD1 KO cells. Moreover, the amount of SAMHD1 in the cells was unaffected by HSV-1 infection (Figure 17. C).

Since SAMHD1 KO leads to increased HSV-1 replication in *trans*-differentiated BLaER1 cells. We attempted to bypass SAMHD1 before HSV-1 infection of macrophage-like cells to see if these types of DNA viruses are restricted by SAMHD1 in a dNTP-dependent manner in BLaER1 cells. Since expression of the late gene ICP5

is dependent on HSV-1 DNA replication, this effect may be due to SAMHD1's enzymatic activity downregulating intracellular dNTP pools. Hence, we reasoned that overcoming SAMHD1 by means other than knockout may also rescue HSV-1 replication in macrophage-like BLaER1 cells. Infections were performed on *trans*-differentiated BLaER1 cells exposed to either dN, Vpx-VLPs, or the specific enzyme inhibitor SIK0001. The magnitude of productive infection indicator ICP5 levels were measured by using flow cytometry at 18 h p.i. (Figure 17. D).

Somewhat surprisingly, in *trans*-differentiated BLaER1 WT cells, all three treatments were not able to rescue HSV replication to levels comparable to those seen in SAMHD1 KO cells. Incubating cells with dN didn't lead to an enhancement of HSV-1 ICP5 level. The dN had no additional effect in cells that were depleted of endogenous SAMHD1. Additionally, the Vpx-VLPs treatment even inhibited HSV-1 replication. These results emphasize the potential differences between BLaER1 cell line and primary MDMs in regards to SAMHD1, which may be necessary to comprehend the restrictive role of this factor for HSV-1 (see also section 3.9.2). We found that SAMHD1 and MX2 can control HSV-1 replication in *trans*-differentiated BLaER1 macrophages to some extent in the current study. Studies conducted on genetically modified MDMs will provide an important reference. In the next part of this thesis, we adapted a methodology that allows genetic loss-of-function studies for virus infections in MDMs.

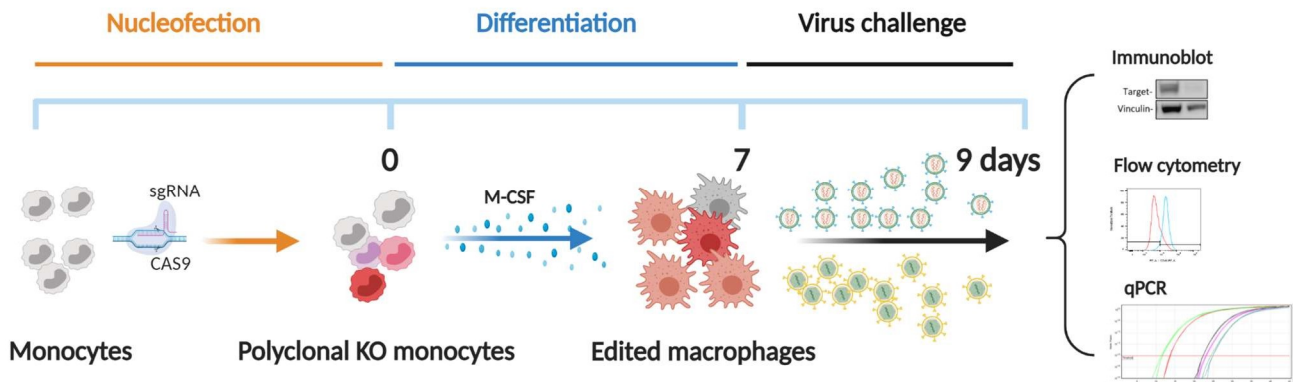## 3.6 Generation of knockouts in MDMs using CRISPR/Cas9

Figure 18: Workflow optimized for efficient gene ablation in MDMs
CD14-positive monocytes were enriched from human PBMC through magnetic negative selection. Nucleofection of the Cas9 nuclease with sgRNA as a RNP complexes was delivered into monocytes. The disrupted gene will be washed out during differentiation, and effects of gene deletion were verified in edited monocytes.

Macrophages are important regulators between viral infection and innate immune responses [85]. Although cell lines have the benefit of being easily accessible, primary macrophages are more relevant to reflect infection *in vivo*. A primary macrophage cell model that is easily amendable to genetic manipulation would be very useful for validating candidate genes of interest from the BLaER1 cell line system. Nevertheless, low editing efficiency in primary macrophage has long been a limitation due to the difficulty of expanding and genetically manipulating *in vitro*. The most significant impediment to deleting genes in myeloid cells is DNA transfection. Despite several strategies have been pursued for gene editing in T cells, there were few silencing methods for either human primary monocytes or MDMs in the literature [435]. The CRISPR/Cas9 system is active in various cell types, but primary human macrophages have long been awaited. Thus in the Keppler laboratory, we developed an high efficiency ribonucleoprotein (RNP) complex transfection method for gene ablation in primary MDMs. We present a reliable and economical system for genetically engineering human primary monocytes before converting them to macrophages. Initially, monocytes are negatively isolated from PBMCs derived from whole blood, buffy coats or blood cones, and subsequently undergo RNP nucleofection. CRISPR/Cas9-modified cells are then seeded and differentiated in macrophage generating medium where cytokines are replenished during the course of the experiment. Depending on the protein's natural turnover rate, the decline of target expression may take longer. We thus decided to validate target protein loss for all candidates at day 7. These edits are robust since they take place at the nucleotide

85

level, even enabling depletion of target with a long lifespan. This methodology is intended to be compatible with assessing a biological outcome using a variety of common assays. For instance, gene modified macrophages from a polyclone culture can be challenged with virus while the level of infection is monitored using flow cytometry (Figure 18). Taken together, the methodologies presented here allow for effective gene deletion in primary macrophages without the need for drug selection or cell populations sorting.

3.7 RNP Nucleofection into MDMs results in efficient gene silencing compared with RNA interference

3.7.1 Primary MDMs are resistant to common forms of transfection
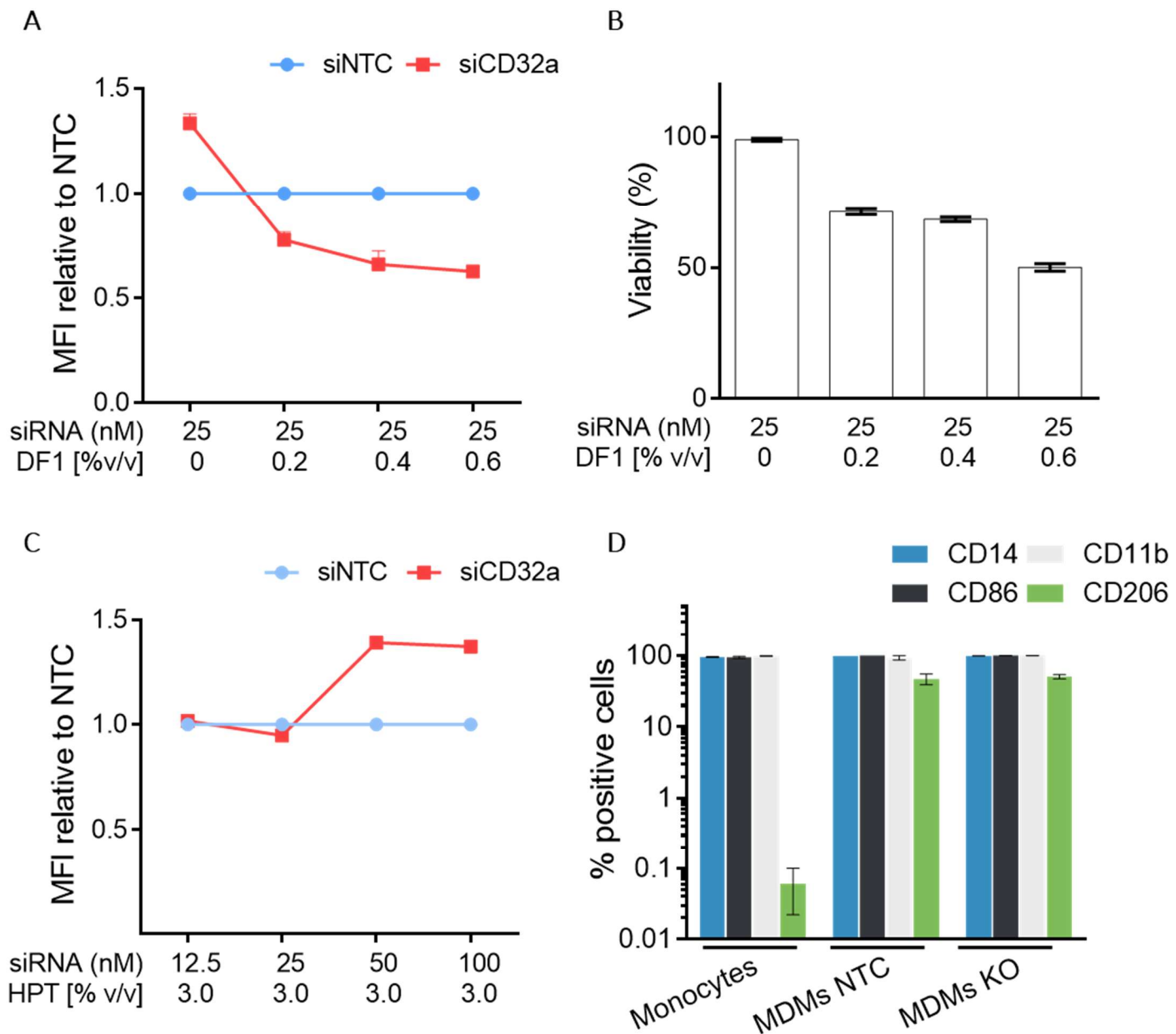
Figure 19: Primary MDMs are largely resistant to transfection and gene silencing by siRNA
Systematic titrations of DharmaFECT1 (DF1) and HiPerFect (HPT). (A) To achieve the maximum transfection efficiency with (B) the minimal effect on cell viability, 25 nM siRNA with varying concentrations of DF1 were utilized. (C) Primary MDMs were transfected with increasing amounts of siRNA with HPT. (D) CRISPR/Cas9-edited primary MDMs have stable and similar myeloid marker expression to unedited MDMs. A panel of myeloid markers (CD14, CD11b, CD86 and CD206) to distinguish monocytes and macrophages were tested by flow cytometry. Bars indicate relative means ± S.D.

To begin optimizing human myeloid cell editing, we targeted CD32a, a phagocytic receptor that is stably expressed on the monocyte/macrophage lineage [436, 437].

These will allow us to assess CD32a effects irrespective of donor-dependent variations. Recently, CD32a expression was proposed to be associated with HIV-1 latency [438-440]. Although the function of CD32a on the cell surface is controversial, it was chosen as a stable target to validate knock-down or knock-out efficiencies in the current study. We first determined whether transfection of siRNAs targeting CD32a enables an efficient knock-down in primary MDMs. MDMs incubated with the transfection reagent can lead to ISG viperin upregulation, indicating that cell type-dependent optimization of RNA transfection is needed, especially when dealing with innate sensing [157]. Therefore, siRNA transfections using DharmaFECT1 (DF1; Dharmacon) or HiPerFect (HPT; Qiagen) were employed, since they had displayed an overall attenuated ISG upregulation upon siRNA transfection in preliminary studies. We thus tested their suitability to promote siRNA uptake in MDMs.

DharmaFECT1 is a widely utilized reagent for siRNA delivery that causes the least amount of ISG expression in MDMs [441]. We performed a screen for the maximum amounts of the DharmaFECT1 required for efficient transfection. A titration series of DharmaFECT1, e.g., 0.5 µL (0.2% [v/v]), 1.0 µL (0.4% [v/v]) and 1.5 µL (0.6% [v/v]) were mixed with 25 nM siRNA and added to 500 µL of warm RPMI medium. HiPerFect transfection reagent is known to offer the benefit of higher siRNA concentrations and high stability in dilution [441]. Therefore, 12.5-100 nM siRNA was taken to determine the minimum amount of siRNA that was required. The introduction of HiPerFect-siRNA complexes to the liquid culture results in a final HiPerFect concentration of 3% [v/v] for the 24-well plate format. Our preliminary experiments investigated the amounts of transfection reagent used in DharmaFECT1 (Figure 19. A) and concentrations of siRNA applied in HiPerFect (Figure 19. C) within the manufacturer's recommended range. After 5 days of primary monocytes differentiation, the matured MDMs were subjected to siRNA transfection (section method 2.2.7) and this transfection was repeated after 48 h. The CD32a knock-down efficiency was quantified by flow cytometry. As shown in Figure 19. A and B, high DharmaFECT1 caused more pronounced knockdown of CD32a, but also caused considerable cell toxicity. For the HiPerFect transfection reagent, which supposedly has a higher efficiency and low toxicity, no target-specific effect of the siRNA was observed (Figure 19. C). Within the experiment, we investigated a final siRNA concentration of 25 nM and 0.2 percent [v/v] of DharmaFECT1 or 3.0 percent [v/v] of HiPerFect, respectively. However, the results

reported here demonstrate that primary macrophages are largely resistant to siRNA transfection using these transfection reagents.

3.7.2 Generation of knockouts in MDMs using CRISPR/Cas9
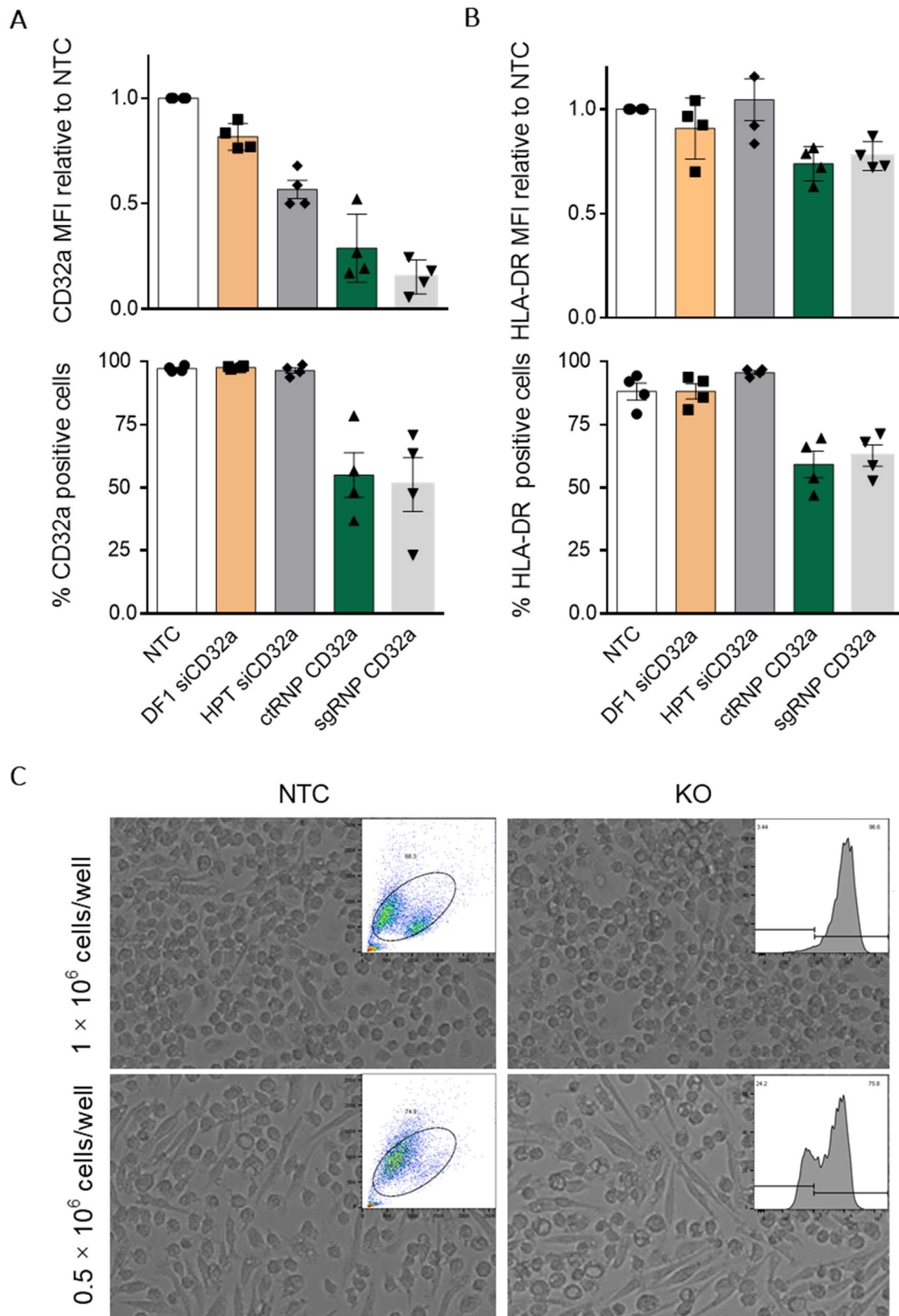
Figure 20: Primary MDMs nucleofected with RNPs have an efficient genetic editing
CD14-positive monocytes were transfected with either siRNA (siCD32a) or gRNA targeting CD32a RNP complex (RNP CD32a). (A) Analysis of CD32a KO efficiency and (B) cell activation marker HLA-DR were measured by flow cytometry. Bars indicate relative means ± S.D, each dot depicts a biological replicate. (C) High seeding density of MDMs decreased polarization and KO efficiency. Following

nucleofection, 0.5-1 million monocytes were seeded in each well of a 24-well plate. Representative images of different seeding cell numbers affect nucleofection. MDMs were first gated on forward and side scatter (FSC and SSC), panels illustrating FACS plots displaying the CD32a percent and WT are displayed as the unshaded histogram.

Both of these transfection reagents, DharmaFECT1 and HiPerFect, failed to achieve higher levels of target knock-down in MDMs (Figure 20. A). The number of CD32a-positive cells remained greater than 90% and CD32a expression (i.e. MFI) was comparable to the control using Dharmafect1. The HiPerFect was more potent compared to DharmaFECT1, the CD32a expression were 50% downregulated despite giving the high ratio of CD32a-positive cells. We decided not to continue an optimization process for this technology, but rather pursue CRISPR/Cas9-mediated gene silencing in cells of the myeloid lineage, which holds great promise. Thus, we next sought to adapt a sgRNA/Cas9-based protocol from human T cells to achieve efficient knockouts in primary MDMs without compromising cell viability [442].

RNPs are primarily made up of two parts: a sgRNA as well as a Cas9 nuclease. The sgRNA is a two-molecule complex composed of target-specific crisprRNA (crRNA) and trans-activating crRNA (tracrRNA) which binds to RNA binding to Cas9 (ctRNP). Because providing surplus sgRNA facilitates effective RNP formation, a 2.5:1 molar ratio of sgRNA and Cas9 was expected as a starting condition (8 M Cas9 per reaction). The EH-100 pulse code in the P3 buffer is identified in a report of Nucleofector conditions for optimally balancing editing effectiveness, cell survival, and cell morphology [418]. RNP concentration has been found to significantly affect the on- to off-target ratio [443]. We also have noticed that both viability and Cas9 uptake can be affected by the number of cells. Thus, 2×10^6 freshly isolated CD14-positive monocytes in 20 μL P3 buffer were transferred on top of 5 μL RNP mix. Cells mixed with the RNP complex, but not electroporated, were used as reference WT. As cell density affects nucleofection significantly, further experiments to confirm the seed density were required. Therefore, either 1×10^6/well or 0.5×10^6/well monocytes after nucleofection were seeded in a 24-well plate, and CD32a KO efficiency were compared by flow cytometry. As illustrated (Figure 20. C), higher seeding density had limited CD32a knockout efficiency compared to lower density of MDMs. Additionally, differentiation is a basic biological function of macrophages, however 1×10^6/well seeding conditions had incomplete polarization according to their forward- and side scatter characteristics

with low granularity after nucleofection. Therefore, the procedure outlined in this protocol has been optimized for $5×10^5$ cells/well seeding in 24-well plate. We observed that approximately 30-70% of cells had reduced expression with ctRNP CD32a nucleofection (Figure 20. A). However, there were some loss of viability after transfection. Given that the Cas9 nuclease was extracted from *E. coli* rather than being purified, macrophages are sensitive to exogenous nucleic acids or proteins. Thus, we reasoned that the condition may not be optimal for RNP nucleofection and monocytes were later electroporated with endotoxin-free Cas9 before being differentiated to macrophages.

Collectively, RNP complexes delivery achieved nearly 80% population-level genetic knockout versus siRNA. This is achieved in freshly isolated monocytes without the need for cell selection after nucleoprotein. While the monocytes converted to mature macrophages, gene editing was stable without an impact on cell viability (Figure 20. B). Either DharmaFECT1 or HiPerFect dual transfection trigger broad HLA-DR activation of MDMs at the time of analysis. In contrast, delivery of RNP did not disturb MDMs activation and morphology. In this study, we found that primary monocytes were accessible to CRISPR/Cas9-based gene-editing in the absence of morphology alterations, implying that this methodology could help researchers better understand gene functions within MDMs.

3.7.3 Multiple sgRNA combinations allow efficient gene knockouts

Figure 21: Detection of CRISPR/Cas9-mediated gene alterations
Knocking out targeted genes based on sgRNA results in the loss of gene products. RNPs containing three distinct guide sequences against the indicated gene were nucleofected into CD14-positive monocytes. (A) The target site of the sgRNAs in the CD32a gene is depicted in diagram. The Protospacer-adjacent motif sequence is written in bold, while the sgRNA target sequence is underlined. (B) The relative contribution of each sgRNA to Indel mutations was evaluated using the online tool ICE analysis.

According to a previous study, knockout efficiencies for individual donors can vary greatly, and using more than two sgRNAs at the same time leads to higher targeting efficiency than using a single gRNA [444]. Therefore, we investigated to see if this method could enhance the disruption of the *CD32a* locus in MDMs. Recently, fully synthetic sgRNAs were developed and chemically modified, which combine the crRNA and tracrRNA into a single unit and don't require guide annealing before RNP complexing [415]. Since synthetic sgRNAs showed improved function and stability, three synthetic CD32a sgRNA composed of RNPs (sgRNP CD32a) were accordingly designed. As shown in Figure 21. A, sgRNA1 and sgRNA2 target exon 1 which is downstream of the start codon, while sgRNA3 was designed to induce cleavage at the intro and the site is 127 nucleotides downstream from sgRNA1. To boost the knockout efficiency, we pooled three gRNAs targeting the same gene in one nucleofection. The loci of interest were PCR-amplified and subsequently sequenced and analyzed at the website ice.synthego.com. We noted deletion of the intervening sequence around the

predicted Cas9 cutting sites (Figure 21. B). To this end, the delivery of combined three sgRNPs obtained a maximum 95% knockout efficiency (i.e., MFI) at the population level (Figure 20. A). The effectiveness of specific sgRNAs were found to differ, CD32a sgRNA1 exhibited the highest editing efficiency, whereas sgRNA1/sgRNA3 and sgRNA2/sgRNA3 combinations resulted in 7% and 5% mutated clones respectively (Figure 21. B). As all the sgRNAs do not show the same efficiency for generation of double strand breaks, the editing efficiency of multiple sgRNAs was higher than that of a single sgRNA. Thus, maximal depletion of each gene was observed when multiple sgRNAs for CD32a were used, resulting in 128 bp deletions as expected. Most importantly, macrophages obtained from both WT and edited monocytes demonstrated classic morphology and expressed associated markers under MDMs-generating conditions (Figure 19. D). Myeloid marker expression did not differ between edited and unedited MDMs. M2 markers (CD86 and CD206) were elevated in macrophages following differentiation, which was consistent with previous report, suggesting CRISPR/Cas9-mediated gene ablation does not disturb primary monocytes differentiation and myeloid gene expression [445]. The effect of nucleofection on innate cell activation was then investigated, and we discovered that either ctRNP or sgRNP delivery did not result in a significant up-regulation of the activation marker HLA-DR compared to the siRNA method. Thus, we have demonstrated that delivery of RNP complexes routinely generates higher knockout efficiency than the siRNA method. This initial work allowed us to knock out CD32a expression ~85% on average (i.e., MFI) of all macrophages in the culture. Using multiple sgRNA combinations, it is indeed possible to induce efficient knockout (maximum 99%) in monocytes before they are differentiated into macrophages. To date, most genetic manipulation has relied on RNAi technologies which are limited by transient and off-target effects [446]. The platform we presented here vastly improved existing human myeloid cell manipulation technology, allowing multiplex KOs to be generated in parallel. The platform was then used to knock out MX2 in primary monocytes.

3.8 MX2 or SAMHD1 knockouts enhance HIV-1 replication in MDMs
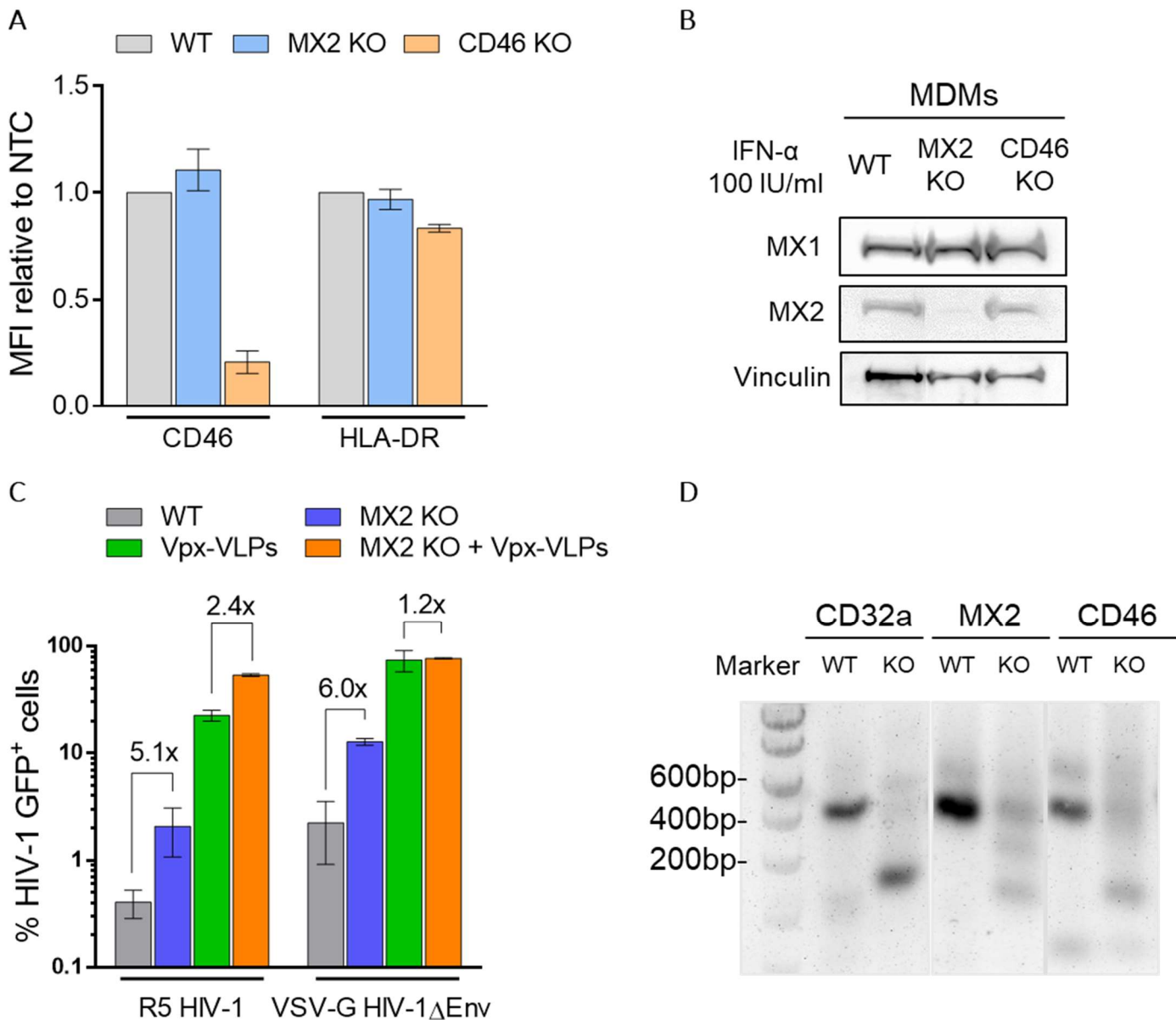
Figure 22: CRISPR/Cas9-edited MDMs are characterized by high knockout efficiency
CRISPR/Cas9 allows high and specific target gene editing and has no gross effects on cell activation. Primary human monocytes were nucleofected with RNPs targeting either CD46 or MX2. (A) Analysis of cells for CD46 and HLA-DR expression were measured by flow cytometry. The data are from two experiments, and the bars indicate relative means to WT ± S.D. (B) Quantification of MX2 KO in primary MDMs. MDMs were treated with IFN-α for 24 h before cells were lysed and tested by immunoblotting. The upper membranes depict MX1 and MX2. Vinculin was used as loading control. Immunoblot images are representative of two independent experiments performed with different donors. (C) MX2 deletion or SAMHD1 degradation enhanced replication of HIV in primary MDMs. MDMs were treated with IFN-α (100 IU/mL) for 24 h and subsequently challenged with two different HIV strains (R5 HIV-1 or VSV-G HIV-1ΔEnv). Cells were harvested and HIV-1 GFP-positive cells were quantified by flow cytometry 48 h p.i., the bars indicate relative means ± S.D. (D) PCR-based analysis of gene editing were performed using primers near the anticipated cutting site and the PCR products were checked on 1% agarose gel.

Encouraged by our results for CD32a KO in MDMs, we reasoned that the conditions for RNP delivery in different target genes might be consistent. We then focused on

MX2, an ISG that is expressed on MDMs after IFN-α treatment. Three distinct sgRNAs were designed to target MX2 exon2. In parallel to generating MX2 or SAMHD1 KO primary MDMs, another surface marker, CD46 (also known as membrane cofactor protein) which is expressed in most nucleated cells, was taken to test the specificity of the CRISPR/Cas9 technology. Using buffer P3, EH-100, specific RNP variants were delivered into monocytes by nucleofection. The edited monocytes were then differentiated into macrophages. As expected, pooling of Cas9-RNPs drastically reduced CD46 level in around 80% population as well as CD32a. Meanwhile, the activation state assessed by HLA-DR was not influenced after editing in either WT or KO MDMs (Figure 22. A). The MX2 gene was then disrupted in primary monocytes from two separate donors using specific sgRNP. The KO efficiency was tested by immunoblotting after monocytes differentiated into MDMs (Figure 22. B). Next, MDMs were treated with IFN-α or Vpx-VLPs for 24 h. The treatment of IFN-α induced strong ISGs MX1 induction in both WT and KO cells. MX2 was only expressed in WT and CD46 KO macrophages, but not MX2 KO cells (Figure 22. B). To assess the cleaving ability of the RNP complex on the target gene, we conducted PCR using a combination of primers which were located at a region of cutting sites for the semi-quantitative assessment of gene length. PCR products of edited monocytes were checked on 1% agarose, a single small band that matches the predicted sizes, indicating that the sgRNAs targeted the expected sites correctly. When compared to non-edited cells, frameshift cleavage products were found only in genomic DNA from polyclonal MDMs cells nucleofected with sgRNP of targets (Figure 22. D), and this is also in line with the semi-immunoblotting results (Figure 22. B). To this end, we identified 5 µL RNP that combined three sgRNAs and 2×10^6 CD14-positive cells under EH100/P3 as the best combination of efficient KOs in the myeloid lineage.

Previous findings suggested that ectopic MX2 expression can disrupt HIV-1 replication, but it's unclear whether over-expression approaches alone are sufficient to confer antiviral activity at physiological levels [309]. For this reason, we explored whether MX2 has a restriction role in genetically modified, primary MDMs upon HIV-1 infection. The MX2 KO MDMs were generated using the above described protocol and infected side-by-side with either R5 HIV-1 GFP or VSV-G HIV-1ΔEnv GFP. To evaluate the MX2 restriction to HIV-1, MDMs were pretreated with 100 IU/mL IFN-α for 24 h induce MX2 expression before being challenged. The MX2 KO efficiency was examined in both WT

and MX2 KO MDMs. Remarkably, MX2 depletion resulted in strong enhancement of VSV-G HIV-1ΔEnv infection (ca. 6-fold) compared to WT MDMs (Figure 22. C). Replication of an R5 macrophage-tropic HIV-1 was also markedly enhanced, 5.1-fold. This demonstrates that MX2 is a mediator of the IFN-mediated HIV-1 resistance in human MDMs. MDMs treated with Vpx-VLPs had a high infection rate, indicating that SAMHD1 actively inhibits HIV-1 replication in this cell type. Of note, Vpx-VLPs treatment of MX2 KO MDMs showed a slightly increased infection of R5 HIV-1 (ca. 2.4-fold) and VSVG HIV-1ΔEnv (ca. 1.2-fold) compared to Vpx-VLPs treatment alone, supporting an MX2-independent SAMHD1 post-entry block. MX2 KO fully rescued HIV-1 in human MDMs. These results suggest that MX2 inhibits HIV-1 infection in primary macrophages as well as in *trans*-differentiated BLaER1 cells. This biological effect upon ablation of a specific ISG reveals such model is appropriate for characterize cell factors in the context of virus restriction.

3.9 MX2 and SAMHD1 are post-entry inhibitors of herpesviruses in MDMs

3.9.1 HSV-1 productively infects MDMs and is sensitive to IFN-α
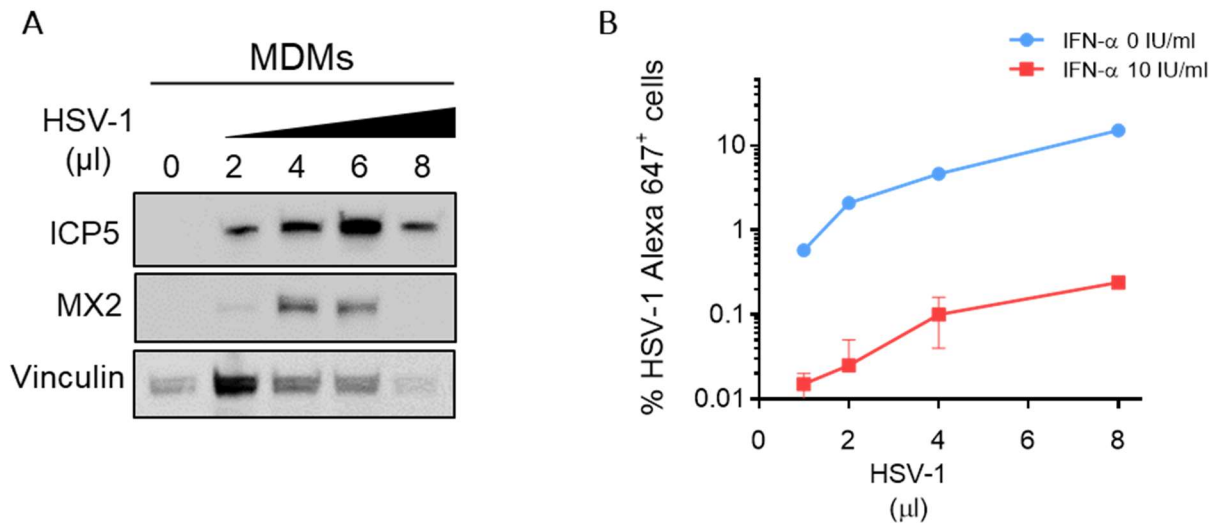
Figure 23: HSV-1 productively infects MDMs and is sensitive to IFN-α
 (A) The levels of ICP5 and MX2 in cell extracts were determined by immunoblotting at the specified time points after infection. (B) Effect of IFN-α pretreatment on the accumulation of viral ICP5. Prior to infection with HSV-1, primary MDMs were either mock or IFN-α (10 IU/mL) treated for 24 h. After 18 h, cells were collected and analyzed for intracellular HSV-1 ICP5 staining by flow cytometry.

It has been reported that HSV-1 productively infects MDMs to some degree [198]. We wanted to explore whether HSV-1 infection can trigger IFN-I response and establish an antiviral state in MDMs. Primary MDMs were exposed to the HSV-1 inoculum for 3 h at 37°C, after three washes with PBS, cultured in complete medium for 18 h. A somewhat dose-dependent induction of the ISG MX2 was observed and higher inoculation doses caused apoptosis in HSV-1-infected MDMs (Figure 23. A). *In vitro* studies have shown that IFN-I can inhibit HSV-1 replication [447]. To confirm these findings, we pretreated MDMs with IFN-α for 24 h prior to HSV-1 infection. As previously reported, HSV-1 was very sensitive to IFN-α pretreatment (Figure 23. B). Although HSV-1 infection of MDMs itself induced ISGs, this IFN-like response is apparently not strong enough to inhibit HSV-1 replication to the same degree as the addition of exogenous IFN.

3.9.2 MX2 and SAMHD1 are post-entry inhibitors of HSV-1 replication in MDMs
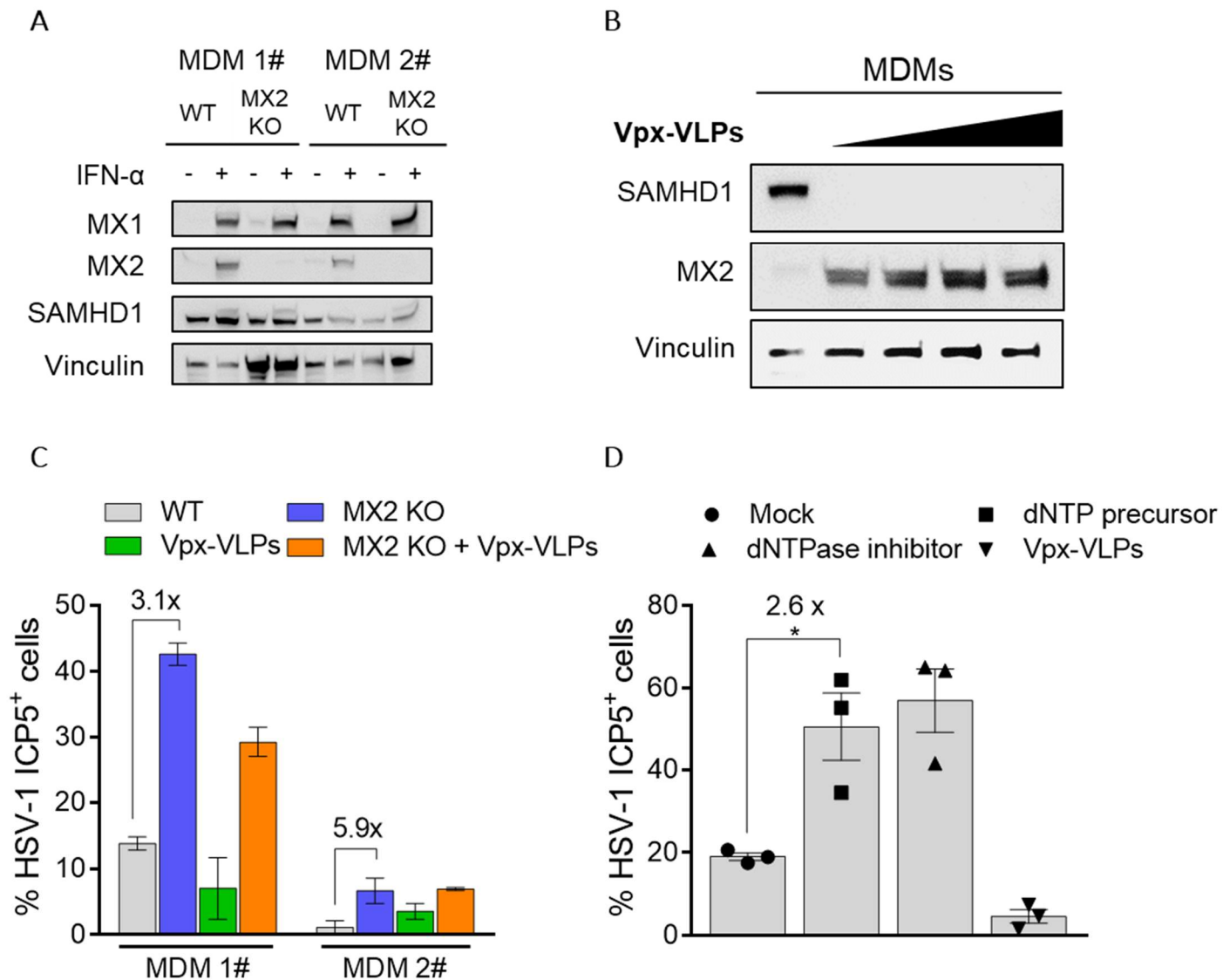
Figure 24: MX2 and SAMHD1 are post-entry inhibitors of HSV-1 in MDMs
(A) MX2 KO primary MDMs from 2 donors were generated and the MX2 KO efficiency was validated by immunoblotting after IFN-α (10 IU/mL) treatment. (B) After 24 h of incubation with Vpx-VLPs, SAMHD1 in WT MDMs was analyzed by immunoblotting. (C) WT, MX2 KO or SAMHD1 degraded MDMs were challenged with HSV-1 at a low MOI, cells were harvested and quantified 18 h p.i. (D) Prior to infection of HSV-1, WT MDMs were provided with dN for 0.5 h, and SIK0001 or Vpx-VLPs for 24 h. Each dot depicts biological replicates. Statistical analysis was performed using two-way ANOVA.

To test whether MX2 can inhibit HSV-1 replication, we generated MX2 KOs in MDMs from two donors (MDM 1# and 2#) and treated them with IFN-α. As shown in Figure 24. A, MX2 level was completely abrogated in both MDM 1# and MDM 2# while MX1 and SAMHD1 expressions were not influenced, suggesting the specifics of our developed protocol. As expected, MX2 KO MDMs were more vulnerable to HSV-1. Immunoblots showed that MX2 KO was efficient within two donors and resulted in 3.1-fold to 5.9-fold increased levels of HSV-1 replication, respectively (Figure 24. C). These

findings point to MX2 as a conceivable restriction factor that prevents DNA and RNA viruses from replicating. To validate SAMHD1's effect on HSV-1, MDMs were pretreated with Vpx-VLPs for 24 h and SAMHD1 degradation was evaluated by western blotting. SAMHD1 was efficiently degraded in MDMs exposed to Vpx-VLPs (Figure 24. B). The WT, MX2 KO, Vpx-VLPs treated MDMs were then infected with HSV-1 and infection levels were evaluated by flow cytometry 18 h p.i. As shown in Figure 24. C, despite that the two cell samples were identically treated, the non-targeting control's baseline infection rate varies due to donor infectivity variability. Thus, each assay was only compared to donor-matched controls, and infection rates were calculated separately.

As the HSV-1 restriction observed HSV-1 restriction corresponds to low dNTP levels in the previous report [267], we investigated if supplying a source of dNTPs could facilitate in overcoming the HSV-1 restriction. MDMs were pretreated with either dN, SIK0001 or Vpx-VLPs and infected with HSV-1 for 18 h. The following day, MDMs were harvested and HSV-1 replication was quantified by flow cytometry. A higher level of ICP5-positive cells was observed only in the dN and SIK0001 treatment, but not for the Vpx-VLPs treated cells (Figure 24. D). dN's adding enhanced HSV-1 replication by 2.6-fold for MDMs, and SIK0001 treatment demonstrated comparable level of dN's enhancement, supporting that providing an excess of dNs as well as small molecule-mediated blocking of SAMHD1's dNTPase activity can relieve the restriction for HSV-1. This suggests that SAMHD1 inhibits HSV-1 in differentiated macrophages through reducing the intracellular pool of dNTPs. Whereas the details of SAMHD1's antiviral activity (dNTPase vs. RNase activity) is debatable, we firstly evaluated if SAMHD1 degrading has an effect on HSV-1 replication. Conversely, HSV-1 replication in Vpx-VLPs treated MDMs was reduced (Figure 24. D). The combination of MX2 KO and Vpx-VLPs' mediated SAMHD1 degradation showed less fold increase of HSV-1 replication than the MX2 KO MDMs, but rescue more replication than the only Vpx-VLPs treated MDMs, indicating that MX2 is a major restriction factor in the IFN-mediated antiviral response (Figure 24. C). SAMHD1 is involved in a complex process that maintains the equilibrium between virus replication and immune response [370]. While Vpx-VLPs treatment showed a substantial decrease in SAMHD1 levels, it induced antiviral MX2 expression, indicating that the ISGs induction triggered by addition of Vpx-VLPs may outweigh the net effect on this virus (Figure 24. B). These

findings provide the hypothesis that Vpx-VLPs pretreatment reduces HSV-1 replication and the possible reason might be the high HSV-1 sensitivity to an IFN response. We demonstrate here that SAMHD1 inhibits HSV-1 replication in MDMs via dNTP triphosphohydrolase activity, which can be partially overcome by exogenous dN or SIK0001. While degradation of SAMHD1 by Vpx-VLPs repressed HSV-1 replication. Collectively, these data suggest that *trans*-differentiated BLaER1 cells respond similarly to MDMs in the perspective of HSV-1 infection. Thus, MX2 and SAMHD1 are post-entry inhibitors of HSV-1 in *trans*-differentiated BLaER1 and primary MDMs.

3.10 Loss of NLRP3 and DDX1 results in enhanced HIV-1 infection and ISGs induction in *trans*-differentiated BLaER1 cells
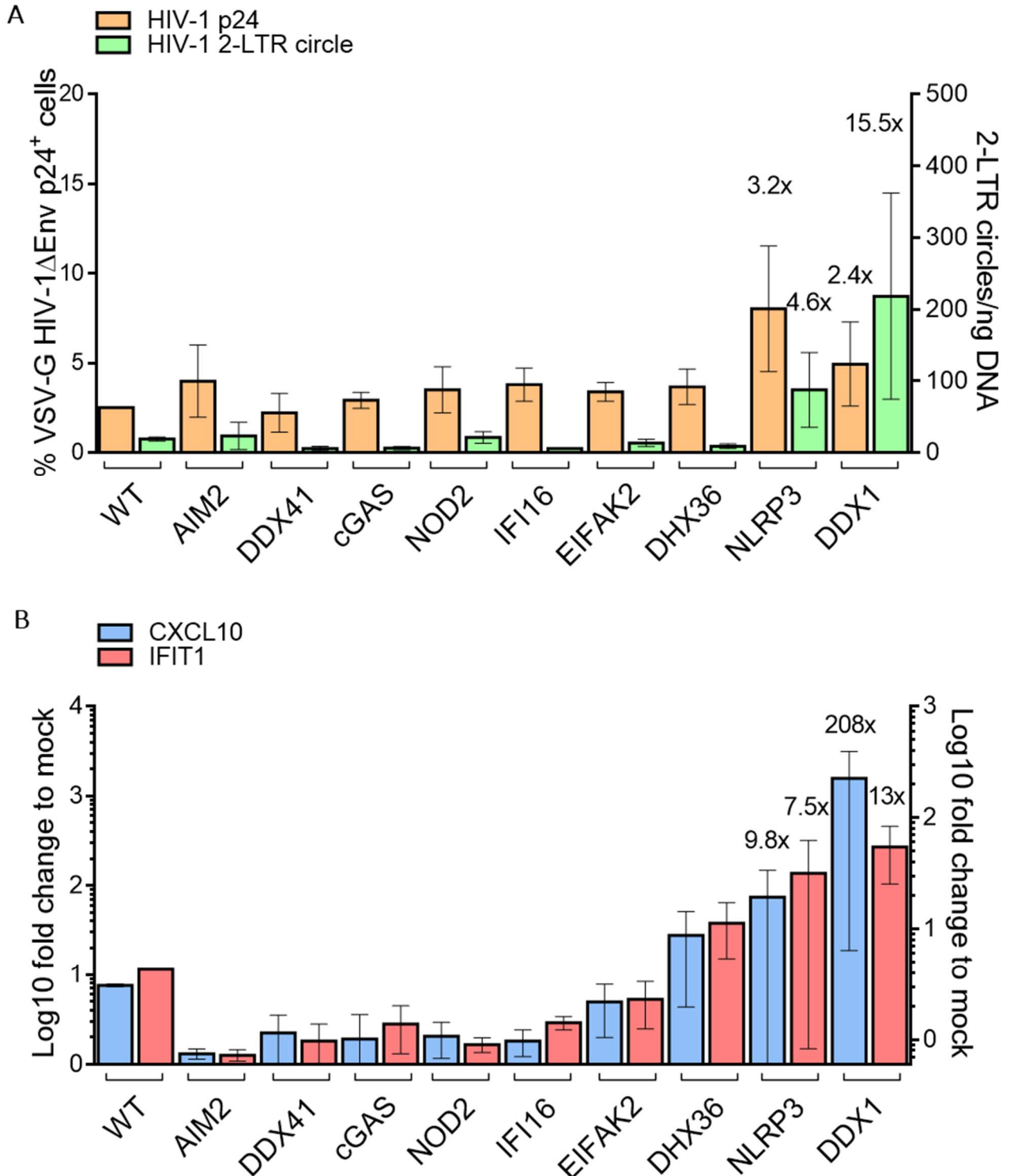
Figure 25: An educated screening for putative sensors and restriction factors of lentiviruses in BLaER1 macrophages indicates a suppressive role of NLRP3 and DDX1 on HIV-1 infection in myeloid cells

Trans-differentiated BLaER1 WT and KO cells (typically three individual cell clones per condition) were challenged with VSV-G HIV-1ΔEnv. Cells were harvested and fixed at 48 h p.i. (A) Cells were stained for intracellular HIV-1 p24 expression and analyzed by flow cytometry. In addition, cells were analyzed

by qPCR for relative levels of episomal 2-LTR circles, (B) CXCL10 and IFIT1 expression levels. Shown are arithmetic means ± SD. Numbers above histograms indicate the factor of increase compared to WT cells.

According to the above findings, *trans*-differentiated BLaER1 cells are similar to primary MDMs in some aspects, making them a viable and valid platform for testing the function of restriction factors. To exploit this system for candidate restriction factor screening, after genetic editing to achieve stable knock out phenotypes, knockout cells were *trans*-differentiated and challenged with VSV-G HIV-1ΔEnv, with virus replication and ISGs induction monitored. To identify novel cellular factors that can modulate HIV-1 infection, we have generated in collaboration with the Hornung laboratory 9 candidate KOs, i.e. for AIM2, DDX41, cGAS, NOD2, IFI16, EIF2AK2, DHX36, NLRP3 and DDX1, and examined their effect on replication of HIV-1. The KOs of AIM2, DDX41, cGAS, NOD2, IFI16, EIF2AK2 and DHX36 had only minor or no effects on VSV-G HIV-1ΔEnv infection (Figure 25.). In contrast, both NLRP3 and DDX1 KOs markedly enhanced the rate of HIV-1 infection. This was evident in the percentage of p24 production (Figure 25. A; 2.4-to 3.2-fold), which was more prominently reflected in 2-LTR circle levels (Figure 25. A; 4.6-to 15.5-fold) in *trans*-differentiated BLaER1 cells.

To test that a loss of these candidate sensors also reduced antiviral IFN induction, IFN-α driven-CXCL10 and IFIT1 mRNA expression were evaluated. Unexpectedly, both infected NLRP3 and DDX1 KO BLaER1 cells showed an increased induction of CXCL10 and IFIT1 mRNA (Figure 25. B), compared to infected WT control cells. The observed low levels of ISG induction is consistent with previous findings in MDMs that HIV-1 infection can be detected at a post-integration step, resulting in a late upregulation of ISGs during the replication cycle [237]. Consideration of the temporal dynamics of infection and innate recognition, this could be explained by two scenarios: (i) KO of NLRP3 or DDX1 allows for an increased sensing of HIV-1 that does, however, not induce anti-viral ISGs. They failed to block reverse transcription (as reported for DDX41), promoting the progress of the early stages of the replication cycle; (ii) these knockouts result in an reduction of HIV-1 sensing and a lack of antiviral ISG induction (removal of a direct constraint on the early post-entry phase of the virus), allowing the replication cycle to progress more efficiently up to integration and viral transcription, inducing as a "secondary post-integration phenotype" the observed induction of ISGs. These data emphasize the significance of multiple protection from host. Collectively,

these results suggest that *trans*-differentiated BLaER1 cells display macrophage-like properties and are permissive to post-entry steps of HIV-1 replication, making them a potential model for studies into the HIV-1 infection of macrophages.

4. Discussion

Both HIV-1 and HSV-1 are a constant threat to human health as they can cause latent infection and a sterilizing cure is still not possible. Macrophages are mononuclear, tissue-like leucocytes that play a significant role in innate immunity to viral eradication. It is well documented that HIV-1 and HSV-1 can successfully infect macrophages *ex vivo* and *in vivo* animal models [130]. Identifying the host-pathogen dynamics that regulate viral replication in human macrophages is therefore crucial. However, the data from the most cell lines may not fully recapitulate phenotypes in primary cells due to several limitations [448]. In the current thesis, we focussed on three critical aims: (i) establish a novel, macrophage-like model in genetically easily amendable BLaER1 cells, (ii) establish an efficient CRISPR/Cas9 knockout methodology for primary human macrophages and (iii) examine putative restriction factors in both cell systems.

4.1 Modeling human primary macrophages with the *trans*-differentiated BLaER1 cells

Immortalized myeloid cell lines are typically proliferating and must be differentiated, which is commonly treated with PMA and/or Vitamin D before exhibiting monocyte or macrophage characteristics [449]. These pre-treatments have the potential to activate a variety of non-PRR signaling pathways, as well as render the cells resistant to PRR stimulation [450]. The best-characterized cell line in this context, BLaER1, was derived from human immortalized immune B cells that can express C/EBPα when pretreated with β-estradiol [393]. Although C/EBP factors have been identified to regulate HIV-1 LTR promoters, of particular relevance is the finding that C/EBPβ is required for efficient replication of HIV-1 in macrophages but not in CD4-positive T cells [451], there is no report of C/EBPα influencing viral replication. Thus, interactions between C/EBPα and HIV-1 could be ignored. We found that BLaER1 cells polarize into an M2 macrophage-like cell morphology after *trans*-differentiating from a proliferative to a post-mitotic state (Figure 13) [393]. Importantly, after *trans*-differentiation, BLaER1 cells became competent for multiple innate immune signaling pathways [389]. Since *trans*-differentiated BLaER1 cells were permissive to the infection or at least post-entry steps of both RNA and DNA viruses (Figure 16 and 17), this study utilizes *trans*-differentiated BLaER1 cells as a model system to investigate effects on virus replication and immune responses in macrophages. Using an optimized work-flow for

knockout generation in BLaER1 cells (Figure 6), we studied the role of the indicated cellular proteins on HIV-1 or HSV-1 infection in *trans*-differentiated cells. We have generated monoclonal KOs of MX2 and SAMHD1, as well as 9 cellular proteins involved in viral sensing and restriction. MX2 is an ISG with a wide range of antiviral activities [310]. We demonstrated that *trans*-differentiated BLaER1 cells responded to IFN-α treatment, and MX2 expression can be induced after IFN-α activation in BLaER1 cells similar to primary macrophages (Figure 14. A). SAMHD1 is a dNTP hydrolase which can block viral gene synthesis while also controlling cell proliferation, differentiation and survival [452]. Remarkably, SAMHD1 protein expression was readily detected in *trans*-differentiated cells BLaER1 cells. Albeit being expressed at a low level, SAMHD1 was sufficient to block lentivirus transduction (Figure 10. A and D). In line with results from primary macrophages [429], SAMHD1 expression was not further increased by IFN-α in BLaER1 cells (Figure 14. A). BLaER1 cells have a fully functional SAMHD1 after *trans*-differentiation and SAMHD1 can be degraded by Vpx-VLPs (Figure 10. B). Based on these reports and also to increase sensitivity of β-estradiol activation, we found that starving BLaER1 cells can enhance *trans*-differentiation suggesting a cell cycle arrest (Figure 8. B). Furthermore, following dN augmentation of the culture medium, BLaER1 cells became more differentiated and more susceptible to lentiviral transduction (Figure 11. A). We speculate that dN pre-treatment elevates cytoplasmic dNTP levels for gene re-programming and in turn also depletes proliferating B cells (Figure 11. B). Consistent with this observation, SAMHD1 KO cells also displayed a mature morphology. The addition of either dN or the SAMHD1 inhibitor SIK0001 increased lentiviral transduction, suggesting that SAMHD1 inhibits transduction by limiting dNTP pools (Figure 10. D). In comparison to the effects of exogenous dN and SIK0001, the rescue effects on Vpx-VLP lentiviral transduction are greatest in MDMs but limited in BLaER1 cells (Figure 10. C and D). We found that Vpx-VLPs pre-incubation deletes SAMHD1 efficiently while triggering ISG induction (Figure 10. B). The MX1 induction indicates an antiviral state was triggered by Vpx-VLPs which in turn inhibited lentiviral transduction.

The presence of specific receptor on macrophages is required for HIV-1 infection, we first measured the levels of CD4, CCR5 and CXCR4 on the BLaER1 cell surface before and after *trans*-differentiation. Freshly isolated primary monocytes and differentiated

macrophages served as a reference. Consistent with previous reports, we found that primary monocytes expressed relatively high levels of CCR5, which decreased to medium levels upon differentiation to MDMs (up to 70% of CCR5-positive cells) [403]. CD4, CCR5, and CXCR4 were expressed on the surface of *in vitro* cultured MDMs, but only at low levels (Figure 9. A) [403]. In BLaER1 cells, we found that CD4 and CCR5 were not expressed, and CXCR4 was only expressed on the surface of proliferating BLaER1 cells. Since the HIV-1 entry receptor complex was either absent or down-regulated upon conversion of BLaER1 cells into a macrophage-like phenotype, we used a single-round HIV-1 in which the viral envelope protein was replaced with that of VSV, which can infect a wide range of cell types, to study post-entry steps of HIV in genetically altered macrophage-like BLaER1 cells.

During the replication cycle of HIV-1, multiple elements are produced that may be recognized by PRRs [151]. However, HIV-1 sensing is a complicated process that is highly dependent on the cell type [453]. In human myeloid cells, such as MDDC [365] or MDMs [182], HIV-1 infection is initially poorly detected and does not provoke detectable activation of NF-kB or production of IFN-ß. It has also been demonstrated that HIV-1 inhibits TLRs mediated responses in alveolar macrophages and macrophage cell line U1 [454]. While others claim that HIV-1 tends to induce ISGs and activate the inflammasome [455, 456]. These inconsistencies could be due to a variety of experimental methods and cell types. In our study, HIV-1 productive infection of BLaER1 cell induced a weak, yet detectable, ISG response, with levels of MX2 remaining undetectable. Our findings are consistent with former research on ISG induction of HIV-infected primary MDMs [457]. In these cells, only dN pretreatment allowed productive infection, yet ISGs were not significantly induced on the protein level and slightly on the mRNA level (Figure 15. A). Inhibition of HIV-1 replication by reverse transcriptase EFV and the integrase inhibitor DTG served as reference controls. Furthermore, dN and small molecule SIK0001 pretreatment overcome the SAMHD1 restriction (Figure 10. D). In combination, these results indicate (i) the ability of HIV-1 to go through post-entry steps in BLaER1 cells, (ii) SAMHD1 may be a relevant restriction in this model system and (iii) that HIV-1 replication prevents strong ISG induction (Figure 15. B). Unexpectedly, the retroviral SMRV, which shows a broad range of permissiveness for cell lines and multiple species, was identified as being integrated and continuously released from BLaER1 cells (Figure 16. B) [421]. Although

primate retroviruses and their components are typically potent agents to interfere with the delicate balance of immune regulation and cytokine production, SMRV apparently did not induce ISGs in BLaER1 cells and did not markedly alter HIV-1 or HSV-1 replication (Figure 14. A, Figure 17. C). Thus, the presence of this endogenous retrovirus still allowed meaningful and well controlled mechanistic studies in the context of infection experiments. MX2 and SAMHD1 were already identified as HIV-1 or HSV-1 restriction factors in BLaER1 cell lines. These findings suggest that *in vitro* model systems of *trans*-differentiated BLaER1 cells can be important to answer critical issues in virology and innate immunity. It's critical that the results of the BLaER1 model be reproduced primary macrophages.

4.2 CRISPR/Cas9 ribonucleoprotein-mediated gene knockout in MDMs

Many studies utilize transformed myeloid cell lines or genetically engineered murine models since they are relatively easy to culture. However, phenotypic differences between transformed cell lines and primary human myeloid cells exist in many biological processes [458]. This is particularly relevant to the context of innate antiviral immunity given the known but as yet not validated cellular factor. Primary human macrophages lack candidate PPRs and restriction factors implicated in innate immune activation in THP-1 cells, murine macrophages, and human PBMCs. Current strategies for identifying genes of interest or significance include overexpression and knockdown [167]. Gene-targeted knockdown studies produce results that are more representative of the effect of a particular gene than overexpression studies, which produce an excess expression profile that may be rare in a normal cell. Some studies combined knockdown and overexpression strategies to assess the effect of a gene. While these techniques suggest a particular role for a gene in viral replication, the majority of the suggested candidate genes were proved with a single report and did not appear to be verified [459, 460]. The experimental differences can also lead to inconsistence data. It was found that HIV-1 ssDNA stimulates IFN-α expression in MDMs through IFI16. However, the experiments were carried out by DNA transfection which does not mimic real infection [461]. The role of MX2 and SAMHD1 as restriction factors was demonstrated mainly on different knockdown or knockout cell lines and our BLaER1 model. It is critical that the results from BLaER1 model be evaluated in primary macrophage.

Because of macrophages' sensitivity (e.g. AIM2 and STING) to foreign genetic material, they are difficult to transfect manipulation [461, 462]. In this study, we recently described that 25 nM SMARTpool siRNA has been tested yielding a 20% knockdown at a final DharmaFECT1 concentration of 0.2% [v/v]. However, increasing the volume of DharmaFECT1 reagent was not ideal for delivering siRNA into primary MDMs as it resulted in unexpected transfection efficiency and cell death (Figure 19. A). Despite the HiPerFect-mediated gene inactivation approach has been routinely used in primary macrophages, we observed that HiPerFect resulted in poor gene knockdown efficiency when siRNA concentration was 25 nM above (Figure 19. C). In addition, HLA-DR activation was induced by both DharmaFECT1 and HiPerFect reagent. siRNA

technology is a powerful tool, but neither of the transfection reagents tested were particularly effective in our primary macrophage studies. Another macrophage model comes from pluripotent stem cells, which can be genetically modified and induced to differentiate into macrophages via hematopoietic differentiation [463]. This method, however, is complicated and costly. Thus, the selection of the macrophage model system and specific experiment methods is critical for evaluating innate immune responses. Although primary cell systems are more difficult to manipulate and donor variables, they yield more physiologically relevant data. Tissue macrophages from HIV-1-infected individuals help to reveal the viral reservoir's relevance and composition *in vivo* [77, 80]. Despite the fact that siRNA-mediated gene inactivation is the most common method for characterizing target gene in macrophages, the high-throughput screening through siRNA is limited. Owing to the difficulty of isolating macrophages from tissues, and transfection subjects macrophages to significant stress that may alter their phenotype [464], we next applied CRISPR/Cas9 edited MDMs to characterize HIV-1 or HSV-1 infection.

Compared to the utility of the RNAi approach which is limited by poor editing efficiencies and specificity, genetic manipulations using the CRISPR/Cas9 system have been shown to be effective in either eliminating non-integrated HIV-1 provirus or specific host factors [465, 466]. Using the CRISPR/Cas9 system, a genome-wide screening of cellular factors that may influence virus replication, is possible [199]. For example, LEDGF and TNPO3 have recently been knocked out in primary CD4-positive T cells via RNP nucleofection, resulting in a coreceptor tropism-independent reduction in HIV-1 infection [467]. CRISPR/Cas9 has also been harnessed to target several HSV-1 genes. The deletion of ICP0 and UL7 *in vitro* was shown to completely inhibit viral replication [468]. Thus, we modified a type-II CRISPR/Cas9 system comprised of endonuclease SpCas9 and two to three pre-selected, target-specific sgRNAs to evaluate the gene ablation efficacy at the targeted loci (e.g., CD32a, CD46, MX2 and SAMHD1). CD14-positive monocytes are most commonly present in peripheral blood and can be typically differentiated *in vitro* into macrophages, making them an ideal tissue source to generate genetically altered primary myeloid cells [469]. Since the major challenges of CRISPR/Cas9 are the efficient delivery of sgRNA/Cas9 and precise genome cleavage efficacy, we have optimized the workflow for efficient gene ablation in monocytes to study primary MDMs biology (Figure 18). In this study, factors

that might influence gene editing were considered, such as cell isolation, sgRNA selection, RNP preparation, nucleofection and cell differentiation.

We first utilized the CRISPR/Cas9 system to knock out two myeloid markers, CD32a and CD46, in order to rapidly genetic modification performance using flow cytometry in freshly isolated monocytes. Liposomal-, viral- and electroporation-based systems are currently used to deliver sgRNA/Cas9 into cells. Liposomal-based systems have a lower delivery efficiency and higher cytotoxicity than the others, while viral vector-based systems can maintain stable transgene expression but cause inflammatory side effects [470]. The nucleofection method has been used to transfer genes without affecting cell viability or causing non-specific immunogenic effects [471, 472]. Importantly, nucleofection is apparently able to circumvent sensing by nucleic acid-specific PRRs in MDMs. After nucleofection, monocytes were cultured in macrophage generation medium to allow targeted gene deletion (Figure 18). The optimal knockout condition and macrophage polarization are affected by the amount of specific RNPs, the LPS-free environment and the cytokine stimulation. We observed that using sgRNAs instead of crRNAs significantly improved gene editing efficiency in MDMs (Figure 20. A). Individual sgRNAs exhibited different editing efficiency were revealed by sanger sequencing analysis, while multiple targeting events may increase the chances of a frameshifting indels improving KO efficiency (Figure 21. B). To improve target gene disturbance, the V3 Cas9 (IDT) was used to generate a few RNP variants with multiple sgRNAs. Using multiple sgRNAs, it is possible sufficient to accomplish an 85% reduction in protein levels of targets at least (Figure 19. A). Further, the consistently robust knockouts were confirmed by ICE analysis (Figure 21. B). Alternatively, polarization conditions causing differential expression of chemokine receptors and PRRs should be considered [473]. The levels of host factors (e.g., ADAM10 and PKC-delta) that positively regulate HIV-1 replication could be altered by macrophage polarization, allowing macrophages to be differentially vulnerable to HIV-1 infection [474, 475]. MDMs stimulated with M-CSF are most similar to tissue macrophages, as opposed to MDMs differentiated with GM-CSF, which are more similar to alveolar macrophages [476]. Aside from the cytokines that were tested, cell density was another important parameter to consider. We observed that seeding monocytes at a lower density increased nucleofection efficiency (Figure 20. C). In the current study CRISPR/Cas9-edited monocytes were differentiated into macrophages

in vitro upon stimulation by M-CSF at low density. Differentiation is a basic biological function of macrophages. The differentiation and maturation state were evaluated by examining typical morphology and quantifying classic myeloid genes expression. Comparison of myeloid markers (CD14 and CD11b) revealed no specific changes following nucleofection. We examined the CD86 and CD206 expression, which are markers of M2 macrophages, since maintenance of normal cell state during the gene editing is critical [477]. We discovered that M2 markers were detectable equally between WT and KO MDMs, suggesting that RNP nucleofection did not affect differentiation (Figure 19. D). Moreover, RNP delivery had no effect on phagocytosis activity and cell activation. Therefore, RNP-mediated gene editing was demonstrated to be highly efficient and specific compared to RNAi.

This study aimed to establish macrophage models for viral infection. Besides the BLaER1 cell line, very few reports in the literature have thus far been dedicated to efficient knockouts in human primary macrophages. We conducted a comparative study of a given siRNA-mediated gene silencing approach and CRISPR/Cas9-mediated gene deletion among primary macrophages. We customized cell isolation, nucleofection and differentiation processes of this methodology. Along with this protocol, the genetically altered primary macrophage can be implemented into immunological and virological-phenotypic assessments. This method is capable of having >100 million monocytes available for from a single donor buffy coat, allowing for genome-wide CRISPR screens to identify genes that affect viral replication. With MX2 and SAMHD1 have been mainly characterized in cell lines for their antiviral capacity. The second goal of this study was to investigate the potency of MX2 and SAMHD1 in blocking viral replication in macrophages. After nucleofection with sgRNP targeting MX2, genetically modified monocytes were stimulated with M-CSF to generate MDMs. MX2 expression was significantly reduced while cell viability was maintained, which is consistent with the inactivation of CD32 and CD46. The functional analysis shows for the very first time that MX2 hinders HIV-1 or HSV-1 replication in primary macrophages, representing a highly physiologically relevant model *ex vivo* compared with human cell lines and animal models (see next section).

4.3 MX2 and SAMHD1 are ISGs to HIV-1 and HSV-1 infection

A plenty of proteins with antiviral activity have been discovered in recent years. Remarkably, several of them prevent not only RNA viruses like HIV-1, but also DNA viruses like HSV-1 from replicating. These cellular proteins include MX2 and SAMHD1. Since they act at post entry steps, we considered them as promising restriction factors and two macrophage models were developed to knockout, validate and compare the inhibitory activity of both factors toward HIV-1 and HSV-1.

MX2 plays a role in suppressing HIV-1 acquisition and replication according to epidemiological and evolutionary evidence [478]. It has been noted in one study that MX2 accumulating at the nuclear pore blocks HIV-1 infection after reverse transcription [479] and/or before viral DNA integration with decreased levels of 2-LTR [480]. However, another study found that MX2 had no impact on the number of 2-LTR circles [275]. Given the ability of HIV-1 viral CA mutants (e.g., G89V, N57S) to evade MX2 restriction, it is proposed that MX2 targets the viral CA [273]. MX2 may be specifically bound to the incoming HIV-1 CA, similar to the primate TRIM5α, CPSF6 or NUP153, but the exact mechanism that affects CA uncoating is unknown [481]. On the other hand, MX2's attachment to HIV-1 CA is not always correlated with virus inhibition, suggesting that MX2 destabilizes viral DNA and/or inhibits the nuclear accumulation indirectly [315]. This restriction may occur via a host factors (e.g., CypA, Nups) dependent mechanism [321]. MX2's ability to prevent HSV-1 dsDNA from reaching the nucleus is dependent on its proper intracellular localization and GTP hydrolysis, which is an evolutionary conserved characteristic among Herpesviridae [274, 325]. The inhibitory roles of MX2 are still poorly understood. One major reason is that experiments from shRNA knock down or CRISPR/Cas9 knock out of MX2 are inconsistent in cell lines [273, 431]. Another explanation is that the MX2 expression levels differ between cell lines and primary cell types. We therefore attempted to construct two specific macrophage models able to elucidate mechanisms of how MX2 inhibits HIV-1 and HSV-1.

MX2 induction by IFN- results in a significant reduction in HIV-1 replication [276]. We have previously shown that *trans*-differentiated BLaER1 cells do not express detectable levels of MX2 in the absence of IFN-α pretreatment (Figure 14. A). We

hypothesized that perturbing MX2 expression may enhance viral infection in macrophage-like cells, as reported by others in various cell lines [319]. To determine whether HIV-1 infection itself leads to the stimulation of endogenous MX2 expression, *trans*-differentiated BLaER1 cells infected with VSV-G pseudotyped HIV-1ΔEnv at low MOI were prepared. For experiments to simultaneously assess whether MX2 was indeed responsible for the inhibition, IFN-α-activated WT and MX2 KO pairs of *trans*-differentiated BLaER1 were challenged with virus at high MOI. We show that MX2 inhibits the replication of HIV-1 by a SAMHD1-independent pathway in *trans*-differentiated BLaER1 cells. The BLaER1 cell model demonstrates similarity to primary macrophages in their ability to support HIV-1 replication, but not stimulate strong MX2 expression. We have shown in this study that MX2 inhibits the replication of HIV-1 in *trans*-differentiated BLaER1 cells, yet the anti-viral activity of MX2 in particular has so far not been demonstrated in terminally differentiated primary cell types. With the aim of reconciling these discoveries, we applied CRISPR/Cas9 to knock out MX2 in primary macrophages. Mechanistically, MX2 appears to hinder nuclear import of the PIC in primary MDMs (Figure 16. C and D), in line with previous reports [273]. Although MX2's role in HIV-1 inhibition was questioned [431], a MX2 knockout rescued infection of R5 HIV-1 or VSV-G pseudotyped HIV-1ΔEnv in primary MDMs (Figure 22. C), which also implies that MX2 inhibition occurs after entry. Our study demonstrates that depletion of MX2 by CRISPR/Cas9 gene editing yields a significant increase in viral replication in primary MDMs. This is reminiscent of our recent observations using the HIV-1-infected BLaER1 cell line model.

In contrast to HIV-1, HSV-1 infection leads to strong innate immune responses, yet the sensors involved for herpesviruses are largely undetermined. In *trans*-differentiated BLaER1 cells, the induction of chemokines and ISGs by HSV-1 replication correlated with the level of productive infection quantified by the abundance of the HSV capsid ICP5 (Figure 17. A and B). Levels of CXCL10 and IFIT1 production were similar to that seen upon treatment of cells with IFN-α at 1000 IU/mL, which was also mirrored by the induction of MX2 by HSV-1 infection (Figure 17. B and C), suggesting that MX2 as an ISG may play a role in HSV-1 restriction in *trans*-differentiated BLaER1 cells and MDMs (Figure 24. B). In primary MDMs, HSV-1 infection induced ISGs in an MOI-dependent fashion (Figure 23. A). These observations suggest HSV-1 has not yet

evolved an effective strategy to evade the activity of cellular MX2. In summary, this shows for the first time that MX2 inhibits HIV-1 and HSV-1 replication in BLaER1 macrophage-like cells and primary MDMs.

SAMHD1 is an ISG that can be activated in an amount of cell lines and primary MDMs [482]. New important roles of DNA repair and DNA degradation have also been unveiled [369, 483]. SAMHD1 is a dNTPase, which contributes to low dNTP abundance and inhibits proviral DNA synthesis HCMV, VACV, EBV and HBV [268, 339, 373, 484-486]. Additional studies showed that SAMHD1 might also contribute to viral inhibition via its RNase and Nuclease activities, although these results require further validation [355, 357]. Phosphorylation regulates SAMHD1's antiviral restriction function but not its dNTPase activity [346], since phospho-SAMHD1 lacks anti-HIV activity but can reduce the dNTP levels [353]. SAMHD1 appears to be sufficient in inhibiting HSV-1 replication by lowering cellular dNTP levels, but HIV-1 restriction may require cofactor as phospho-SAMHD1 abolished only HIV-1 but not HSV-1 restriction. We observed that inhibition of SAMHD1 dNTPase activity leads to a significant increase in HIV-1 replication in both *trans*-differentiated BLaER1 cells and primary MDMs (Figure 10. C and D). To discover more about SAMHD1's role in viral restriction in primary macrophages, MX2/SAMHD1 double knockout cells should be generated, since an interplay of these factors has been suggested [375]. SAMHD1 has been shown to inhibit HSV-1 via its dNTPase activity [267]. The SAMHD1 knockout enhanced HSV-1 replication to levels comparable to the MX2 knockout in *trans*-differentiated BLaER1 (Figure 17. A). SAMHD1 has been shown to be inhibited by the small molecule SIK0001 or to be overcome by dN treatment, which allowed HSV-1 to escape the SAMHD1 restriction. Interestingly, exogenous dN and SIK0001, but not Vpx-VLPs treatment, overcame the SAMHD1-mediated restriction of HSV-1 in *trans*-differentiated BLaER1 cells (Figure 17. D) and primary MDMs (Figure 24. D). The lack of intracellular dNTPs, which are regulated by SAMHD1, appears to be the mechanism. However, Vpx-VLPs-mediated SAMHD1 degradation had a inhibitory effect on HSV-1 replication. The possibility was that Vpx-VLPs induced antiviral state while HSV-1 was highly susceptible to IFN sensitivity. Enhanced ISG MX1 transcripts were already found in *trans*-differentiated BLaER1 cells treated with Vpx-VLPs without viral challenge (Figure 10. B). In line with this observation, Vpx-VLPs treatment appears to be able to induce a broad antiviral state in primary MDMs (Figure 24. B). Although Vpx-

VLPs are devoid of the viral RNA genome, they are capable of fusing and eliciting an ISG response. One explanation could be that plasmid DNA used during the production of 293T cells may contaminate the Vpx-VLPs production and induce innate responses. Membrane disruptions, such as infection-induced fusion events, can trigger the STING→TBK-1→ IRF-3 signaling, which helps macrophages resist virus entry [487]. Similarly, macrophages have been shown to detect the fusion of herpesviruses or liposomes independently of cGAS [488]. Infection with enveloped viruses triggers intracellular Ca^{2+} oscillations upon virus entry and virus-cell membrane fusion is detected by the host contributing to IFN antiviral responses [488, 489]. Thus, dissection of virus-specific and methodology-driven responses in these virus-host interaction models will be critical to understanding the underlying biological processes with relevance to virus pathology.

Our findings show that HSV-1 is not able to escape SAMHD1 restriction in both *trans*-differentiated BLaER1 cells and MDMs. We found no evidence that HSV-1 counteract SAMHD1's effects in this study, as SAMHD1 is not degraded during infection. Unlike retroviruses, some large dsDNA viruses, such as vaccinia virus, have extra dNTP biosynthesis machinery, including TK and RNR, to enhance a measurable increase in dNTP concentrations. In contrast with HIV-2 and the related SIV, which encode Vpx proteins to antagonize SAMHD1, the β- and γ-herpesviruses utilize protein kinases to phosphorylate SAMHD1 on T592 without affecting its protein level. However, whether α-herpesviruses HSV-1 counteract the restriction of SAMHD1 by phosphorylation is unknown. Future studies will examine the functions of phospho-SAMHD1 to explain the mechanistic differences between inhibition of HIV-1 and HSV-1 in MDMs.

4.4 Limitations of the study

Collectively, we demonstrate that *trans*-differentiated BLaER1 cells express myeloid surface markers, known restriction factors, and are highly phagocytic. Furthermore, we developed a rapid and efficient protocol to knockout genes in primary macrophages. Both of these genetically modifiable macrophage cell models for HIV-1 and HSV-1 infection were validated for the role of cellular MX2 and SAMHD1 in restricting viral replication. Although these model systems provide feasible ways for validation of

genes that can positively or negatively affect HIV-1 and HSV-1 infection, there are still a number of limitations of the current work:

Firstly, while generating *trans*-differentiated BLaER1 cells allowing rapid genetic and functional screens these cells lack the HIV-1 entry receptor complex, requiring the use of alternative, less physiological entry pathways of this lentivirus.

Secondly, while the presence of the newly discovered SMRV coinfection did not appear to significantly affect HIV-1 or HSV-1 replication, it is still unclear to what extent this retrovirus may modulate innate immunity in this screening system that could affect the biological outcome.

Thirdly, our results are consistent with the notion that MX2 restricts HIV-1 replication after cDNA synthesis and at steps that coincide with nuclear import. This conclusion is based, however, only on the quantification of episomal levels of HIV-1 2-LTR circles. Molecular mechanisms how MX2 exhibits antiviral functions require further analysis, including the role of the viral capsid and the interplay with CPSF6 and nucleoporins.

Fourthly, SAMHD1 is likely to inhibit viral replication at multiple level with its dNTPase activity, single-stranded DNA/RNA binding, and nuclease activities. We present evidence that overcoming SAMHD1 in BLaER1 cells as well as in primary MDMs increases their susceptibility to infection with HIV-1 and HSV-1. However, our findings did not yet identify common and different mechanisms for the restriction of the DNA herpesviruses and the RNA retroviruses. Specifically, it will be interesting to study a panel of MX2 or SAMHD1 deletion and missense mutant proteins, e.g. lacking the N-terminal NLS or lacking GTPase function.

Fifthly, an educated screening for putative sensors and restriction factors of lentiviruses in the *trans*-differentiated BLaER1 cell model indicates a thus far unappreciated suppressive role of NLRP3 and DDX1 on early HIV-1 infection in myeloid cells. However, due to time restrictions we were unable to extend these interesting findings to primary macrophage models which lack NLRP3 or DDX1.

4.5 Conclusions and perspectives

The aim of this thesis was to explore virus-host interactions in aspects of macrophage innate immune functions in response to HIV-1 and HSV-1. We address these questions by characterizing and advancing genetic manipulation of two cell models, the *trans*-differentiated macrophage-like BLaER1 cells and MDMs. As proof-of-concept, we focused on the activities of the putative antiviral factors MX2 and SAMHD1 on both HIV-1 and HSV-1 replication. We demonstrated that (i) the BLaER1 cell model can be used as a complementary tool for CRISPR/Cas9-mediated screening for and studying of candidate cellular genes involved in virus replication; (ii) CRISPR/Cas9-mediated gene editing can be applied successfully and efficiently to MDMs, thus providing a highly relevant methodology to study virus-host interaction in physiologically relevant primary cells; and (iii) BLaER1 macrophage-like cells and MDMs display similar response patterns to virus infection, validating the usefulness of the BLaER1 model system. CRISPR/Cas9-based gene editing provides a powerful methodology to explore or corroborate the function of specific host factors involved in viral inhibition. Already established knockouts in BLaER1 cells have been applied for screening of candidate factors for sensing and restriction of viral replication. Mimicking the BLaER1 workflows, CRISPR/Cas9 system can be efficiently applied to primary human cells of the monocyte/macrophage lineage. Thus, limitations to high-throughput KO analysis in primary cell types are lessened. We then addressed how this technique can be utilized to study virus-host interactions, specifically the roles of MX2 and SAMHD1 in restricting HIV-1 or HSV-1.

MX proteins belong to the dynamin-like GTPase family and play important roles in cellular trafficking [315]. MX2 has been discovered to interact with HIV-1 nucleocapsid complexes *in vitro*, suggesting that MX2 might be interfering with the HIV-1 uncoating process [490]. MX2 is also thought to block HIV-1 nuclear import by targeting the CA and interacting with other cellular proteins. For an additional post-nuclear entry block, MX2 inhibits nuclear maturation of the PIC [480]. However, the mechanism by which MX2 prevents HIV-1 infection in the early stages is unknown, as MX2-resistant CA proteins are also bound by MX2 [321]. Of note, HIV-1 CA can directly interact with other host cell factors during post-entry steps in cell lines, i.e. CypA, CPSF6, certain nucleoporins and transportins [321]. HIV-1 CA mutants G89V, N57A/S, N74D and

A92E, as well as combined knockouts of MX2 and other CA-binding factors in macrophage models will be important. The demonstration that MX2 blocks early steps of the HIV-1 replication, specifically PIC nuclear import or integration, will now allow further mechanistic studies in macrophages. During HSV-1 replication, CA docks onto a host nuclear pore complex, followed by the viral genome translocating into the nucleoplasm via the nuclear pore, where it is transcribed and replicated in order to spread infection. MX2 prohibits HSV-1 genomes from reaching the nucleus [274]. The function study of MX2 variants revealed that the anti-herpesvirus mechanism differs from the anti-HIV-1 in that it requires both GTP binding and hydrolysis [309]. The nuclear binding is reduced when Nup214 or Nup358 are knocked down, suggesting that nucleoporins are an important cellular factor in HSV-1 CA-nucleus anchoring [327]. Currently, no interaction of MX2 with HSV-1 CA or nucleoporins could be demonstrated. Thus, further work is needed to elucidate the pathogen-specific mode of action of MX2 and specific mutants. To validate whether MX2 is engaged in the modulation of protein transport through nuclear pores, we will generate MX2 GTP hydrolysis defective mutant T151A and binding-deficient mutants K131A, variants of HIV-1/HSV-1 CA and ablate expression of different nucleoporins (e.g., CPSF6, TNPO3, LEDGF) in MDMs. MX2 has evolved adaptively in human populations, and a polymorphism in the gene affects MX2 expression in response to IFN-α as well as HIV-1 infection susceptibility [491]. Therefore, the potential of harnessing MX2 would provide new antiretroviral therapies.

SAMHD1 has recently been discovered to play roles in virology and immunology [370]. It restricts retroviruses RT, ERT and gap repair through its dNTPase activity. Aside from the known dNTP-binding active site, SAMHD1 has exonuclease activities [356]. As a negative regulator, it prevents the excess accumulation of endogenous nucleic acids that cause autoinflammatory diseases [204]. Mutations of SAMHD1 are frequently observed in solid tumors and chronic lymphocytic leukemia [369]. Because dNTPs are a fundamental substrate for DNA synthesis, we sought to broaden SAMHD1's role in restricting DNA virus in primary MDMs. Evidently, the findings in this study prove the assertion that SAMHD1 restricts HSV-1 replication capacity in a way observed in HIV-1 lentiviruses by diminishing cellular dNTPs. Interestingly, neither HIV-1 nor HSV-1 evolved to counteract SAMHD1 during replication. T592 phosphorylation of SAMHD1 is thought to be a critical post-translational modification.

SAMHD1 has been found to become delocalized and inactivated by HCMV-dependent phosphorylation [492]. HSV-1 infection, on the other hand, does not cause T592 phosphorylation, and SAMHD1 inhibits HSV-1 regardless of its T592 phosphorylation state [374]. The most recent evidence on SAMHD1 restriction in HSV-1 and HIV-1 underlines the ambiguous relationship for both dNTPase activity and phosphorylation state. Based on previous work, it is possible to generate phosphomimetic, dNase, or RNase mutants that provides perspective into the regulation of the SAMHD1 imposed restriction to HIV/HSV infection in primary MDMs [442].

The genetic ablation of the restriction factors MX2 and SAMHD1 in both macrophage systems increased HIV-1 or HSV-1 infection, demonstrating the systems' power for genotype-phenotype interrogation. Efficient ablation of *CCR5* has been achieved in HSCT by CRISPR/Cas9 [493], given the importance of macrophages in viral infection, further investigations into cellular factors involved in viral sensing, restriction as well as their interaction with the virus, may facilitate the development of novel therapies. To identify putative post-entry sensors and restriction factors in primary MDMs, we will target multiple nucleic acid sensing modalities that previously proposed in BLaER1: TLRs (TLR3, TLR7, TLR8, TLR9), RLRs (RIG-I, MDA5, LGP2), NLRs (NLRP3, NOD2), cGAS and OAS enzymes, non-RLR helicases (DDX1/DDX21/DHX36, DHX9, DHX36, DDX41, DDX3), as well as DNA damage components (RAD50, Mre11, Ku70/Ku80/PKC-delta) in primary MDMs. Beyond this example of reverse genetics, CRISPR-mediated interference (CRISPRi) or activation (CRISPRa) of target genes may broaden its range of applications [419, 494]. Those wild-type or engineered "countermeasure-resistant" restriction factors, e.g., SERINC5, TRIM5α/R332G/R335G, APOBEC3G/D128K and Tetherin/T45I, that are weakly expressed in infected cells could be activated by CRISPRa to provide strong restrictive capacities against HIV-1 infection [253]. Based on the findings of this study, the development of restriction factor-based therapeutics could open up new therapeutic avenues for viral control by combining intrinsic cellular sensing and antiviral immunity activation.

References

1.   Rambaut, A., et al., *The causes and consequences of HIV evolution.* 2004. **5**(1): p. 52-61.

2.   Faria, N.R., et al., *The early spread and epidemic ignition of HIV-1 in human populations.* 2014. **346**(6205): p. 56-61.

3.   Hemelaar, J.J.T.i.m.m., *The origin and diversity of the HIV-1 pandemic.* 2012. **18**(3): p. 182-192.

4.   Sharp, P.M. and B.H.J.C.S.H.p.i.m. Hahn, *Origins of HIV and the AIDS pandemic.* 2011. **1**(1): p. a006841.

5.   Bbosa, N., et al., *HIV subtype diversity worldwide.* 2019. **14**(3): p. 153-160.

6.   UNAIDS. *WHO. HIV Statistics.* 2019.

7.   Hollingsworth, T.D., R.M. Anderson, and C.J.T.J.o.i.d. Fraser, *HIV-1 transmission, by stage of infection.* 2008. **198**(5): p. 687-693.

8.   Boily, M.-C., et al., *Heterosexual risk of HIV-1 infection per sexual act: systematic review and meta-analysis of observational studies.* 2009. **9**(2): p. 118-129.

9.   Reis Machado, J., et al., *Mucosal immunity in the female genital tract, HIV/AIDS.* 2014. **2014**.

10.   Baggaley, R.F., et al., *Risk of HIV-1 transmission for parenteral exposure and blood transfusion: a systematic review and meta-analysis.* 2006. **20**(6): p. 805-812.

11.   Cullen, B.R.J.C., *HIV-1 auxiliary proteins: making connections in a dying cell.* 1998. **93**(5): p. 685-692.

12.   Li, G., E.J.M. De Clercq, and M.B. Reviews, *HIV genome-wide protein associations: a review of 30 years of research.* 2016. **80**(3): p. 679-731.

13.   Scherer, L., J. Rossi, and M.J.G.t. Weinberg, *Progress and prospects: RNA-based therapies for treatment of HIV infection.* 2007. **14**(14): p. 1057-1064.

14.   Cicala, C., J. Arthos, and A.S.J.J.o.t.m. Fauci, *HIV-1 envelope, integrins and co-receptor use in mucosal transmission of HIV.* 2011. **9**(1): p. 1-10.

15.   Xu, H., X. Wang, and R.S.J.I.r. Veazey, *Mucosal immunology of HIV infection.* 2013. **254**(1): p. 10-33.

16.   Shen, R., H.E. Richter, and P.D.J.A.j.o.r.i. Smith, *Early HIV‑1 target cells in human vaginal and ectocervical mucosa.* 2011. **65**(3): p. 261-267.

17.   Ahmed, Z., et al., *The role of human dendritic cells in HIV-1 infection.* 2015. **135**(5): p. 1225-1233.

18.   Février, M., K. Dorgham, and A.J.V. Rebollo, *CD4+ T cell depletion in human immunodeficiency virus (HIV) infection: role of apoptosis.* 2011. **3**(5): p. 586-612.

19.   Moir, S., T.-W. Chun, and A.S.J.A.r.o.p.m.o.d. Fauci, *Pathogenic mechanisms of HIV disease.* 2011. **6**: p. 223-248.

20.   Chereshnev, V., et al., *Pathogenesis and treatment of HIV infection: the cellular, the immune system and the neuroendocrine systems perspective.* 2013. **32**(3): p. 282-306.

21.   Cohen, M.S., O.D. Council, and J.S.J.J.o.t.I.A.S. Chen, *Sexually transmitted infections and HIV in the era of antiretroviral treatment and prevention: the biologic basis for epidemiologic synergy.* 2019. **22**: p. e25355.

22.   Rosadas, C. and G.P.J.F.i.m. Taylor, *Mother-to-child HTLV-1 transmission: unmet research needs.* 2019. **10**: p. 999.

23.   Rerks-Ngarm, S., et al., *Vaccination with ALVAC and AIDSVAX to prevent HIV-1 infection in Thailand.* 2009. **361**(23): p. 2209-2220.

24.   Cohen, J., *Combo of two HIV vaccines fails its big test*. 2020, American Association for the Advancement of Science.

25.   Gupta, R.K., et al., *HIV-1 drug resistance before initiation or re-initiation of first-line antiretroviral therapy in low-income and middle-income countries: a systematic review and meta-regression analysis.* 2018. **18**(3): p. 346-355.

26.   Zhu, T., et al., *Genotypic and phenotypic characterization of HIV-1 patients with primary infection.* 1993. **261**(5125): p. 1179-1181.

27.   Maréchal, V., et al., *Human immunodeficiency virus type 1 entry into macrophages mediated by macropinocytosis.* 2001. **75**(22): p. 11166-11177.

28.   Mondor, I., S. Ugolini, and Q.J.J.J.o.v. Sattentau, *Human immunodeficiency virus type 1 attachment to HeLa CD4 cells is CD4 independent and gp120 dependent and requires cell surface heparans.* 1998. **72**(5): p. 3623-3634.

29.   Nguyen, D.G. and J.E.J.E.j.o.i. Hildreth, *Involvement of macrophage mannose receptor in the binding and transmission of HIV by macrophages.* 2003. **33**(2): p. 483-493.

30.   Von Lindern, J.J., et al., *Potential role for CD63 in CCR5-mediated human immunodeficiency virus type 1 infection of macrophages.* 2003. **77**(6): p. 3624-3633.

31.   Rich, E., et al., *Increased susceptibility of differentiated mononuclear phagocytes to productive infection with human immunodeficiency virus-1 (HIV-1).* 1992. **89**(1): p. 176-183.

32.   O'Brien, W.A., et al., *Kinetics of human immunodeficiency virus type 1 reverse transcription in blood mononuclear phagocytes are slowed by limitations of nucleotide precursors.* 1994. **68**(2): p. 1258-1263.

33.   Jacque, J.-M. and M.J.N. Stevenson, *The inner-nuclear-envelope protein emerin regulates HIV-1 infectivity.* 2006. **441**(7093): p. 641-645.

34.   Benaroch, P., et al., *HIV-1 assembly in macrophages.* 2010. **7**(1): p. 1-10.

35.   Welsch, S., et al., *HIV-1 buds predominantly at the plasma membrane of primary human macrophages.* 2007. **3**(3): p. e36.

36.   Raposo, G., et al., *Human macrophages accumulate HIV ‑ 1 particles in MHC II compartments.* 2002. **3**(10): p. 718-729.

37.   Verani, A., G. Gras, and G.J.M.i. Pancino, *Macrophages and HIV-1: dangerous liaisons.* 2005. **42**(2): p. 195-212.

38.   Micci, L., et al., *CD4 depletion in SIV-infected macaques results in macrophage and microglia infection with rapid turnover of infected cells.* 2014. **10**(10): p. e1004467.

39.   Merino, K.M., et al., *Role of monocyte/macrophages during HIV/SIV infection in adult and pediatric acquired immune deficiency syndrome.* 2017. **8**: p. 1693.

40.   Coombs, R.W., P.S. Reichelderfer, and A.L.J.A. Landay, *Recent observations on HIV type-1 infection in the genital tract of men and women.* 2003. **17**(4): p. 455-480.

41.   Goodenow, M.M., et al., *HIV‑1 fitness and macrophages.* 2003. **74**(5): p. 657-666.

42.   Dupont, M. and Q.J.J.V. Sattentau, *Macrophage cell-cell interactions promoting HIV-1 infection.* 2020. **12**(5): p. 492.

43.   Yagi, Y., et al., *Inhibition of DC‑SIGN‑mediated transmission of human immunodeficiency virus type 1 by Toll‑like receptor 3 signalling in breast milk macrophages.* 2010. **130**(4): p. 597-607.

44.   Bergamaschi, A. and G.J.R. Pancino, *Host hindrance to HIV-1 replication in monocytes and macrophages.* 2010. **7**(1): p. 1-17.

45.   Smythies, L.E., et al., *Human intestinal macrophages display profound inflammatory anergy despite avid phagocytic and bacteriocidal activity.* 2005. **115**(1): p. 66-75.

46.   Shen, R., et al., *Macrophages in vaginal but not intestinal mucosa are monocyte-like and permissive to human immunodeficiency virus type 1 infection.* 2009. **83**(7): p. 3258-3267.

47.   Sattentau, Q.J., M.J.C.h. Stevenson, and microbe, *Macrophages and HIV-1: an unhealthy constellation.* 2016. **19**(3): p. 304-310.

48.   Joseph, S.B., et al., *HIV-1 target cells in the CNS.* 2015. **21**(3): p. 276-289.

49.   van Furth, R. and Z.A.J.T.J.o.e.m. Cohn, *The origin and kinetics of mononuclear phagocytes.* 1968. **128**(3): p. 415-435.

50.   Bellingan, G.J., et al., *In vivo fate of the inflammatory macrophage during the resolution of inflammation: inflammatory macrophages do not die locally, but emigrate to the draining lymph nodes.* 1996. **157**(6): p. 2577-2585.

51.   Murphy, J., et al., *The prolonged life-span of alveolar macrophages.* 2008. **38**(4): p. 380-385.

52.   Swingler, S., et al., *Apoptotic killing of HIV-1–infected macrophages is subverted by the viral envelope glycoprotein.* 2007. **3**(9): p. e134.

53.   Reynoso, R., et al., *HIV-1 induces telomerase activity in monocyte-derived macrophages, possibly safeguarding one of its reservoirs.* 2012. **86**(19): p. 10327-10337.

54.   Schnell, G., et al., *HIV-1 replication in the central nervous system occurs in two distinct cell types.* 2011. **7**(10): p. e1002286.

55.   Lacey, D.C., et al., *Defining GM-CSF–and macrophage-CSF–dependent macrophage responses by in vitro models.* 2012. **188**(11): p. 5752-5765.

56.   Koppensteiner, H., R. Brack-Werner, and M.J.R. Schindler, *Macrophages and their relevance in Human Immunodeficiency Virus Type I infection.* 2012. **9**(1): p. 1-11.

57.   Osborn, L., S. Kunkel, and G.J.J.P.o.t.N.A.o.S. Nabel, *Tumor necrosis factor alpha and interleukin 1 stimulate the human immunodeficiency virus enhancer by activation of the nuclear factor kappa B.* 1989. **86**(7): p. 2336-2340.

58.   Herbein, G. and A.J.R. Varin, *The macrophage in HIV-1 infection: from activation to deactivation?* 2010. **7**(1): p. 1-15.

59.   Shapiro, L., et al., *Interleukin 18 stimulates HIV type 1 in monocytic cells.* 1998. **95**(21): p. 12550-12555.

60.   Fantuzzi, L., F. Belardelli, and S.J.J.o.l.b. Gessani, *Monocyte/macrophage‑derived CC chemokines and their modulation by HIV‑1 and cytokines: A complex network of interactions influencing viral replication and AIDS pathogenesis.* 2003. **74**(5): p. 719-725.

61.   Herbein, G. and K.A.J.T.i.i. Khan, *Is HIV infection a TNF receptor signalling-driven disease?* 2008. **29**(2): p. 61-67.

62.   Fisher, B.S., et al., *Liver macrophage-associated inflammation correlates with SIV burden and is substantially reduced following cART.* 2018. **14**(2): p. e1006871.

63.   Aids, D.C.o.A.E.o.A.-H.d.S.G.J., *Factors associated with specific causes of death amongst HIV-positive individuals in the D: A: D Study.* 2010. **24**(10): p. 1537-1548.

64.   Gannon, P., M.Z. Khan, and D.L.J.C.o.i.n. Kolson, *Current understanding of HIV-associated neurocognitive disorders pathogenesis.* 2011. **24**(3): p. 275.

65.   Papasavvas, E., et al., *IL-13 acutely augments HIV-specific and recall responses from HIV-1-infected subjects in vitro by modulating monocytes.* 2005. **175**(8): p. 5532-5540.

66.   Clerici, M. and G.M.J.I.t. Shearer, *A TH1→TH2 switch is a critical step in the etiology of HIV infection.* 1993. **14**(3): p. 107-111.

67.   Cassol, E., et al., *Macrophage polarization and HIV‑1 infection.* 2010. **87**(4): p. 599-608.

68.   Pierson, T., J. McArthur, and R.F.J.A.r.o.i. Siliciano, *Reservoirs for HIV-1: mechanisms for viral persistence in the presence of antiviral immune responses and antiretroviral therapy.* 2000. **18**(1): p. 665-708.

69.   Alexaki, A. and B.J.P.P. Wigdahl, *HIV-1 infection of bone marrow hematopoietic progenitor cells and their role in trafficking and viral dissemination.* 2008. **4**(12): p. e1000215.

70.   Churchill, M.J., et al., *HIV reservoirs: what, where and how to target them.* 2016. **14**(1): p. 55.

71.   Eisele, E. and R.F.J.I. Siliciano, *Redefining the viral reservoirs that prevent HIV-1 eradication.* 2012. **37**(3): p. 377-388.

72.   Blankson, J.N., et al., *Biphasic decay of latently infected CD4+ T cells in acute human immunodeficiency virus type 1 infection.* 2000. **182**(6): p. 1636-1642.

73.   Ganor, Y., et al., *The adult penile urethra is a novel entry site for HIV-1 that preferentially targets resident urethral macrophages.* 2013. **6**(4): p. 776-786.

74.   Cribbs, S.K., et al., *Healthy HIV-1-infected individuals on highly active antiretroviral therapy harbor HIV-1 in their alveolar macrophages.* 2015. **31**(1): p. 64-70.

75.   Zalar, A., et al., *Macrophage HIV-1 infection in duodenal tissue of patients on long term HAART.* 2010. **87**(2): p. 269-271.

76.   Kandathil, A.J., et al., *No recovery of replication-competent HIV-1 from human liver macrophages.* 2018. **128**(10): p. 4501-4509.

77.   Ganor, Y., et al., *HIV-1 reservoirs in urethral macrophages of patients under suppressive antiretroviral therapy.* 2019. **4**(4): p. 633-644.

78.   Cattin, A., et al., *HIV-1 is rarely detected in blood and colon myeloid cells during viral-suppressive antiretroviral therapy.* 2019. **33**(8): p. 1293.

79.   Shen, R., et al., *Stromal down-regulation of macrophage CD4/CCR5 expression and NF-κB activation mediates HIV-1 non-permissiveness in intestinal macrophages.* 2011. **7**(5): p. e1002060.

80.   Ko, A., et al., *Macrophages but not astrocytes harbor HIV DNA in the brains of HIV-1-infected aviremic individuals on suppressive antiretroviral therapy.* 2019. **14**(1): p. 110-119.

81.   González-Scarano, F. and J.J.N.r.i. Martín-García, *The neuropathogenesis of AIDS.* 2005. **5**(1): p. 69-81.

82.   Kelly, J., et al., *Human macrophages support persistent transcription from unintegrated HIV-1 DNA.* 2008. **372**(2): p. 300-312.

83.   Zastre, J.A., et al., *Up‑regulation of P‑glycoprotein by HIV protease inhibitors in a human brain microvessel endothelial cell line.* 2009. **87**(4): p. 1023-1036.

84.   Persaud, D., et al., *Absence of detectable HIV-1 viremia after treatment cessation in an infant.* 2013. **369**(19): p. 1828-1835.

85.   Venzke, S. and O.T.J.E.r.o.c.i. Keppler, *Role of macrophages in HIV infection and persistence.* 2006. **2**(4): p. 613-626.

86.   Eriksson, S., et al., *Comparative analysis of measures of viral reservoirs in HIV-1 eradication studies.* 2013. **9**(2): p. e1003174.

87.   Siliciano, J.D., et al., *Long-term follow-up studies confirm the stability of the latent reservoir for HIV-1 in resting CD4+ T cells.* 2003. **9**(6): p. 727-728.

88.   Yang, L.P., et al., *Productive infection of neonatal CD8+ T lymphocytes by HIV-1.* 1998. **187**(7): p. 1139-1144.

89.   Moir, S. and A.S.J.N.R.I. Fauci, *B cells in HIV infection and disease.* 2009. **9**(4): p. 235-245.

90.   Honeycutt, J.B., et al., *Macrophages sustain HIV replication in vivo independently of T cells.* 2016. **126**(4): p. 1353-1366.

91.   McElrath, M.J., R.M. Steinman, and Z.A.J.T.J.o.c.i. Cohn, *Latent HIV-1 infection in enriched populations of blood monocytes and T cells from seropositive patients.* 1991. **87**(1): p. 27-30.

92.   Wong, J.K., S.A.J.C.O.i.H. Yukl, and AIDS, *Tissue reservoirs of HIV.* 2016. **11**(4): p. 362.

93.   Strain, M., et al., *Heterogeneous clearance rates of long-lived lymphocytes infected with HIV: intrinsic stability predicts lifelong persistence.* 2003. **100**(8): p. 4819-4824.

94.   Zhang, Y., et al., *In vivo kinetics of human natural killer cells: the effects of ageing and acute and chronic viral infection.* 2007. **121**(2): p. 258-265.

95.   Cole, J.L., et al., *Ineffective platelet production in thrombocytopenic human immunodeficiency virus–infected patients.* 1998. **91**(9): p. 3239-3246.

96.   Collin, M., N. McGovern, and M.J.I. Haniffa, *Human dendritic cell subsets.* 2013. **140**(1): p. 22-30.

97.   Otero, M., et al., *Peripheral blood dendritic cells are not a major reservoir for HIV type 1 in infected individuals on virally suppressive HAART.* 2003. **19**(12): p. 1097-1103.

98.   Heesters, B.A., R.C. Myers, and M.C.J.N.R.I. Carroll, *Follicular dendritic cells: dynamic antigen libraries.* 2014. **14**(7): p. 495-504.

99.   McDonald, D., et al., *Recruitment of HIV and its receptors to dendritic cell-T cell junctions.* 2003. **300**(5623): p. 1295-1297.

100.   Moses, A.V., et al., *Human immunodeficiency virus infection of human brain capillary endothelial cells occurs via a CD4/galactosylceramide-independent mechanism.* 1993. **90**(22): p. 10474-10478.

101.   Li, G.-H., L. Henderson, and A.J.C.H.r. Nath, *Astrocytes as an HIV reservoir: mechanism of HIV infection.* 2016. **14**(5): p. 373-381.

102.   Llewellyn, G.N., et al., *HIV-1 infection of microglial cells in a reconstituted humanized mouse model and identification of compounds that selectively reverse HIV latency.* 2018. **24**(2): p. 192-203.

103.   Williams, K.C., et al., *Perivascular macrophages are the primary cell type productively infected by simian immunodeficiency virus in the brains of macaques: implications for the neuropathogenesis of AIDS.* 2001. **193**(8): p. 905-916.

104.   Matsuzawa, T., et al., *Immunological function of Langerhans cells in HIV infection.* 2017. **87**(2): p. 159-167.

105.   Kandathil, A.J., S. Sugawara, and A.J.R. Balagopal, *Are T cells the only HIV-1 reservoir?* 2016. **13**(1): p. 1-10.

106.   Iversen, A.K., et al., *Longitudinal and cross-sectional studies of HIV-1 RNA and DNA loads in blood and the female genital tract.* 2004. **117**(2): p. 227-235.

107.   Trifonova, R.T., et al., *Myeloid cells in intact human cervical explants capture HIV and can transmit it to CD4 T cells.* 2018. **9**: p. 2719.

108.   Smith, D.M., et al., *The prostate as a reservoir for HIV-1.* 2004. **18**(11): p. 1600-1602.

109.   Darcis, G., R.W. Coombs, and C.J.A. Van Lint, *Exploring the anatomical HIV reservoirs: role of the testicular tissue.* 2016. **30**(18): p. 2891.

110.   Sundstrom, J.B., et al., *Human tissue mast cells are an inducible reservoir of persistent HIV infection.* 2007. **109**(12): p. 5293-5300.

111.   Cassol, E., et al., *Monocyte‐derived macrophages and myeloid cell lines as targets of HIV‐1 replication and persistence.* 2006. **80**(5): p. 1018-1030.

112.   Winston, J.A., et al., *Nephropathy and establishment of a renal reservoir of HIV type 1 during primary infection.* 2001. **344**(26): p. 1979-1984.

113.   Ho, J.E. and P.Y.J.H. Hsue, *Cardiovascular manifestations of HIV infection.* 2009. **95**(14): p. 1193-1202.

114.   Arduino, P.G., S.R.J.J.o.o.p. Porter, and medicine, *Herpes Simplex Virus Type 1 infection: overview on relevant clinico‐pathological features.* 2008. **37**(2): p. 107-121.

115.   Mahiet, C., et al., *Structural variability of the herpes simplex virus 1 genome in vitro and in vivo.* 2012. **86**(16): p. 8592-8601.

116.   James, C., et al., *Herpes simplex virus: global infection prevalence and incidence estimates, 2016.* 2020. **98**(5): p. 315.

117.   Looker, K.J., et al., *Global and regional estimates of the contribution of herpes simplex virus type 2 infection to HIV incidence: a population attributable fraction analysis using published epidemiological data.* 2020. **20**(2): p. 240-249.

118.   Whitley, R.J. and B.J.T.l. Roizman, *Herpes simplex virus infections.* 2001. **357**(9267): p. 1513-1518.

119.   Fatahzadeh, M. and R.A.J.J.o.t.A.A.o.D. Schwartz, *Human herpes simplex virus infections: epidemiology, pathogenesis, symptomatology, diagnosis, and management.* 2007. **57**(5): p. 737-763.

120.   Kaufman, H.E., et al., *HSV-1 DNA in tears and saliva of normal adults.* 2005. **46**(1): p. 241-247.

121.   Kimberlin, D.W.J.T.L.G.H., *Why neonatal herpes matters.* 2017. **5**(3): p. e234-e235.

122.   Munawwar, A. and S.J.J.o.l.p. Singh, *Human herpesviruses as copathogens of HIV infection, their role in HIV transmission, and disease progression.* 2016. **8**(1): p. 5.

123.   Nicoll, M.P., J.T. Proença, and S.J.F.m.r. Efstathiou, *The molecular basis of herpes simplex virus latency.* 2012. **36**(3): p. 684-705.

124.   Winter, G.J.J.o.P.P., *Herpes simplex: treatment and vaccination.* 2020. **2**(5): p. 222-223.

125.   Grünewald, K., et al., *Three-dimensional structure of herpes simplex virus from cryo-electron tomography.* 2003. **302**(5649): p. 1396-1398.

126.   Laine, R.F., et al., *Structural analysis of herpes simplex virus by optical super-resolution imaging.* 2015. **6**(1): p. 1-10.

127.   Connolly, S.A., T.S. Jardetzky, and R.J.N.r.M. Longnecker, *The structural basis of herpesvirus entry.* 2020: p. 1-12.

128.   Roizman, B. and R.J.J.A.r.o.m. Whitley, *An inquiry into the molecular basis of HSV latency and reactivation.* 2013. **67**: p. 355-374.

129.   Everett, R.D., *HSV-1 biology and life cycle*, in *Herpes Simplex Virus*. 2014, Springer. p. 1-17.

130.   Carr, D.J.J.J.o.v., *Herpes simplex virus 1, macrophages, and the cornea.* 2017. **91**(21).

131.   LaVail, J.H., W.E. Johnson, and L.C.J.J.o.C.N. Spencer, *Immunohistochemical identification of trigeminal ganglion neurons that innervate the mouse cornea: relevance to intercellular spread of herpes simplex virus.* 1993. **327**(1): p. 133-140.

132.   Shivkumar, M., et al., *Herpes simplex virus 1 interaction with myeloid cells in vivo.* 2016. **90**(19): p. 8661-8672.

133.   Chinnery, H.R., P.G. McMenamin, and S.J.J.P.A.-E.J.o.P. Dando, *Macrophage physiology in the eye.* 2017. **469**(3-4): p. 501-515.

134.   Miettinen, J.J., S. Matikainen, and T.A.J.J.o.v. Nyman, *Global secretome characterization of herpes simplex virus 1-infected human primary macrophages.* 2012. **86**(23): p. 12770-12778.

135.   Kodukula, P., et al., *Macrophage control of herpes simplex virus type 1 replication in the peripheral nervous system.* 1999. **162**(5): p. 2895-2905.

136.   Ellermann-Eriksen, S.J.V.J., *Macrophages and cytokines in the early defence against herpes simplex virus.* 2005. **2**(1): p. 1-30.

137.   Lee, D.H. and H.J.J.o.v. Ghiasi, *Roles of M1 and M2 macrophages in herpes simplex virus 1 infectivity.* 2017. **91**(15).

138.   Chen, S.-H., J.E. Oakes, and R.N.J.A.r. Lausch, *Synergistic anti-HSV effect of tumor necrosis factor alpha and interferon gamma in human corneal fibroblasts is associated with interferon beta induction.* 1993. **22**(1): p. 15-29.

139.   Güler, M.L., et al., *Genetic susceptibility to Leishmania: IL-12 responsiveness in TH1 cell development.* 1996. **271**(5251): p. 984-987.

140.   Cao, Y., et al., *Interleukin‐4 regulates proteoglycan‐induced arthritis by specifically suppressing the innate immune response.* 2007. **56**(3): p. 861-870.

141.   Melchjorsen, J., et al., *Induction of cytokine expression by herpes simplex virus in human monocyte-derived macrophages and dendritic cells is dependent on virus replication and is counteracted by ICP27 targeting NF-κB and IRF-3.* 2006. **87**(5): p. 1099-1108.

142.   Piacentini, R., et al., *HSV-1 and Alzheimer's disease: more than a hypothesis.* 2014. **5**: p. 97.

143.   White, K.A., et al., *Diet-induced obesity prolongs neuroinflammation and recruits CCR2+ monocytes to the brain following herpes simplex virus (HSV)-1 latency in mice.* 2016. **57**: p. 68-78.

144.   Colonna, M. and O.J.A.r.o.i. Butovsky, *Microglia function in the central nervous system during health and neurodegeneration.* 2017. **35**: p. 441-468.

145.   Block, M.L., L. Zecca, and J.-S.J.N.R.N. Hong, *Microglia-mediated neurotoxicity: uncovering the molecular mechanisms.* 2007. **8**(1): p. 57-69.

146.   Javier, R.T., et al., *A herpes simplex virus transcript abundant in latently infected neurons is dispensable for for establishment of the latent state.* 1988. **166**(1): p. 254-257.

147.   Feldman, L.T., et al., *Spontaneous molecular reactivation of herpes simplex virus type 1 latency in mice.* 2002. **99**(2): p. 978-983.

148.   Horan, K.A., et al., *Proteasomal degradation of herpes simplex virus capsids in macrophages releases DNA to the cytosol for recognition by DNA sensors.* 2013. **190**(5): p. 2311-2319.

149.   Lucinda, N., et al., *Dendritic cells, macrophages, NK and CD8+ T lymphocytes play pivotal roles in controlling HSV-1 in the trigeminal ganglia by producing IL1-beta, iNOS and granzyme B.* 2017. **14**(1): p. 1-15.

150.   Paludan, S.R., et al., *Recognition of herpesviruses by the innate immune system.* 2011. **11**(2): p. 143-154.

151.   Iwasaki, A.J.I., *Innate immune recognition of HIV-1.* 2012. **37**(3): p. 389-398.

152.   Amarante-Mendes, G.P., et al., *Pattern recognition receptors and the host cell death molecular machinery.* 2018. **9**: p. 2379.

153.   Tang, D., et al., *PAMP s and DAMP s: signal 0s that spur autophagy and immunity.* 2012. **249**(1): p. 158-175.

154.   Iwasaki, A.J.A.r.o.m., *A virological view of innate immune recognition.* 2012. **66**: p. 177-196.

155.   Medzhitov, R. and C.A.J.S. Janeway, *Decoding the patterns of self and nonself by the innate immune system.* 2002. **296**(5566): p. 298-300.

156.   Nasr, N., et al., *HIV-1 infection of human macrophages directly induces viperin which inhibits viral production.* 2012. **120**(4): p. 778-788.

157.   Decalf, J., et al., *Sensing of HIV-1 entry triggers a type I interferon response in human primary macrophages.* 2017. **91**(15).

158.   Leib, D.A., et al., *Interferons regulate the phenotype of wild-type and mutant herpes simplex viruses in vivo.* 1999. **189**(4): p. 663-672.

159.   Orzalli, M.H., et al., *cGAS-mediated stabilization of IFI16 promotes innate signaling during herpes simplex virus infection.* 2015. **112**(14): p. E1773-E1781.

160.   Melchjorsen, J., et al., *Early innate recognition of herpes simplex virus in human primary macrophages is mediated via the MDA5/MAVS-dependent and MDA5/MAVS/RNA polymerase III-independent pathways.* 2010. **84**(21): p. 11350-11358.

161.   Karaba, A.H., et al., *Herpes simplex virus type 1 inflammasome activation in proinflammatory human macrophages is dependent on NLRP3, ASC, and caspase-1.* 2020. **15**(2): p. e0229570.

162.   Medzhitov, R.J.N., *Recognition of microorganisms and activation of the immune response.* 2007. **449**(7164): p. 819-826.

163.   Lazear, H.M., J.W. Schoggins, and M.S.J.I. Diamond, *Shared and distinct functions of type I and type III interferons.* 2019. **50**(4): p. 907-923.

164.   González-Navajas, J.M., et al., *Immunomodulatory functions of type I interferons.* 2012. **12**(2): p. 125-135.

165.   Zanoni, I., F. Granucci, and A.J.F.i.i. Broggi, *Interferon (IFN)-λ takes the helm: immunomodulatory roles of type III IFNs.* 2017. **8**: p. 1661.

166.   Platanias, L.C.J.N.R.I., *Mechanisms of type-I-and type-II-interferon-mediated signalling.* 2005. **5**(5): p. 375-386.

167.   Gélinas, J.-F., et al., *Multiple inhibitory factors act in the late phase of HIV-1 replication: a systematic review of the literature.* 2018. **82**(1).

168.   Schneider, W.M., M.D. Chevillotte, and C.M.J.A.r.o.i. Rice, *Interferon-stimulated genes: a complex web of host defenses.* 2014. **32**: p. 513-545.

169.   Sirén, J., et al., *IFN-α regulates TLR-dependent gene expression of IFN-α, IFN-β, IL-28, and IL-29.* 2005. **174**(4): p. 1932-1937.

170.   Yan, N. and Z.J.J.N.i. Chen, *Intrinsic antiviral immunity.* 2012. **13**(3): p. 214.

171.   Tartour, K., et al., *IFITM proteins are incorporated onto HIV-1 virion particles and negatively imprint their infectivity.* 2014. **11**(1): p. 1-14.

172.   Hrecka, K., et al., *Vpx relieves inhibition of HIV-1 infection of macrophages mediated by the SAMHD1 protein.* 2011. **474**(7353): p. 658-661.

173.   Tada, T., et al., *MARCH8 inhibits HIV-1 infection by reducing virion incorporation of envelope glycoproteins.* 2015. **21**(12): p. 1502-1507.

174.   Krapp, C., et al., *Guanylate binding protein (GBP) 5 is an interferon-inducible inhibitor of HIV-1 infectivity.* 2016. **19**(4): p. 504-514.

175.   Van den Bergh, R., et al., *Transcriptome analysis of monocyte-HIV interactions.* 2010. **7**(1): p. 1-16.

176.   Liu, L., et al., *A whole genome screen for HIV restriction factors.* 2011. **8**(1): p. 1-15.

177.   Bergamaschi, A., et al., *The CDK inhibitor p21Cip1/WAF1 is induced by FcγR activation and restricts the replication of human immunodeficiency virus type 1 and related primate lentiviruses in human macrophages.* 2009. **83**(23): p. 12253-12265.

178.   Suspène, R., et al., *Genetic editing of herpes simplex virus 1 and Epstein-Barr herpesvirus genomes by human APOBEC3 cytidine deaminases in culture and in vivo.* 2011. **85**(15): p. 7594-7602.

179. Chin, K.-C. and P.J.P.o.t.N.A.o.S. Cresswell, *Viperin (cig5), an IFN-inducible antiviral protein directly induced by human cytomegalovirus.* 2001. **98**(26): p. 15125-15130.

180. Pardieu, C., et al., *The RING-CH ligase K5 antagonizes restriction of KSHV and HIV-1 particle release by mediating ubiquitin-dependent endosomal degradation of tetherin.* 2010. **6**(4): p. e1000843.

181. Guha, D. and V.J.I.S.R.N. Ayyavoo, *Innate immune evasion strategies by human immunodeficiency virus type 1.* 2013. **2013**.

182. Rasaiyaah, J., et al., *HIV-1 evades innate immune recognition through specific cofactor recruitment.* 2013. **503**(7476): p. 402-405.

183. Gringhuis, S.I., et al., *HIV-1 blocks the signaling adaptor MAVS to evade antiviral host defense after sensing of abortive HIV-1 RNA by the host helicase DDX3.* 2017. **18**(2): p. 225-235.

184. Manel, N. and D.R.J.C. Littman, *Hiding in plain sight: how HIV evades innate immune responses.* 2011. **147**(2): p. 271-274.

185. Harman, A.N., et al., *HIV blocks interferon induction in human dendritic cells and macrophages by dysregulation of TBK1.* 2015. **89**(13): p. 6575-6584.

186. Doehle, B.P., et al., *Human immunodeficiency virus type 1 mediates global disruption of innate antiviral signaling and immune defenses within infected cells.* 2009. **83**(20): p. 10395-10405.

187. Solis, M., et al., *RIG-I-mediated antiviral signaling is inhibited in HIV-1 infection by a protease-mediated sequestration of RIG-I.* 2011. **85**(3): p. 1224-1236.

188. Foster, J.L., et al., *Mechanisms of HIV-1 Nef function and intracellular signaling.* 2011. **6**(2): p. 230-246.

189. Clerzius, G., J.F. Gélinas, and A.J.R.i.m.v. Gatignol, *Multiple levels of PKR inhibition during HIV‐1 replication.* 2011. **21**(1): p. 42-53.

190. Takata, M.A., et al., *CG dinucleotide suppression enables antiviral defence targeting non-self RNA.* 2017. **550**(7674): p. 124-127.

191. Yan, N., et al., *The cytosolic exonuclease TREX1 inhibits the innate immune response to human immunodeficiency virus type 1.* 2010. **11**(11): p. 1005-1013.

192. Melchjorsen, J., J. SIREN, and I.J.T.J.o.g.v. JULKUNEN, *PALUDAN SR AND MATIKAINEN S. 2006. Induction of cytokine expression by herpes simplex virus in human monocyte-derived macrophages and dendritic cells is dependent on virus replication and is counteracted by ICP27 targeting NF-kappaB and IRF-3.* **87**: p. 1099-1108.

193. Roy, A., et al., *Nuclear innate immune DNA sensor IFI16 is degraded during lytic reactivation of Kaposi's sarcoma-associated herpesvirus (KSHV): role of IFI16 in maintenance of KSHV latency.* 2016. **90**(19): p. 8822-8841.

194. Melroe, G.T., N.A. DeLuca, and D.M.J.J.o.v. Knipe, *Herpes simplex virus 1 has multiple mechanisms for blocking virus-induced interferon production.* 2004. **78**(16): p. 8411-8420.

195.   Verpooten, D., et al., *Control of TANK-binding kinase 1-mediated signaling by the γ134. 5 protein of herpes simplex virus 1.* 2009. **284**(2): p. 1097-1105.

196.   Mogensen, T.H., et al., *Suppression of proinflammatory cytokine expression by herpes simplex virus type 1.* 2004. **78**(11): p. 5883-5890.

197.   Wang, S., et al., *Herpes simplex virus 1 serine/threonine kinase US3 hyperphosphorylates IRF3 and inhibits beta interferon production.* 2013. **87**(23): p. 12814-12827.

198.   Christensen, M.H., et al., *HSV – 1 ICP 27 targets the TBK 1 – activated STING signalsome to inhibit virus –induced type I IFN expression.* 2016. **35**(13): p. 1385-1399.

199.   Park, R.J., et al., *A genome-wide CRISPR screen identifies a restricted set of HIV host dependency factors.* 2017. **49**(2): p. 193-203.

200.   Stremlau, M., et al., *The cytoplasmic body component TRIM5α restricts HIV-1 infection in Old World monkeys.* 2004. **427**(6977): p. 848-853.

201.   Reszka, N., et al., *Simian TRIM5α proteins reduce replication of herpes simplex virus.* 2010. **398**(2): p. 243-250.

202.   Sheehy, A.M., et al., *Isolation of a human gene that inhibits HIV-1 infection and is suppressed by the viral Vif protein.* 2002. **418**(6898): p. 646-650.

203.   Hancock, M.H., J.A. Corcoran, and J.R.J.V. Smiley, *Herpes simplex virus regulatory proteins VP16 and ICP0 counteract an innate intranuclear barrier to viral gene expression.* 2006. **352**(1): p. 237-252.

204.   Maelfait, J., et al., *Restriction by SAMHD1 limits cGAS/STING-dependent innate and adaptive immune responses to HIV-1.* 2016. **16**(6): p. 1492-1501.

205.   Van Damme, N., et al., *The interferon-induced protein BST-2 restricts HIV-1 release and is downregulated from the cell surface by the viral Vpu protein.* 2008. **3**(4): p. 245-252.

206.   Usami, Y., Y. Wu, and H.G.J.N. Göttlinger, *SERINC3 and SERINC5 restrict HIV-1 infectivity and are counteracted by Nef.* 2015. **526**(7572): p. 218-223.

207.   Orzalli, M.H., N.A. DeLuca, and D.M.J.P.o.t.N.A.o.S. Knipe, *Nuclear IFI16 induction of IRF-3 signaling during herpesviral infection and degradation of IFI16 by the viral ICP0 protein.* 2012. **109**(44): p. E3008-E3017.

208.   You, H., et al., *Herpes simplex virus type 1 abrogates the antiviral activity of Ch25h via its virion host shutoff protein.* 2017. **143**: p. 69-73.

209.   Su, C., G. Zhan, and C.J.V.j. Zheng, *Evasion of host antiviral innate immunity by HSV-1, an update.* 2016. **13**(1): p. 1-9.

210.   He, B., M. Gross, and B.J.P.o.t.N.A.o.S. Roizman, *The γ134. 5 protein of herpes simplex virus 1 complexes with protein phosphatase 1α to dephosphorylate the α subunit of the eukaryotic translation initiation factor 2 and preclude the shutoff of protein synthesis by double-stranded RNA-activated protein kinase.* 1997. **94**(3): p. 843-848.

211.   Henrick, B.M., et al., *HIV-1 structural proteins serve as PAMPs for TLR2 heterodimers significantly increasing infection and innate immune activation.* 2015. **6**: p. 426.

212. Brun, P., et al., *Herpes simplex virus type 1 engages toll like receptor 2 to recruit macrophages during infection of enteric neurons.* 2018. **9**: p. 2148.

213. Cardinaud, S., et al., *Triggering of TLR‑3, ‑4, NOD2, and DC‑SIGN reduces viral replication and increases T‑cell activation capacity of HIV‑infected human dendritic cells.* 2017. **47**(5): p. 818-829.

214. Reinert, L.S., et al., *TLR3 deficiency renders astrocytes permissive to herpes simplex virus infection and facilitates establishment of CNS infection in mice.* 2012. **122**(4): p. 1368-1376.

215. Zhang, S.-Y., et al., *TLR3 deficiency in patients with herpes simplex encephalitis.* 2007. **317**(5844): p. 1522-1527.

216. Miettinen, M., et al., *IFNs activate toll-like receptor gene expression in viral infections.* 2001. **2**(6): p. 349-355.

217. Tanji, H., et al., *Structural reorganization of the Toll-like receptor 8 dimer induced by agonistic ligands.* 2013. **339**(6126): p. 1426-1429.

218. Lepelley, A., et al., *Innate sensing of HIV-infected cells.* 2011. **7**(2): p. e1001284.

219. Gringhuis, S.I., et al., *HIV-1 exploits innate signaling by TLR8 and DC-SIGN for productive infection of dendritic cells.* 2010. **11**(5): p. 419.

220. Khatamzas, E., et al., *Snapin promotes HIV‑1 transmission from dendritic cells by dampening TLR 8 signaling.* 2017. **36**(20): p. 2998-3011.

221. Heil, F., et al., *Species-specific recognition of single-stranded RNA via toll-like receptor 7 and 8.* 2004. **303**(5663): p. 1526-1529.

222. Rasmussen, S.B., et al., *Type I interferon production during herpes simplex virus infection is controlled by cell-type-specific viral recognition through Toll-like receptor 9, the mitochondrial antiviral signaling protein pathway, and novel recognition systems.* 2007. **81**(24): p. 13315-13324.

223. Iversen, M.B., et al., *Expression of type III interferon (IFN) in the vaginal mucosa is mediated primarily by dendritic cells and displays stronger dependence on NF-κB than type I IFNs.* 2010. **84**(9): p. 4579-4586.

224. Martinelli, E., et al., *HIV-1 gp120 inhibits TLR9-mediated activation and IFN-α secretion in plasmacytoid dendritic cells.* 2007. **104**(9): p. 3396-3401.

225. Xing, J., et al., *Herpes simplex virus 1 tegument protein US11 downmodulates the RLR signaling pathway via direct interaction with RIG-I and MDA-5.* 2012. **86**(7): p. 3528-3540.

226. Zhao, J., et al., *A viral deamidase targets the helicase domain of RIG-I to block RNA-induced activation.* 2016. **20**(6): p. 770-784.

227. Bandyopadhyay, S.K., et al., *Transcriptional induction by double-stranded RNA is mediated by interferon-stimulated response elements without activation of interferon-stimulated gene factor 3.* 1995. **270**(33): p. 19624-19629.

228. Schlee, M.J.I., *Master sensors of pathogenic RNA–RIG-I like receptors.* 2013. **218**(11): p. 1322-1335.

229.   Bode, C., et al., *Human plasmacytoid dendritic cells elicit a Type I Interferon response by sensing DNA via the cGAS‑STING signaling pathway.* 2016. **46**(7): p. 1615-1621.

230.   Miyashita, M., et al., *DDX60, a DEXD/H box helicase, is a novel antiviral factor promoting RIG-I-like receptor-mediated signaling.* 2011. **31**(18): p. 3802-3819.

231.   Kim, T., et al., *Aspartate-glutamate-alanine-histidine box motif (DEAH)/RNA helicase A helicases sense microbial DNA in human plasmacytoid dendritic cells.* 2010. **107**(34): p. 15181-15186.

232.   Naji, S., et al., *Host cell interactome of HIV-1 Rev includes RNA helicases involved in multiple facets of virus production.* 2012. **11**(4): p. M111. 015313.

233.   Zhang, Z., et al., *DDX1, DDX21, and DHX36 helicases form a complex with the adaptor molecule TRIF to sense dsRNA in dendritic cells.* 2011. **34**(6): p. 866-878.

234.   SCHRÖDER, H.C., et al., *Binding of Tat protein to TAR region of human immunodeficiency virus type 1 blocks TAR-mediated activation of (2´-5´) oligoadenylate synthetase.* 1990. **6**(5): p. 659-672.

235.   Ryman, K.D., et al., *Effects of PKR/RNase L-dependent and alternative antiviral pathways on alphavirus replication and pathogenesis.* 2002. **15**(1): p. 53-76.

236.   Drappier, M. and T.J.C.o.i.v. Michiels, *Inhibition of the OAS/RNase L pathway by viruses.* 2015. **15**: p. 19-26.

237.   Jakobsen, M.R., et al., *IFI16 senses DNA forms of the lentiviral replication cycle and controls HIV-1 replication.* 2013. **110**(48): p. E4571-E4580.

238.   Crill, E.K., S.R. Furr‑Rogers, and I.J.G. Marriott, *RIG‑I is required for VSV‑induced cytokine production by murine glia and acts in combination with DAI to initiate responses to HSV‑1.* 2015. **63**(12): p. 2168-2180.

239.   Takaoka, A., et al., *DAI (DLM-1/ZBP1) is a cytosolic DNA sensor and an activator of innate immune response.* 2007. **448**(7152): p. 501-505.

240.   Atluri, V.S.R., et al., *Effect of cocaine on HIV infection and inflammasome gene expression profile in HIV infected macrophages.* 2016. **6**(1): p. 1-12.

241.   Maruzuru, Y., et al., *Herpes simplex virus 1 VP22 inhibits AIM2-dependent inflammasome activation to enable efficient viral replication.* 2018. **23**(2): p. 254-265. e7.

242.   Gao, D., et al., *Cyclic GMP-AMP synthase is an innate immune sensor of HIV and other retroviruses.* 2013. **341**(6148): p. 903-906.

243.   Su, C. and C.J.J.o.v. Zheng, *Herpes simplex virus 1 abrogates the cGAS/STING-mediated cytosolic DNA-sensing pathway via its virion host shutoff protein, UL41.* 2017. **91**(6).

244.   Guo, H., et al., *HIV-1 infection induces interleukin-1β production via TLR8 protein-dependent and NLRP3 inflammasome mechanisms in human monocytes.* 2014. **289**(31): p. 21716-21726.

245.   Wang, W., et al., *STING promotes NLRP3 localization in ER and facilitates NLRP3 deubiquitination to activate the inflammasome upon HSV-1 infection.* 2020. **16**(3): p. e1008335.

246.   Wang, Q., et al., *CARD8 is an inflammasome sensor for HIV-1 protease activity*. 2021.

247.   You, H., et al., *β-catenin is required for the cGAS/STING signaling pathway but antagonized by the herpes simplex virus 1 US3 protein*. 2020. **94**(5).

248.   Cooper, A., et al., *HIV-1 causes CD4 cell death through DNA-dependent protein kinase during viral integration*. 2013. **498**(7454): p. 376-379.

249.   Ferguson, B.J., et al., *DNA-PK is a DNA sensor for IRF-3-dependent innate immunity*. 2012. **1**: p. e00047.

250.   Sakurai, Y., et al., *DNA double strand break repair enzymes function at multiple steps in retroviral infection*. 2009. **6**(1): p. 1-13.

251.   Chiu, Y.-H., J.B. MacMillan, and Z.J.J.C. Chen, *RNA polymerase III detects cytosolic DNA and induces type I interferons through the RIG-I pathway*. 2009. **138**(3): p. 576-591.

252.   Yoh, S.M., et al., *PQBP1 is a proximal sensor of the cGAS-dependent innate response to HIV-1*. 2015. **161**(6): p. 1293-1305.

253.   Rosa, A., et al., *HIV-1 Nef promotes infection by excluding SERINC5 from virion incorporation*. 2015. **526**(7572): p. 212-217.

254.   Sato, A., M.M. Linehan, and A.J.P.o.t.N.A.o.S. Iwasaki, *Dual recognition of herpes simplex viruses by TLR2 and TLR9 in dendritic cells*. 2006. **103**(46): p. 17343-17348.

255.   Lu, J., et al., *The IFITM proteins inhibit HIV-1 infection*. 2011. **85**(5): p. 2126-2137.

256.   Wakim, L.M., et al., *Enhanced survival of lung tissue-resident memory CD8+ T cells during infection with influenza virus due to selective expression of IFITM3*. 2013. **14**(3): p. 238-245.

257.   Smith, S., et al., *Interferon-induced transmembrane protein 1 restricts replication of viruses that enter cells via the plasma membrane*. 2019. **93**(6).

258.   Liu, S.-Y., et al., *Interferon-inducible cholesterol-25-hydroxylase broadly inhibits viral entry by production of 25-hydroxycholesterol*. 2013. **38**(1): p. 92-105.

259.   Bauman, D.R., et al., *25-Hydroxycholesterol secreted by macrophages in response to Toll-like receptor activation suppresses immunoglobulin A production*. 2009. **106**(39): p. 16764-16769.

260.   Park, K. and A.L.J.J.o.l.b. Scott, *Cholesterol 25‑hydroxylase production by dendritic cells and macrophages is regulated by type I interferons*. 2010. **88**(6): p. 1081-1087.

261.   Tiwari, V. and D.J.T.J.o.g.v. Shukla, *Phosphoinositide 3 kinase signalling may affect multiple steps during herpes simplex virus type-1 entry*. 2010. **91**(Pt 12): p. 3002.

262.   Lahaye, X., et al., *NONO detects the nuclear HIV capsid to promote cGAS-mediated innate immune activation*. 2018. **175**(2): p. 488-501. e22.

263.   Henriet, S., et al., *Tumultuous relationship between the human immunodeficiency virus type 1 viral infectivity factor (Vif) and the human APOBEC-3G and APOBEC-3F restriction factors*. 2009. **73**(2): p. 211-232.

264.   Tognarelli, E.I., et al., *Herpes simplex virus evasion of early host antiviral responses.* 2019. **9**: p. 127.

265.   Oliva, H., et al., *Increased expression with differential subcellular location of cytidine deaminase APOBEC3G in human CD4+ T-cell activation and dendritic cell maturation.* 2016. **94**(7): p. 689-700.

266.   Laguette, N., et al., *SAMHD1 is the dendritic-and myeloid-cell-specific HIV-1 restriction factor counteracted by Vpx.* 2011. **474**(7353): p. 654-657.

267.   Kim, E.T., et al., *SAMHD1 restricts herpes simplex virus 1 in macrophages by limiting DNA replication.* 2013. **87**(23): p. 12949-12956.

268.   Lahouassa, H., et al., *SAMHD1 restricts the replication of human immunodeficiency virus type 1 by depleting the intracellular pool of deoxynucleoside triphosphates.* 2012. **13**(3): p. 223-228.

269.   Cribier, A., et al., *Phosphorylation of SAMHD1 by cyclin A2/CDK1 regulates its restriction activity toward HIV-1.* 2013. **3**(4): p. 1036-1043.

270.   Allouch, A., et al., *p21-mediated RNR2 repression restricts HIV-1 replication in macrophages by inhibiting dNTP biosynthesis pathway.* 2013. **110**(42): p. E3997-E4006.

271.   Zhang, J., D.T. Scadden, and C.S.J.T.J.o.c.i. Crumpacker, *Primitive hematopoietic cells resist HIV-1 infection via p21 Waf1/Cip1/Sdi1.* 2007. **117**(2): p. 473-481.

272.   Ku, C.C., et al., *Herpes simplex virus-1 induces expression of a novel MxA isoform that enhances viral replication.* 2011. **89**(2): p. 173-182.

273.   Goujon, C., et al., *Human MX2 is an interferon-induced post-entry inhibitor of HIV-1 infection.* 2013. **502**(7472): p. 559-562.

274.   Crameri, M., et al., *MxB is an interferon-induced restriction factor of human herpesviruses.* 2018. **9**(1): p. 1-16.

275.   Liu, Z., et al., *The interferon-inducible MxB protein inhibits HIV-1 infection.* 2013. **14**(4): p. 398-410.

276.   Kane, M., et al., *MX2 is an interferon-induced inhibitor of HIV-1 infection.* 2013. **502**(7472): p. 563-566.

277.   Allouch, A., et al., *The TRIM family protein KAP1 inhibits HIV-1 integration.* 2011. **9**(6): p. 484-495.

278.   Wang, X., et al., *Moloney leukemia virus 10 (MOV10) protein inhibits retrovirus replication.* 2010. **285**(19): p. 14346-14355.

279.   Tyagi, M. and F.J.R. Kashanchi, *New and novel intrinsic host repressive factors against HIV-1: PAF1 complex, HERC5 and others.* 2012. **9**(1): p. 1-3.

280.   Peterlin, B.M., et al., *Hili inhibits HIV replication in activated T cells.* 2017. **91**(11).

281.   Toth, A.M., et al., *Interferon Action and the Double-Stranded RNA-Dependent Enzymes ADAR1 Adenosine Deaminase and PKR Protein Kinase.* 2006. **81**: p. 369-434.

282.   Jiménez, V.C., et al., *G3BP1 restricts HIV-1 replication in macrophages and T-cells by sequestering viral RNA.* 2015. **486**: p. 94-104.

283.   Benayas, B., et al., *Tetraspanin CD81 regulates HSV-1 infection.* 2020. **209**: p. 489-498.

284.   Han, K., D.I. Lou, and S.L.J.P.G. Sawyer, *Identification of a genomic reservoir for new TRIM genes in primate genomes.* 2011. **7**(12): p. e1002388.

285.   Ozato, K., et al., *TRIM family proteins and their emerging roles in innate immunity.* 2008. **8**(11): p. 849-860.

286.   Singh, R., et al., *Association of TRIM22 with the type 1 interferon response and viral control during primary HIV-1 infection.* 2011. **85**(1): p. 208-216.

287.   Zhu, Y., et al., *Zinc-finger antiviral protein inhibits HIV-1 infection by selectively targeting multiply spliced viral mRNAs for degradation.* 2011. **108**(38): p. 15834-15839.

288.   Gao, G., X. Guo, and S.P.J.S. Goff, *Inhibition of retroviral RNA production by ZAP, a CCCH-type zinc finger protein.* 2002. **297**(5587): p. 1703-1706.

289.   McMillan, N.A., et al., *HIV-1 Tat directly interacts with the interferon-induced, double-stranded RNA-dependent kinase, PKR.* 1995. **213**(2): p. 413-424.

290.   Lussignol, M., et al., *The herpes simplex virus 1 Us11 protein inhibits autophagy through its interaction with the protein kinase PKR.* 2013. **87**(2): p. 859-871.

291.   Razzak, M.J.N.R.U., *Schlafen 11 naturally blocks HIV.* 2012. **9**(11): p. 605-605.

292.   Li, M., et al., *Codon-usage-based inhibition of HIV protein synthesis by human schlafen 11.* 2012. **491**(7422): p. 125-128.

293.   Malathi, K., et al., *Small self-RNA generated by RNase L amplifies antiviral innate immunity.* 2007. **448**(7155): p. 816-819.

294.   Woods, M.W., et al., *Human HERC5 restricts an early stage of HIV-1 assembly by a mechanism correlating with the ISGylation of Gag.* 2011. **8**(1): p. 1-18.

295.   Wilson, S.J., et al., *Inhibition of HIV-1 particle assembly by 2′, 3′-cyclic-nucleotide 3′-phosphodiesterase.* 2012. **12**(4): p. 585-597.

296.   Ghimire, D., M. Rai, and R.J.J.o.G.V. Gaur, *Novel host restriction factors implicated in HIV-1 replication.* 2018. **99**(4): p. 435-446.

297.   Hotter, D., D. Sauter, and F.J.S.G. Kirchhoff, *Guanylate binding protein 5: Impairing virion infectivity by targeting retroviral envelope glycoproteins.* 2017. **8**(1): p. 31-37.

298.   Zhang, Y., J. Lu, and X.J.V. Liu, *MARCH2 is upregulated in HIV-1 infection and inhibits HIV-1 production through envelope protein translocation or degradation.* 2018. **518**: p. 293-300.

299.   Lodermeyer, V., et al., *90K, an interferon-stimulated gene product, reduces the infectivity of HIV-1.* 2013. **10**(1): p. 1-18.

300.   Miyagi, E., et al., *Vpu enhances HIV-1 virus release in the absence of Bst-2 cell surface down-modulation and intracellular depletion.* 2009. **106**(8): p. 2868-2873.

301.   Zenner, H.L., et al., *Herpes simplex virus 1 counteracts tetherin restriction via its virion host shutoff activity.* 2013. **87**(24): p. 13115-13123.

302.   Blondeau, C., et al., *Tetherin restricts herpes simplex virus 1 and is antagonized by glycoprotein M.* 2013. **87**(24): p. 13124-13133.

303.   Shen, G., et al., *Herpes simplex virus 1 counteracts viperin via its virion host shutoff protein UL41.* 2014. **88**(20): p. 12163-12166.

304.   Miyakawa, K., et al., *BCA2/Rabring7 promotes tetherin-dependent HIV-1 restriction.* 2009. **5**(12): p. e1000700.

305.   Lenschow, D.J., et al., *IFN-stimulated gene 15 functions as a critical antiviral molecule against influenza, herpes, and Sindbis viruses.* 2007. **104**(4): p. 1371-1376.

306.   Okumura, A., et al., *Innate antiviral response targets HIV-1 release by the induction of ubiquitin-like protein ISG15.* 2006. **103**(5): p. 1440-1445.

307.   Katzenell, S. and D.A.J.J.o.v. Leib, *Herpes simplex virus and interferon signaling induce novel autophagic clusters in sensory neurons.* 2016. **90**(9): p. 4706-4719.

308.   Mahboubi, B., et al., *Host SAMHD1 protein restricts endogenous reverse transcription of HIV-1 in nondividing macrophages.* 2018. **15**(1): p. 1-11.

309.   Staeheli, P. and O.J.J.o.v. Haller, *Human MX2/MxB: a potent interferon-induced postentry inhibitor of herpesviruses and HIV-1.* 2018. **92**(24).

310.   Haller, O., et al., *Mx GTPases: dynamin-like antiviral machines of innate immunity.* 2015. **23**(3): p. 154-163.

311.   Gao, S., et al., *Structural basis of oligomerization in the stalk region of dynamin-like MxA.* 2010. **465**(7297): p. 502-506.

312.   Schulte, B., et al., *Restriction of HIV-1 requires the N-terminal region of MxB as a capsid-binding motif but not as a nuclear localization signal.* 2015. **89**(16): p. 8599-8610.

313.   Daumke, O., et al., *Structure of the MxA stalk elucidates the assembly of ring-like units of an antiviral module.* 2010. **1**(1): p. 502-506.

314.   Gao, S., et al., *Structure of myxovirus resistance protein a reveals intra-and intermolecular domain interactions required for the antiviral function.* 2011. **35**(4): p. 514-525.

315.   King, M.C., G. Raposo, and M.A.J.P.o.t.N.A.o.S. Lemmon, *Inhibition of nuclear import and cell-cycle progression by mutated forms of the dynamin-like GTPase MxB.* 2004. **101**(24): p. 8957-8962.

316.   Melén, K., et al., *Human MxB protein, an interferon-α-inducible GTPase, contains a nuclear targeting signal and is localized in the heterochromatin region beneath the nuclear envelope.* 1996. **271**(38): p. 23478-23486.

317.   Hofer, U.J.N.R.M., *Interfering with HIV infection.* 2013. **11**(11): p. 743-743.

318.   Goujon, C., et al., *Transfer of the amino-terminal nuclear envelope targeting domain of human MX2 converts MX1 into an HIV-1 resistance factor.* 2014. **88**(16): p. 9017-9026.

319.   Busnadiego, I., et al., *Host and viral determinants of Mx2 antiretroviral activity.* 2014. **88**(14): p. 7738-7752.

320.   Yamashita, M. and A.N.J.T.i.m. Engelman, *Capsid-dependent host factors in HIV-1 infection.* 2017. **25**(9): p. 741-755.

321.   Kane, M., et al., *Nuclear pore heterogeneity influences HIV-1 infection and the antiviral activity of MX2.* 2018. **7**: p. e35738.

322.   Patzina, C., O. Haller, and G.J.J.o.B.C. Kochs, *Structural requirements for the antiviral activity of the human MxA protein against Thogoto and influenza A virus.* 2014. **289**(9): p. 6020-6027.

323.   Goujon, C., et al., *A triple-arginine motif in the amino-terminal domain and oligomerization are required for HIV-1 inhibition by human MX2.* 2015. **89**(8): p. 4676-4680.

324.   Betancor, G., et al., *The GTPase domain of MX2 interacts with the HIV-1 capsid, enabling its short isoform to moderate antiviral restriction.* 2019. **29**(7): p. 1923-1933. e3.

325.   Schilling, M., et al., *Human MxB protein is a pan-herpesvirus restriction factor.* 2018. **92**(17).

326.   Schulze, A., P. Gripon, and S.J.H. Urban, *Hepatitis B virus infection initiates with a large surface protein–dependent binding to heparan sulfate proteoglycans.* 2007. **46**(6): p. 1759-1768.

327.   Copeland, A.M., W.W. Newcomb, and J.C.J.J.o.v. Brown, *Herpes simplex virus replication: roles of viral proteins and nucleoporins in capsid-nucleus attachment.* 2009. **83**(4): p. 1660-1668.

328.   Vasudevan, A.A.J., et al., *MXB inhibits murine cytomegalovirus.* 2018. **522**: p. 158-167.

329.   Achuthan, V., et al., *Capsid-CPSF6 interaction: master regulator of nuclear HIV-1 positioning and integration.* 2019. **1**(1): p. 39.

330.   Gelais, C.S., et al., *Identification of cellular proteins interacting with the retroviral restriction factor SAMHD1.* 2014. **88**(10): p. 5834-5844.

331.   Tramentozzi, E., et al., *The dNTP triphosphohydrolase activity of SAMHD1 persists during S-phase when the enzyme is phosphorylated at T592.* 2018. **17**(9): p. 1102-1114.

332.   Szaniawski, M.A., et al., *SAMHD1 phosphorylation coordinates the anti-HIV-1 response by diverse interferons and tyrosine kinase inhibition.* 2018. **9**(3).

333.   Ji, X., et al., *Mechanism of allosteric activation of SAMHD1 by dGTP.* 2013. **20**(11): p. 1304-1309.

334.   Zhu, C., et al., *Structural insight into dGTP-dependent activation of tetrameric SAMHD1 deoxynucleoside triphosphate triphosphohydrolase.* 2013. **4**(1): p. 1-9.

335.   Amie, S.M., R.A. Bambara, and B.J.J.o.B.C. Kim, *GTP is the primary activator of the anti-HIV restriction factor SAMHD1.* 2013. **288**(35): p. 25001-25006.

336.   Baldauf, H.-M., et al., *SAMHD1 restricts HIV-1 infection in resting CD4+ T cells.* 2012. **18**(11): p. 1682-1688.

337. Riess, M., et al., *Interferons induce expression of SAMHD1 in monocytes through down-regulation of miR-181a and miR-30a.* 2017. **292**(1): p. 264-277.

338. Jin, C., et al., *MicroRNA-181 expression regulates specific post-transcriptional level of SAMHD1 expression in vitro.* 2014. **452**(3): p. 760-767.

339. Franzolin, E., et al., *The deoxynucleotide triphosphohydrolase SAMHD1 is a major regulator of DNA precursor pools in mammalian cells.* 2013. **110**(35): p. 14272-14277.

340. de Silva, S., et al., *Promoter methylation regulates SAMHD1 gene expression in human CD4+ T cells.* 2013. **288**(13): p. 9284-9292.

341. Ballana, E. and J.A.J.T.i.m. Esté, *SAMHD1: at the crossroads of cell proliferation, immune responses, and virus restriction.* 2015. **23**(11): p. 680-692.

342. Tang, C., et al., *Impaired dNTPase activity of SAMHD1 by phosphomimetic mutation of Thr-592.* 2015. **290**(44): p. 26352-26359.

343. Gramberg, T., et al., *Restriction of diverse retroviruses by SAMHD1.* 2013. **10**(1): p. 1-12.

344. Sze, A., et al., *Host restriction factor SAMHD1 limits human T cell leukemia virus type 1 infection of monocytes via STING-mediated apoptosis.* 2013. **14**(4): p. 422-434.

345. St Gelais, C., et al., *SAMHD1 restricts HIV-1 infection in dendritic cells (DCs) by dNTP depletion, but its expression in DCs and primary CD4+ T-lymphocytes cannot be upregulated by interferons.* 2012. **9**(1): p. 1-15.

346. Welbourn, S., et al., *Restriction of virus infection but not catalytic dNTPase activity is regulated by phosphorylation of SAMHD1.* 2013. **87**(21): p. 11516-11524.

347. Van Cor-Hosmer, S.K., et al., *Restricted 5′-end gap repair of HIV-1 integration due to limited cellular dNTP concentrations in human primary macrophages.* 2013. **288**(46): p. 33253-33262.

348. Mlcochova, P., et al., *A G1‑like state allows HIV‑1 to bypass SAMHD 1 restriction in macrophages.* 2017. **36**(5): p. 604-616.

349. Mlcochova, P., et al., *DNA damage induced by topoisomerase inhibitors activates SAMHD 1 and blocks HIV‑1 infection of macrophages.* 2018. **37**(1): p. 50-62.

350. Lee, E.J., et al., *SAMHD1 acetylation enhances its deoxynucleotide triphosphohydrolase activity and promotes cancer cell proliferation.* 2017. **8**(40): p. 68517.

351. Welbourn, S. and K.J.V. Strebel, *Low dNTP levels are necessary but may not be sufficient for lentiviral restriction by SAMHD1.* 2016. **488**: p. 271-277.

352. Bhattacharya, A., et al., *Effects of T592 phosphomimetic mutations on tetramer stability and dNTPase activity of SAMHD1 can not explain the retroviral restriction defect.* 2016. **6**(1): p. 1-12.

353. White, T.E., et al., *The retroviral restriction ability of SAMHD1, but not its deoxynucleotide triphosphohydrolase activity, is regulated by phosphorylation.* 2013. **13**(4): p. 441-451.

354.   Goncalves, A., et al., *SAMHD1 is a nucleic‑acid binding protein that is mislocalized due to aicardi‑goutières syndrome‑associated mutations.* 2012. **33**(7): p. 1116-1122.

355.   Choi, J., et al., *SAMHD1 specifically restricts retroviruses through its RNase activity.* 2015. **12**(1): p. 1-12.

356.   Seamon, K.J., et al., *SAMHD1 is a single-stranded nucleic acid binding protein with no active site-associated nuclease activity.* 2015. **43**(13): p. 6486-6499.

357.   Ryoo, J., et al., *The ribonuclease activity of SAMHD1 is required for HIV-1 restriction.* 2014. **20**(8): p. 936-941.

358.   Brandariz-Nuñez, A., et al., *Contribution of oligomerization to the anti-HIV-1 properties of SAMHD1.* 2013. **10**(1): p. 1-12.

359.   Goujon, C., et al., *With a little help from a friend: increasing HIV transduction of monocyte-derived dendritic cells with virion-like particles of SIV MAC.* 2006. **13**(12): p. 991-994.

360.   Goujon, C., et al., *Characterization of simian immunodeficiency virus SIVSM/human immunodeficiency virus type 2 Vpx function in human myeloid cells.* 2008. **82**(24): p. 12335-12345.

361.   Hofmann, H., et al., *The Vpx lentiviral accessory protein targets SAMHD1 for degradation in the nucleus.* 2012. **86**(23): p. 12552-12560.

362.   Descours, B., et al., *SAMHD1 restricts HIV-1 reverse transcription in quiescent CD4+ T-cells.* 2012. **9**(1): p. 1-8.

363.   Hollenbaugh, J.A., et al., *dNTP pool modulation dynamics by SAMHD1 protein in monocyte-derived macrophages.* 2014. **11**(1): p. 1-12.

364.   Pertel, T., C. Reinhard, and J.J.R. Luban, *Vpx rescues HIV-1 transduction of dendritic cells from the antiviral state established by type 1 interferon.* 2011. **8**(1): p. 1-16.

365.   Lahaye, X., et al., *The capsids of HIV-1 and HIV-2 determine immune detection of the viral cDNA by the innate sensor cGAS in dendritic cells.* 2013. **39**(6): p. 1132-1142.

366.   Hertoghs, N., et al., *SAMHD1 degradation enhances active suppression of dendritic cell maturation by HIV-1.* 2015. **194**(9): p. 4431-4437.

367.   Puigdomènech, I., et al., *SAMHD1 restricts HIV-1 cell-to-cell transmission and limits immune detection in monocyte-derived dendritic cells.* 2013. **87**(5): p. 2846-2856.

368.   Antonucci, J.M., et al., *SAMHD1 impairs HIV-1 gene expression and negatively modulates reactivation of viral latency in CD4+ T cells.* 2018. **92**(15).

369.   Coquel, F., et al., *SAMHD1 acts at stalled replication forks to prevent interferon induction.* 2018. **557**(7703): p. 57-61.

370.   Chen, S., et al., *SAMHD1 suppresses innate immune responses to viral infections and inflammatory stimuli by inhibiting the NF-κB and interferon pathways.* 2018. **115**(16): p. E3798-E3807.

371. Antonucci, J.M., et al., *SAMHD1-mediated HIV-1 restriction in cells does not involve ribonuclease activity.* 2016. **22**(10): p. 1072-1074.

372. Sommer, A.F., et al., *Restrictive influence of SAMHD1 on Hepatitis B Virus life cycle.* 2016. **6**(1): p. 1-14.

373. Hollenbaugh, J.A., et al., *Host factor SAMHD1 restricts DNA viruses in non-dividing myeloid cells.* 2013. **9**(6): p. e1003481.

374. Badia, R., et al., *Inhibition of herpes simplex virus type 1 by the CDK6 inhibitor PD-0332991 (palbociclib) through the control of SAMHD1.* 2016. **71**(2): p. 387-394.

375. Buffone, C., et al., *The ability of SAMHD1 to block HIV-1 but not SIV requires expression of MxB.* 2019. **531**: p. 260-268.

376. McElrath, M., J. Pruett, and Z.J.P.o.t.N.A.o.S. Cohn, *Mononuclear phagocytes of blood and bone marrow: comparative roles as viral reservoirs in human immunodeficiency virus type 1 infections.* 1989. **86**(2): p. 675-679.

377. Jäger, J., et al., *Human lung tissue explants reveal novel interactions during Legionella pneumophila infections.* 2014. **82**(1): p. 275-285.

378. Fain, J.N., D.S. Tichansky, and A.K.J.M. Madan, *Most of the interleukin 1 receptor antagonist, cathepsin S, macrophage migration inhibitory factor, nerve growth factor, and interleukin 18 release by explants of human adipose tissue is by the non–fat cells, not by the adipocytes.* 2006. **55**(8): p. 1113-1121.

379. Jayakumar, P., et al., *Tissue-resident macrophages are productively infected ex vivo by primary X4 isolates of human immunodeficiency virus type 1.* 2005. **79**(8): p. 5220-5226.

380. Patterson, B.K., et al., *Susceptibility to human immunodeficiency virus-1 infection of human foreskin and cervical tissue grown in explant culture.* 2002. **161**(3): p. 867-873.

381. Folks, T., et al., *Characterization of a promonocyte clone chronically infected with HIV and inducible by 13-phorbol-12-myristate acetate.* 1988. **140**(4): p. 1117-1122.

382. Pise-Masison, C.A. and C.A.J.V. Holland, *Restricted replication of the HIV-1 T-lymphotropic isolate NL4-3 in HL-60 cells.* 1995. **206**(1): p. 641-645.

383. Butera, S.T., et al., *Oscillation of the human immunodeficiency virus surface receptor is regulated by the state of viral activation in a CD4+ cell model of chronic infection.* 1991. **65**(9): p. 4645-4653.

384. Kurt-Jones, E.A., M.H. Orzalli, and D.M.J.C.B.o.H.V. Knipe, *Innate immune mechanisms and herpes simplex virus infection and disease.* 2017: p. 49-75.

385. Kitano, K., et al., *Differentiating agents facilitate infection of myeloid leukemia cell lines by monocytotropic HIV-1 strains [published erratum appears in Blood 1991 Apr 1; 77 (7): 1624].* 1990.

386. Leglise, M.C., et al., *Leukemic cell maturation: phenotypic variability and oncogene expression in HL60 cells: a review.* 1988. **13**(3): p. 319-337.

387. Mitchell, P.S., et al., *Evolutionary analyses suggest a function of MxB immunity proteins beyond lentivirus restriction.* 2015. **11**(12): p. e1005304.

388.   Ranganath, N., et al., *Type I interferon responses are impaired in latently HIV infected cells.* 2016. **13**(1): p. 1-9.

389.   Gaidt, M.M., et al., *Human monocytes engage an alternative inflammasome pathway.* 2016. **44**(4): p. 833-846.

390.   Borzillo, G.V., et al., *Macrophage lineage switching of murine early pre-B lymphoid cells expressing transduced fms genes.* 1990. **10**(6): p. 2703-2714.

391.   DeKoter, R.P. and H.J.S. Singh, *Regulation of B lymphocyte and macrophage development by graded expression of PU. 1.* 2000. **288**(5470): p. 1439-1441.

392.   Rapino, F., et al., *C/EBPα induces highly efficient macrophage transdifferentiation of B lymphoma and leukemia cell lines and impairs their tumorigenicity.* 2013. **3**(4): p. 1153-1163.

393.   Gaidt, M.M., et al., *Modeling Primary Human Monocytes with the Trans–Differentiation Cell Line BLaER1*, in *Innate Immune Activation.* 2018, Springer. p. 57-66.

394.   Ihle, J.N.J.C.i., *Interleukin-3 and hematopoiesis.* 1992. **51**: p. 65-106.

395.   Greulich, W., et al., *TLR8 is a sensor of RNase T2 degradation products.* 2019. **179**(6): p. 1264-1275. e13.

396.   Vierbuchen, T., et al., *The human-associated archaeon Methanosphaera stadtmanae is recognized through its RNA and induces TLR8-dependent NLRP3 inflammasome activation.* 2017. **8**: p. 1535.

397.   Kuffour, E.O., et al., *USP18 (UBP43) abrogates p21-mediated inhibition of HIV-1.* 2018. **92**(20).

398.   Andreeva, L., et al., *cGAS senses long and HMGB/TFAM-bound U-turn DNA by forming protein–DNA ladders.* 2017. **549**(7672): p. 394-398.

399.   Ginhoux, F. and M.J.I. Guilliams, *Tissue-resident macrophage ontogeny and homeostasis.* 2016. **44**(3): p. 439-449.

400.   Röszer, T.J.C., *Understanding the biology of self-renewing macrophages.* 2018. **7**(8): p. 103.

401.   Kedzierska, K., C.L. Maslin, and S.M.J.M.C.R.-O. Crowe, *Cells of the macrophage lineage and their role in the pathogenesis of HIV-1 infection: an update.* 2004. **1**(3): p. 351-360.

402.   Crowe, S., T. Zhu, and W.A.J.J.o.l.b. Muller, *The contribution of monocyte infection and trafficking to viral persistence, and maintenance of the viral reservoir in HIV infection.* 2003. **74**(5): p. 635-641.

403.   Sonza, S., et al., *Human immunodeficiency virus type 1 replication is blocked prior to reverse transcription and integration in freshly isolated peripheral blood monocytes.* 1996. **70**(6): p. 3863-3869.

404.   Fire, A., et al., *Potent and specific genetic interference by double-stranded RNA in Caenorhabditis elegans.* 1998. **391**(6669): p. 806-811.

405.   Whitehead, K.A., R. Langer, and D.G.J.N.r.D.d. Anderson, *Knocking down barriers: advances in siRNA delivery.* 2009. **8**(2): p. 129-138.

406.   Sugimura, R., et al., *Haematopoietic stem and progenitor cells from human pluripotent stem cells.* 2017. **545**(7655): p. 432-438.

407.   Tebas, P., et al., *Gene editing of CCR5 in autologous CD4 T cells of persons infected with HIV.* 2014. **370**(10): p. 901-910.

408.   Mock, U., et al., *mRNA transfection of a novel TAL effector nuclease (TALEN) facilitates efficient knockout of HIV co-receptor CCR5.* 2015. **43**(11): p. 5560-5571.

409.   Silva, G., et al., *Meganucleases and other tools for targeted genome engineering: perspectives and challenges for gene therapy.* 2011. **11**(1): p. 11-27.

410.   Doudna, J.A. and E.J.S. Charpentier, *The new frontier of genome engineering with CRISPR-Cas9.* 2014. **346**(6213).

411.   Cong, L., et al., *Multiplex genome engineering using CRISPR/Cas systems.* 2013. **339**(6121): p. 819-823.

412.   Hsu, P.D., E.S. Lander, and F.J.C. Zhang, *Development and applications of CRISPR-Cas9 for genome engineering.* 2014. **157**(6): p. 1262-1278.

413.   Gaj, T., C.A. Gersbach, and C.F.J.T.i.b. Barbas III, *ZFN, TALEN, and CRISPR/Cas-based methods for genome engineering.* 2013. **31**(7): p. 397-405.

414.   Makarova, K.S., et al., *Evolution and classification of the CRISPR–Cas systems.* 2011. **9**(6): p. 467-477.

415.   Jinek, M., et al., *A programmable dual-RNA–guided DNA endonuclease in adaptive bacterial immunity.* 2012. **337**(6096): p. 816-821.

416.   Kim, H. and J.-S.J.N.R.G. Kim, *A guide to genome engineering with programmable nucleases.* 2014. **15**(5): p. 321-334.

417.   Brinkman, E.K., et al., *Kinetics and fidelity of the repair of Cas9-induced double-strand DNA breaks.* 2018. **70**(5): p. 801-813. e6.

418.   Freund, E.C., et al., *Efficient gene knockout in primary human and murine myeloid cells by non-viral delivery of CRISPR-Cas9.* 2020. **217**(7).

419.   Qi, L.S., et al., *Repurposing CRISPR as an RNA-guided platform for sequence-specific control of gene expression.* 2013. **152**(5): p. 1173-1183.

420.   Schmid-Burgk, J.L., et al., *OutKnocker: a web tool for rapid and simple genotyping of designer nuclease edited cell lines.* 2014. **24**(10): p. 1719-1723.

421.   Pizzato, M., et al., *A one-step SYBR Green I-based product-enhanced reverse transcriptase assay for the quantitation of retroviruses in cell culture supernatants.* 2009. **156**(1-2): p. 1-7.

422.   Kuffour, E.O., et al., *ISG15 deficiency enhances HIV-1 infection by accumulating misfolded p53.* 2019. **10**(4).

423.   Finkelshtein, D., et al., *LDL receptor and its family members serve as the cellular receptors for vesicular stomatitis virus.* 2013. **110**(18): p. 7306-7311.

424. Bakir, T.M.J.S.P.J., *The role of SAMHD1 expression and its relation to HIV-2 (Vpx) gene production.* 2018. **26**(6): p. 903-908.

425. Ravot, E., et al., *High efficiency lentiviral gene delivery in non‐dividing cells by deoxynucleoside treatment.* 2002. **4**(2): p. 161-169.

426. Seamon, K.J., et al., *Small molecule inhibition of SAMHD1 dNTPase by tetramer destabilization.* 2014. **136**(28): p. 9822-9825.

427. Schnyder, J. and M.J.T.J.o.e.m. Baggiolini, *Role of phagocytosis in the activation of macrophages.* 1978. **148**(6): p. 1449-1457.

428. Chen, S., et al., *SAMHD1 suppression of antiviral immune responses.* 2019. **27**(3): p. 254-267.

429. Schmidt, S., et al., *SAMHD1's protein expression profile in humans.* 2015. **98**(1): p. 5-14.

430. Doyle, T., C. Goujon, and M.H.J.N.r.M. Malim, *HIV-1 and interferons: who's interfering with whom?* 2015. **13**(7): p. 403-413.

431. Opp, S., et al., *MxB is not responsible for the blocking of HIV-1 infection observed in alpha interferon-treated cells.* 2016. **90**(6): p. 3056-3064.

432. Vermeire, J., et al., *Quantification of reverse transcriptase activity by real-time PCR as a fast and accurate method for titration of HIV, lenti-and retroviral vectors.* 2012. **7**(12): p. e50859.

433. Stang, A., et al., *Unintended spread of a biosafety level 2 recombinant retrovirus.* 2009. **6**(1): p. 1-6.

434. Gardner, M.B., M. Endres, and P. Barry, *The simian retroviruses SIV and SRV*, in *The retroviridae*. 1994, Springer. p. 133-276.

435. Burke, B., et al., *Macrophages in gene therapy: cellular delivery vehicles and in vivo targets.* 2002. **72**(3): p. 417-428.

436. Mendoza-Coronel, E. and E.J.F.i.i. Ortega, *Macrophage polarization modulates FcγR- and CD13-mediated phagocytosis and reactive oxygen species production, independently of receptor membrane expression.* 2017. **8**: p. 303.

437. Pilling, D., et al., *Identification of markers that distinguish monocyte-derived fibrocytes from monocytes, macrophages, and fibroblasts.* 2009. **4**(10): p. e7475.

438. Descours, B., et al., *CD32a is a marker of a CD4 T-cell HIV reservoir harbouring replication-competent proviruses.* 2017. **543**(7646): p. 564-567.

439. Abdel-Mohsen, M., et al., *CD32 is expressed on cells with transcriptionally active HIV but does not enrich for HIV DNA in resting T cells.* 2018. **10**(437).

440. Osuna, C.E., et al., *Evidence that CD32a does not mark the HIV-1 latent reservoir.* 2018. **561**(7723): p. E20-E28.

441. Jensen, K., et al., *Comparison of small interfering RNA (siRNA) delivery into bovine monocyte-derived macrophages by transfection and electroporation.* 2014. **158**(3-4): p. 224-232.

442.	Hultquist, J.F., et al., *CRISPR–Cas9 genome engineering of primary CD4+ T cells for the interrogation of HIV–host factor interactions.* 2019. **14**(1): p. 1-27.

443.	Pattanayak, V., et al., *High-throughput profiling of off-target DNA cleavage reveals RNA-programmed Cas9 nuclease specificity.* 2013. **31**(9): p. 839-843.

444.	Zhou, J., et al., *Dual sgRNAs facilitate CRISPR/Cas9‑mediated mouse genome targeting.* 2014. **281**(7): p. 1717-1725.

445.	Sander, J., et al., *Cellular differentiation of human monocytes is regulated by time-dependent interleukin-4 signaling and the transcriptional regulator NCOR2.* 2017. **47**(6): p. 1051-1066. e12.

446.	Housden, B.E. and N.J.N.b. Perrimon, *Comparing CRISPR and RNAi-based screening technologies.* 2016. **34**(6): p. 621-623.

447.	Danastas, K., M. Miranda-Saksena, and A.L.J.I.J.o.M.S. Cunningham, *Herpes Simplex Virus Type 1 Interactions with the Interferon System.* 2020. **21**(14): p. 5150.

448.	Garotta, G., et al., *GM‑1, a Clone of the Monoblastic Phagocyte U937 That Expresses a Large Respiratory Burst Capacity Upon Activation With Interferon‑γ.* 1991. **49**(3): p. 294-301.

449.	Schwende, H., et al., *Differences in the state of differentiation of THP‑1 cells induced by phorbol ester and 1, 25‑dihydroxyvitamin D3.* 1996. **59**(4): p. 555-561.

450.	Chanput, W., et al., *Transcription profiles of LPS-stimulated THP-1 monocytes and macrophages: a tool to study inflammation modulating effects of food-derived compounds.* 2010. **1**(3): p. 254-261.

451.	Henderson, A. and K.J.P.o.t.N.A.o.S. Calame, *CCAAT/enhancer binding protein (C/EBP) sites are required for HIV-1 replication in primary macrophages but not CD4+ T cells.* 1997. **94**(16): p. 8714-8719.

452.	Li, M., et al., *Roles of SAMHD1 in antiviral defense, autoimmunity and cancer.* 2017. **27**(4): p. e1931.

453.	Lahaye, X. and N.J.C.o.i.v. Manel, *Viral and cellular mechanisms of the innate immune sensing of HIV.* 2015. **11**: p. 55-62.

454.	Nicol, M.Q., et al., *Human immunodeficiency virus infection alters tumor necrosis factor alpha production via Toll-like receptor-dependent pathways in alveolar macrophages and U1 cells.* 2008. **82**(16): p. 7790-7798.

455.	Diget, E.A., et al., *Characterization of HIV-1 infection and innate sensing in different types of primary human monocyte-derived macrophages.* 2013. **2013**.

456.	Chattergoon, M.A., et al., *HIV and HCV activate the inflammasome in monocytes and macrophages via endosomal Toll-like receptors without induction of type 1 interferon.* 2014. **10**(5): p. e1004082.

457.	Woelk, C.H., et al., *Interferon gene expression following HIV type 1 infection of monocyte-derived macrophages.* 2004. **20**(11): p. 1210-1222.

458.	Giri, M.S., et al., *Microarray data on gene modulation by HIV‑1 in immune cells: 2000–2006.* 2006. **80**(5): p. 1031-1043.

459.	Meier, A., et al., *MyD88-dependent immune activation mediated by human immunodeficiency virus type 1-encoded Toll-like receptor ligands.* 2007. **81**(15): p. 8180-8191.

460.	Gantier, M.P., et al., *TLR7 is involved in sequence-specific sensing of single-stranded RNAs in human macrophages.* 2008. **180**(4): p. 2117-2124.

461.	Jønsson, K., et al., *IFI16 is required for DNA sensing in human macrophages by promoting production and function of cGAMP.* 2017. **8**(1): p. 1-17.

462.	Fernandes-Alnemri, T., et al., *AIM2 activates the inflammasome and cell death in response to cytoplasmic DNA.* 2009. **458**(7237): p. 509-513.

463.	Kambal, A., et al., *Generation of HIV-1 resistant and functional macrophages from hematopoietic stem cell–derived induced pluripotent stem cells.* 2011. **19**(3): p. 584-593.

464.	Mosser, D.M. and J.P.J.N.r.i. Edwards, *Exploring the full spectrum of macrophage activation.* 2008. **8**(12): p. 958-969.

465.	Mefferd, A.L., et al., *Insights into the mechanisms underlying the inactivation of HIV-1 proviruses by CRISPR/Cas.* 2018. **520**: p. 116-126.

466.	Hildreth, A.D., L. Riggan, and T.E.J.S.p. O'Sullivan, *CRISPR-Cas9 Ribonucleoprotein-Mediated Genomic Editing in Primary Innate Immune Cells.* 2020. **1**(3): p. 100113.

467.	Hultquist, J.F., et al., *A Cas9 ribonucleoprotein platform for functional genetic studies of HIV-host interactions in primary human T cells.* 2016. **17**(5): p. 1438-1452.

468.	van Diemen, F.R. and R.J.J.C.m. Lebbink, *CRISPR/Cas9, a powerful tool to target human herpesviruses.* 2017. **19**(2): p. e12694.

469.	Barkal, A.A., et al., *Engagement of MHC class I by the inhibitory receptor LILRB1 suppresses macrophages and is a target of cancer immunotherapy.* 2018. **19**(1): p. 76-84.

470.	Boissel, L., et al., *Comparison of mRNA and lentiviral based transfection of natural killer cells with chimeric antigen receptors recognizing lymphoid antigens.* 2012. **53**(5): p. 958-965.

471.	Tsong, T.Y.J.E. and e.i.c. biology, *Electroporation of cell membranes.* 1989: p. 149-163.

472.	Bian, S., et al., *High-throughput in situ cell electroporation microsystem for parallel delivery of single guide RNAs into mammalian cells.* 2017. **7**(1): p. 1-13.

473.	MARZIO, P.D., et al., *Chemokine receptor regulation and HIV type 1 tropism in monocyte-macrophages.* 1998. **14**(2): p. 129-138.

474.	Friedrich, B.M., et al., *A functional role for ADAM10 in human immunodeficiency virus type-1 replication.* 2011. **8**(1): p. 1-14.

475.	Contreras, X., et al., *Protein kinase C-delta regulates HIV-1 replication at an early post-entry step in macrophages.* 2012. **9**(1): p. 1-11.

476.	Hume, D.A.J.C.o.i.i., *The mononuclear phagocyte system.* 2006. **18**(1): p. 49-53.

477.	Pereira, C., et al., *Dynamics of CD86 expression on allergic inflammation-new insights.* 2009. **3**(2): p. 128-131.

478. Stein, D.R., et al., *Mx2 Expression Is Associated with Reduced Susceptibility to HIV Infection in Highly Exposed HIV Seronegative Sex Workers from Nairobi, Kenya.* 2014. **30**(S1): p. A82-A82.

479. Goujon, C. and M.H.J.J.o.v. Malim, *Characterization of the alpha interferon-induced postentry block to HIV-1 infection in primary human macrophages and T cells.* 2010. **84**(18): p. 9254-9266.

480. Matreyek, K.A., et al., *Host and viral determinants for MxB restriction of HIV-1 infection.* 2014. **11**(1): p. 1-20.

481. Lee, K., et al., *Flexible use of nuclear import pathways by HIV-1.* 2010. **7**(3): p. 221-233.

482. Pauls, E., et al., *Restriction of HIV-1 replication in primary macrophages by IL-12 and IL-18 through the upregulation of SAMHD1.* 2013. **190**(9): p. 4736-4741.

483. Daddacha, W., et al., *SAMHD1 promotes DNA end resection to facilitate DNA repair by homologous recombination.* 2017. **20**(8): p. 1921-1935.

484. Kim, E.T., et al., *SAMHD1 modulates early steps during human cytomegalovirus infection by limiting NF-κB activation.* 2019. **28**(2): p. 434-448. e6.

485. Deutschmann, J. and T.J.V. Gramberg, *SAMHD1… and Viral Ways around It.* 2021. **13**(3): p. 395.

486. Chen, Z., et al., *Inhibition of Hepatitis B virus replication by SAMHD1.* 2014. **450**(4): p. 1462-1468.

487. Noyce, R.S., et al., *Membrane perturbation elicits an IRF3-dependent, interferon-independent antiviral response.* 2011. **85**(20): p. 10926-10931.

488. Holm, C.K., et al., *Virus-cell fusion as a trigger of innate immunity dependent on the adaptor STING.* 2012. **13**(8): p. 737-743.

489. Hare, D.N., et al., *Membrane perturbation-associated Ca2+ signaling and incoming genome sensing are required for the host response to low-level enveloped virus particle entry.* 2016. **90**(6): p. 3018-3027.

490. Fricke, T., et al., *MxB binds to the HIV-1 core and prevents the uncoating process of HIV-1.* 2014. **11**(1): p. 1-14.

491. Sironi, M., et al., *Evolutionary analysis identifies an MX2 haplotype associated with natural resistance to HIV-1 infection.* 2014. **31**(9): p. 2402-2414.

492. De Meo, S., et al., *SAMHD1 phosphorylation and cytoplasmic relocalization after human cytomegalovirus infection limits its antiviral activity.* 2020. **16**(9): p. e1008855.

493. Mandal, P.K., et al., *Efficient ablation of genes in human hematopoietic stem and effector cells using CRISPR/Cas9.* 2014. **15**(5): p. 643-652.

494. Konermann, S., et al., *Genome-scale transcriptional activation by an engineered CRISPR-Cas9 complex.* 2015. **517**(7536): p. 583-588.

Acknowledgements

Affidavit

Affidavit

XIAO, Qianhao
Surname, first name

Feodor-Lynen-Straße 23
Street

81377 München
Zip code, town, country

I hereby declare, that the submitted thesis entitled:

Generation of macrophage models to investigate the effect of host factors restricting HIV and HSV infection

……………………………………………………………………………………………………….

is my own work. I have only used the sources indicated and have not made unauthorized use of services of a third party. Where the work of others has been quoted or reproduced, the source is always given.

I further declare that the submitted thesis or parts thereof have not been presented as part of an examination degree to any other university.

Munich, 29.11.2021
place, date

Qianhao Xiao
Signature doctoral candidate

Curriculum vitae

Qianhao Xiao

14.11.1990, Shiyan, China

Qianhao@mvp.lmu.de

Research areas

HIV infection; Innate immunity

Education

2016-2021, Virology (Ph.D.), Max von Pettenkofer-Institut, Munich, Germany

2013-2016, Pathogen biology (M.Med), Wuhan University, China

2009-2013, Biotechnology (B.Sc.), Northwest A&F University, China

Credentials

Biosafety Level 3 Laboratory authorization (Munich, Germany)

Laboratory Animal Technician certification (Wuhan, China)

Grants (contribution)

Cellular and viral determinants of innate HIV recognition in macrophages (DFG: Grant No. SPP1923)

The mechanisms of neuronal injury caused by activation of macrophages (M1/M2) in the rhesus macaque model of NeuroAIDS (NSFC: Grant No. 81471943)

HIV and/or HCV Infection and Neuron Injury (NSFC: Grant No. 81271334)

The Establishment of Nonhuman Primate Model for Anti-HIV/SIV factors screening (NMP: Grant No. 2014ZX10001003005)

Congress Communications

2018 28th Annual Meeting of the Society for Virology (GfV/DDV) in Würzburg (Poster presentations)

2018 SPP 1923 International Symposium in Heidelberg (Poster presentations)

List of publications (not associated with PhD thesis)

1) **Xiao QH**, Li J, Yu Q, et al. Distinct compartmentalization in the CNS of SHIVKU-1-infected Chinese rhesus macaque is associated with severe neuropathology. JAIDS Journal of Acquired Immune Deficiency Syndromes, 2015, 70(5): e168.

2) Liu H, **Xiao QH**, Liu J B, et al. SIV infection impairs the central nervous system in Chinese rhesus macaques. Journal of Neuroimmune Pharmacology, 2016, 11(3): 592-600.

3) Liu JB, **Xiao QH**, Zhou R, et al. Comparative Analysis of Immune Activation Markers of CD8+ T Cells in Lymph Nodes of Different Origins in SIV-Infected Chinese Rhesus Macaques. Frontiers in Immunology, 2016, 7.

4) Li JB, Liu J, **Xiao QH**, et al. Comparative analysis of lymphocyte and cytokine profiles in peripheral and enteric lymph nodes of SIV-infected Chinese rhesus macaques. Journal of Neuroimmune Pharmacology, 2015, 10: S82.

5) Sun L, Zhou Y, Wang X, Li JL, Zhou L, Sang M, Zhuang K, **Xiao QH**, et al. HIV infection and/or Heroin use dysregulate the plasma exosome miRNA expression. Journal of Neuroimmune Pharmacology volume 15, 2020,pages400-408

6) Liu H, Liu JB, Meng FZ, Xu XQ, Wang Y, Xian QY, Zhou RH, **Xiao QH**, et al. CD4+ T Cell Depletion Does Not Affect the Level of Viremia in Chronically SHIVSF162P3N-Infected Chinese Cynomolgus Monkeys. Researchsquare DOI: 10.21203/rs.3.rs-53973/v1